Nuclear Studies with Neutron-Capture γ Rays

B. ARAD, G. BEN-DAVID

Department of Nuclear Physics, Soreq Nuclear Research Center, Yavne, Israel

and

Department of Physics, Bar-Ilan University, Ramat-Gan, Israel

Thermal neutron-capture γ rays have found applications in a variety of nuclear reaction studies requiring γ rays in the energy region up to 11 MeV. The importance of these γ-ray sources is that they provide very high intensities, which exceed by two orders of magnitude the intensities per unit energy interval obtainable from other sources. The experiments performed with these sources are reviewed in this article, and the advantages and disadvantages of the method are discussed.

CONTENTS

I. INTRODUCTION

I.1 Neutron-Capture γ Rays

Thermal neutrons are readily absorbed by most nuclei, forming a capture nucleus with an excitation energy in the region of 8 MeV, and in some cases up to 11 MeV. With the exception of a few light nuclei, this excitation energy is insufficient to cause emission of charged particles, and the compound nucleus deexcites to its ground state with the emission of γ rays. Usually cascades of γ rays are emitted during the deexcitation process, and many nuclear levels not populated by radioactive decay or in other reactions can be reached in this way.

Neutron-capture γ rays were first reported by Lea (1934), but very few data on the subject were published during the following decade. The development of the nuclear chain reactor by Fermi in 1944 provided for the first time a copious source of thermal neutrons which permitted precision studies of capture γ rays. During the following few years various types of γ spectrometers, including scintillation detectors, crystal diffraction spectrometers, and pair- and Compton-spectrometers, were used in these investigations. An early review of these methods has been given by Bäckström (1959). A great many studies were published during the following period, including compila-

tions of energies and intensities of the capture γ radiation by Groshev *et al.* (1959) and Bartholomew and Higgs (1958). Owing to the complex nature of many of the spectra it was not always possible in the earlier work to evaluate accurately the details of the decay schemes, since the precision spectrometers with their low efficiencies did not permit the use of coincidence techniques. The development of high precision and relatively high efficiency lithium drifted germanium detectors has given new impetus to the study of capture γ radiation, and permitted new compilations of capture γ rays (Groshev *et al.*, 1967, 1968, 1969).

In the studies mentioned above, the capture γ radiation itself was the subject of the research. It was not until 1959 that the potentialities of thermal neutron capture γ rays as a high intensity γ source for studies of nuclear reactions began to be realized. The capture γ radiation is characterized by a line spectrum, with the individual lines having well-defined energies with an energy resolution of the order of a few electron volts. This is because the energy of the neutron-capture compound state is itself well defined, being equal to the sum of the neutron binding energy and the thermal neutron energy (the latter of the order of 0.03 eV). The widths of the primary capture γ lines are therefore given by a convolution of the widths of the nuclear levels populated in the primary transition with the thermal Doppler broadening caused by the motion of the source nuclei, the latter usually predominating. The over-all width is thus a few eV, which is many orders of magnitude less than the widths of lines from photon sources based on the use of charged particle reactions. For example, in the earlier photonuclear work using betatron bremstrahlung, resolutions of the order of a few hundred keV were quite usual (e.g., Fuller and Hayward, 1956), and even with recent developments the best resolution obtained with similar techniques is of the order of a few tens of keV. It thus turns out that the intensities of the thermal neutron-capture γ rays, per unit energy interval, exceed by more than two orders of magnitude the available intensities obtainable from other types of photon sources in this energy region.

The high intensities and the fact that the capture γ beams have sharply defined energies can be of great advantage in certain types of experiments. One drawback is that they do not provide a full range of energies. However, several methods are available for modifying the natural line energy to a certain extent, thus increasing the scope of application of these beams. The energy of the neutron-capture γ ray is determined by the energy of the incoming neutrons (usually thermal), the neutron binding energy, and the energy of the level reached in the de-excitation process. Changes in the γ energy can be produced by the following methods: (a) using epithermal instead of thermal neutrons for the (n, γ) source; (b) rapidly rotating the target so as to cause a Doppler shift of the γ energy in the target frame of reference; (c) inserting a nuclear resonant scatterer in the path of the γ beam and utilizing the scattered beam at a given angle (which defines the energy shift); and (d) inserting a Compton scatterer and using the scattered beam at a given angle. These methods will be discussed in greater detail later in this review.

I.2 The Use of the Nuclear Reactor to Generate High Intensity Neutron-Capture γ-Ray Beams

Photonuclear studies using capture γ rays were first carried out by Eriksen and Zalesky (1954) but the general advantage of using the nuclear reactor to produce capture γ rays was first pointed out by Knoepfel *et al.* (1959) and Jarczyk *et al.* (1959).

To apply this technique, the target generating the capture γ rays is usually irradiated adjacent to the reactor core. Typical early experimental arrangements have been discussed by Jarczyk *et al.* (1961). Since the γ beam produced must generally be filtered from the reactor neutrons and γ background, a tangential beam tube is more convenient than a radial one for the target irradiation. Borated paraffin is a suitable material for filtering the neutrons from the beam. For example, 1.2 m of a mixed water–paraffin filter reduces the fast neutron component by a factor of 10^7, and the capture γ rays in the region of 7 MeV by a factor of only 20. Where a radial beam tube is used, an additional absorber may be required to reduce the fission γ rays in the beam. This can be achieved by using a 10 cm bismuth plug adjacent to the reactor core. In one of the early experiments of Ben-David and Huebschmann (1962), the capture γ source was irradiated in the reactor thermal column thus reducing the problem of fast neutron background.

The capture γ ray source intensity depends linearly on the thermal neutron cross section, the available thermal neutron flux, and the yield $I_\gamma(E_i)$ of the specific capture γ ray of energy E_i. Tables of I_γ for the various capture γ ray sources are listed in the compilations of Groshev *et al.* (1967, 1968, 1969). While the γ energies are often known to within 1 or 2 keV, the relative intensities vary considerably between the different references. Very intense γ sources are available using this method. For example a 10 Kg iron source at a thermal neutron flux of $10^{13}n$ $cm^{-2}\cdot sec^{-1}$ gives a yield of 10^8 photons of 7.632 MeV $cm^{-2}\cdot sec^{-1}$ at a target position 5 meters from the source.

The shape of these γ lines is determined mainly by the thermal Doppler broadening. Metzger (1959) has shown that this is given by a Gaussian form with a characteristic Doppler width Δ. The value of Δ is of

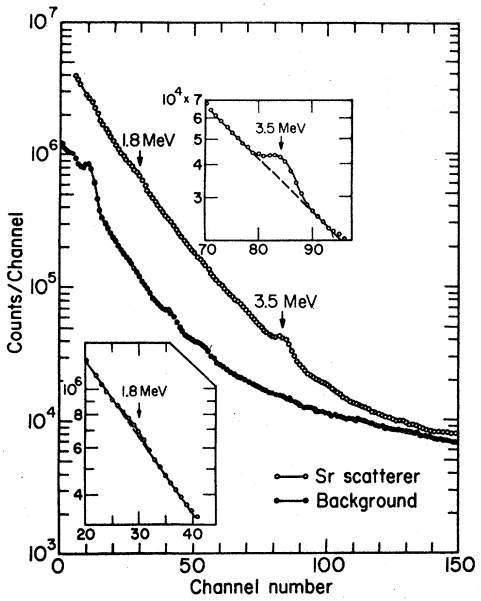

FIG. 1. Pulse height distribution for a Sr source and scatterer. The background was obtained with no scatterer in the beam. [Hans *et al.* (1965)].

the order of 4–8 eV for capture γ rays of 7 MeV, in the normal temperature range. The Doppler width varies with the square root of the effective source temperature, and this effect has been used in several of the experiments discussed in this review.

During the last few years, neutron-capture γ rays have been used to study a wide variety of photonuclear reactions, including resonance γ fluorescence, capture γ Mössbauer phenomena, photoneutron emission, photofission, etc. These applications of capture γ rays are discussed in the succeeding chapters.

II. RESONANCE FLUORESCENCE OF LOW-LYING LEVELS

The phenomenon of resonance fluorescence may be used to study the widths of levels which are beyond the reach of the usual electronic techniques. Two methods of achieving resonance fluorescence in low-lying levels are discussed below.

II.1 Recoil Compensation by Means of a Previous (n, γ) Transition

II.1.1 The Basic Principle

When a level of energy E de-excites to the ground state by γ-ray emission, the energy of the γ ray is less than the level separation energy by an amount $E^2/2Mc^2$, due to the recoil of the nucleus. If this γ ray is now absorbed by a similar nucleus, energy is again expended in nuclear recoil and the excitation energy is less than the original level separation by a total of E^2/Mc^2. In order to obtain resonance fluorescence, this energy difference must be compensated for. Metzger (1959) has described various methods of compensation relying on the introduction of a Doppler shift in the γ-ray energy. This shift may be achieved by mechanical or thermal methods, or by making use of the recoil from a previous nuclear decay or reaction. In this section we deal with the last-mentioned method.

Consider a level of a stable isotope strongly populated in the (n, γ) process by a primary γ transition of energy E_1, this level then de-exciting to the ground state through a second transition of energy E_2. If the lifetime τ of the intermediate level is less than τ_{co}—the average time between successive collisions of the nucleus—the second transition occurs while the nucleus is recoiling with essentially the full recoil energy. (Typical collision times in condensed media are of the order of 2×10^{-14} seconds.) The energy of the secondary γ ray observed at an angle θ to the direction of the recoiling nucleus is then given by

$$E_2' = E_2[1+(V/c)\cos\theta], \tag{2.1a}$$

where V is the recoil velocity. Applying momentum conservation this can be expressed as:

$$E_2' = E_2[1+(E_1/Mc^2)\cos\theta]. \tag{2.1b}$$

As discussed above, to permit resonance fluorescence the difference $E_2'-E_2$ must be equal to the total recoil energy. Thus the resonance condition is given by:

$$(E_2E_1/Mc^2)\cos\theta = E_2^2/Mc^2. \tag{2.2}$$

An angle θ can be found which satisfies Eq. (2.2), provided that $E_1 \geq E_2$; therefore at this angle the secondary γ rays from the source can be used to produce resonance fluorescence in the appropriate scatterer.

In order to permit resonance fluorescence by (n, γ) recoil compensation, it is necessary to have two adjacent stable isotopes—the lighter isotope serving as the (n, γ) source, and the heavier isotope as the resonant scatterer. It is also important that the lighter nucleus have a relatively large thermal neutron-capture cross section, and that the capture nucleus have an appropriate level strongly populated from the capture state and decaying to the ground state with a high branching ratio. Such cases are not too common, but there are a few which have been studied by Fleischman (1963) and Hans *et al.* (1965).

II.1.2 Experimental

In the experiment carried out by Hans *et al.* (1966), the γ-ray source is placed near the reactor core in a thermal flux of about $10^{13}n$ cm^{-2}·sec^{-1}. Both slow and fast neutrons are removed from the beam by a filter consisting of ^{10}B and polyethylene. The collimated γ-ray beam then passes through an absorber and impinges on the resonant scatterer target. The γ rays resonantly scattered from this target were detected

at a backward angle by a 4×4 in. NaI(Tl) detector, and the spectra analyzed with a 400 channel analyzer. A typical spectrum for a ^{87}Sr (n, γ) source and ^{88}Sr resonant scatterer is shown in Fig. 1.

The level widths were determined using the self-absorption technique. In this method a resonant absorber (of the same material as the resonant target) and a nonresonant absorber are alternately placed in the primary beam between the source and the resonant scatterer. The self-absorption ratio R is given by $R=(I_n-I_r)/I_n$, where I_n is the intensity of scattered γ rays using the nonresonant absorber, and I_r the corresponding intensity using the resonant absorber.

II.1.3 Analysis and Results

The comprehensive review article by Metzger (1959) gives a complete analysis of recoil compensated resonance fluorescence. The elastic scattering cross section of an isolated nuclear level at target temperature T for γ rays of energy E is given by

$$\sigma_{\gamma\gamma}(E, T)=\sigma_{\max}{}^{0}\psi(x, t), \tag{2.3}$$

where

$$\sigma_{\max}{}^{0}=2\pi\lambda\!\!\!^{-2}g(\Gamma_0/\Gamma)^2. \tag{2.4}$$

Here $\lambda\!\!\!^{-}$ is the γ wavelength divided by 2π, g is the spin factor $[g=(2j_e+1)/(2j_g+1)]$, where j_e and j_g are the spins of the excited and ground states, respectively, Γ_0 is the partial level width for the ground state transition, and Γ is the total width. The Doppler integral $\psi(x, t)$ takes into account line broadening caused by the thermal motion of the scattering nuclei and is defined by

$$\psi(x, t)=\frac{1}{2(\pi t)^{1/2}}\int_{-\infty}^{+\infty}\frac{\exp[-(x-y)^2/4t]}{1+y^2}\,dy, \tag{2.5}$$

where $x=2(E-E_r)/\Gamma$, E_r being the peak energy of the resonance level, and $t=(\Delta/\Gamma)^2$, where Δ is the Doppler width defined by

$$\Delta=E_r(2kT'/M_0c^2)^{1/2}. \tag{2.6}$$

Here M_0c^2 is the rest mass of the scattering nucleus, k is the Boltzmann constant, and T' is the effective temperature discussed by Lamb (1939).

For values of $t\gg1$, and distances from the peak energy $|E-E_r|\lesssim\Delta$, the Doppler integral of Eq. (2.5) can be expressed in its asymptotic pure Doppler form

$$\psi(x, t)\rightarrow(\pi^{1/2}\Gamma/2\Delta)\exp[(E-E_r)^2/\Delta^2]. \tag{2.7a}$$

At the other extreme, when $t\ll1$, or for distances from the peak energy $|E-E_r|\gg\Delta$, this integral can be expressed in its asymptotic Lorentzian form:

$$\psi(x, t)\rightarrow1\Big/1+\left(\frac{2(E-E_r)}{\Gamma}\right)^2. \tag{2.7b}$$

Arad *et al.* (1967) have discussed the validity of these two approximations in regions of physical interest, and have found more accurate approximations which can be used to derive qualitative results from an experiment. However, for quantitative analysis the exact expression for $\psi(x, t)$ is necessary in most cases. Tables of $\psi(x, t)$ appear in the literature, but errors of up to 2% were reported in the early tabulations. Since the use of Tables can introduce interpolation errors, it is preferable to use a computer program to calculate these functions. An efficient Fortran subroutine is PSICHI, originally developed by O'Shea and Thacher (1963) for reactor calculations.

The self-absorption ratio R, defined above, can be evaluated from the scattering cross section of Eq. (2.3). For the case of resonant scattering with an incident white γ spectrum, Metzger (1959) has shown that R is given by the expression

$$R=NDg\pi\lambda\!\!\!^{-2}(\Gamma_0/\Gamma)\psi(0, t/2), \tag{2.8}$$

where N is the absorber atomic density, and D is its thickness, with the other parameters as defined in Eqs. (2.3)–(2.5). This derivation is for thin scatterers and absorbers.

The beam broadening induced by the primary γ transition, of the order of E_2V/c, is about 100 eV for the transitions considered here. This is considerably more than the over-all level width of a few eV, and fulfills the requirement of a white incident spectrum in the derivation of Eq. (2.8), which can therefore be used to evaluate the level parameters.

Table I summarizes the values of $g\Gamma_0$ obtained by Hans *et al.* (1966) for the elements B, Se, and Sr. Where g is known, Γ_0 is given separately. The errors range between 10% and 35%.

TABLE I. Values of $g\Gamma_0$ for various levels in B, Se, and Sr. From Hans *et al.* (1965).

Nucleus	Energy (MeV)	$g\Gamma_0$ (MeV)	Γ_0 (MeV)
^{11}B	2.14	50	100
	4.46	600	400
	5.03	500	
^{78}Se	3.35	46	
	4.57	180	
	5.21	280	
^{88}Sr	1.83	15	3
	3.5	450	

II.1.4 Conclusions

The recoil compensation method of measuring the width of low-lying nuclear levels, described here, is rather limited. It has been carried out only for a few cases. This is because the conditions essential for resonance scattering are too restrictive. Other methods for carrying out such measurements are discussed in

Sec. IV where it is concluded that resonance fluorescence using low-energy bremsstrahlung is the best method for these low-energy levels.

II.2 Recoilless Nuclear Resonance Absorption (Mössbauer Effect)

II.2.1 The Basic Principle

As discussed above, nuclear recoil causes an energy loss of E^2/Mc^2 both in the emission and absorption of the γ ray. Usually this energy loss is large enough to prevent resonance absorption, which cannot occur without compensation. However, under certain conditions discussed by Mössbauer (1958) (low photon energy, low temperature, and strong crystal binding) the whole crystal takes up the recoil energy. The emission and absorption lines then coincide, so that the well-known Mössbauer resonance absorption can occur.

Mössbauer spectroscopy has found application in a wide variety of fields in solid state physics, chemistry, and nuclear physics. Usually radioactive sources populating appropriate low-energy levels are used in this work, but there are a few cases in which low-lying levels suitable for Mössbauer studies can only be populated via an (n, γ) reaction. An example is the 29.4-keV level in ^{40}K. The γ transition to this level imparts to the ^{40}K nuclei recoil energies up to 800 eV, which is sufficient to displace the atoms from their normal lattice sites. Nevertheless, Hafemeister and Brooks-Shera (1965) succeeded in obtaining a Mössbauer effect with this reaction. They used various capture γ-ray sources containing natural K, and a KCl absorber enriched in ^{40}K. They found a linewidth corresponding to a half-life of 4.3 ± 0.9 nsec, in good agreement with the directly measured value of $4.26\pm$ 0.08 nsec found by Boulter *et al.* (1969). This shows that the source line is not appreciably affected by any radiation damage occuring as a result of recoil during the (n, γ) process. However, in Mössbauer studies using a ^{119}Sn radioactive source Hannaford *et al.* (1965) reported the presence of a second line attributed to such radiation damage.

Additional Mössbauer (n, γ) experiments have been carried out by Tseng *et al.* (1968) on ^{40}K, by Fink and Kienle (1965) on ^{156}Gd and ^{158}Gd, by Gal *et al.* (1968) on ^{158}Gd, by Bauminger *et al.* (1968a) on ^{162}Dy, and by Bauminger *et al.* (1968b) on ^{178}Hf and ^{180}Hf.

II.2.2 Experimental

A typical Mössbauer (n, γ) experiment is that carried out by Tseng *et al.* (1968). The thermal neutron beam from the reactor core emerges through collimators in the reactor shielding wall and impinges on a ^{39}K target, producing 29.4-keV γ rays by the neutron-capture reaction. The γ rays are detected after passing through an absorber enriched in ^{40}K. Either the target or the absorber is oscillated in a conventional Mössbauer transmission experiment. The beam tube is fitted with a special tapered collimator consisting of alternate layers of lead and plastic. The background is reduced by insertion of a 1.5-mm thick lead sheet in the beam. The neutron flux in this experiment was $10^8 n$ cm^{-2}·sec^{-1}, which is at least ten times higher than reported in other experiments of this type. For measurements at liquid nitrogen temperature, a simple styrofoam box was used, the neutron beam entering and leaving through the walls. This offered the advantage of simplicity, but caused 10% higher background than with a thin metal cryostat.

II.2.3 Results and Discussion

(i) *Potassium-40*

The results obtained by Tseng *et al.* (1968) are evaluated for a wide variety of K compounds. The data obtained with KF, K, and KCl targets are in agreement with the earlier work of Hafemeister and Brooks-Shera (1965) but have considerably improved accuracy. Inspection of these results shows that there is almost no observable isomer shift from one target to the next, and that the line width is limited to a narrow range from 2.55–3.3 mm/sec for all these materials.

The fact that all the compounds give a single unshifted line indicated (a) that $\langle \delta r^2 \rangle / \langle r^2 \rangle$, the fractional difference between the nuclear radius in the ground state and the first excited state, is small; and (b) that the electron configuration of the K atom in the various compounds retains its K^+ ion structure and hence does not produce large electric field gradients or appreciable magnetic fields at the nucleus. Even for the case of the KCl source, where a strong electric field gradient could be expected, no quadrupole splitting was observed and an upper estimate of $e^2qQ<12$ MHz was given for this splitting.

The observed isomer shift of ^{40}K between K metal and KF was used to evaluate $\langle \delta r^2 \rangle / \langle r^2 \rangle$. After correcting for the thermal shift due to the difference between the Debye temperatures of K and KF, an upper limit of $\langle \delta r^2 \rangle / \langle r^2 \rangle < 5 \times 10^{-4}$ was found, in agreement with the prediction of Goldstein and Talmi (1956).

(ii) *Rare Earth Elements*

In ^{156}Gd and ^{158}Gd, measured by Fink and Kienle (1965), and in ^{162}Dy measured by Bauminger *et al.* (1968a), the observed linewidth was much broader than the natural linewidth (by a factor of 3 in the case of Gd and 6.5 in the case of Dy).

For Gd, sources and absorbers of metal and oxide were used in all possible combinations. With Gd_2O_3 as a source and Gd metal as absorber, the transmission line was about 10% broader than in the "mirror" experiment which used a metal source and an oxide

absorber. In addition, it was found that for the oxide source the recoilless absorption probability was only 0.6 of that found for the metal source. From the very small measured isomer shifts, Fink and Kienle deduced the values

$$\langle \delta r^2 \rangle / \langle r^2 \rangle = 5.7 \times 10^{-5} \quad \text{for } ^{156}\text{Gd}$$
$$= 2.9 \times 10^{-5} \quad \text{for } ^{158}\text{Gd}$$

while Gal *et al.* (1968) obtained a value of 6.4×10^{-5} for ^{158}Gd. These values are an order-of-magnitude less than those predicted by theory.

In order to obtain a relatively narrow unsplit line for Dy, Bauminger *et al.* (1968a) used a ^{162}DyGa garnet as absorber. They studied the 80.7-keV 2^+ level of $^{162}Dy_2O_3$ source. As the effective magnetic and the electric field gradients in Dy_2O_3 had been previously determined, this experiment could be used to deduce the g factor of the first excited 2^+ rotational state of ^{162}Dy. A value of $g = 0.38 \pm 0.02$ was found, in agreement with the predictions of Nathan and Nilson (1965).

II.2.4 Conclusions

Some interesting nuclear data for the rare-earth and ^{40}K nuclei have been obtained using the (n, γ) Mössbauer technique. However, owing to the complexity of these experiments there is clearly no advantage in using this technique if suitable radioactive Mössbauer sources are available. In the case of ^{40}K no such alternative source exists and this atom can only be studied by the (n, γ) Mössbauer method. Unfortunately, since the K atom seems to retain its strong K^+ ion structure in all its compounds, and the ratio $\langle \delta r^2 \rangle / \langle r^2 \rangle$ is extremely small, little useful chemical or magnetic information can be obtained from these experiments.

III. RESONANCE FLUORESCENCE OF INDIVIDUAL HIGHLY EXCITED NUCLEAR LEVELS

III.1 Introduction

Many investigations have been carried out on photonuclear reactions below 40 MeV. The cross sections for the (γ, n) reaction in this energy region is characterized by the giant resonance behavior. Goldhaber and Teller (1948) explained this behavior in terms of a dipole oscillation of the proton fluid of the nucleus against the neutron fluid by using a collective hydrodynamical model. The theory of the giant resonance absorption process has been developed by Wilkinson (1956) using the independent particle shell model. This model and the derived statistical model of photonuclear reactions can in fact be shown (Brink, 1957) to be equivalent to the Goldhaber and Teller picture.

Nuclear elastic scattering of γ rays offers an alternative method of studying this basic reaction. Early studies were carried out by Gaerttner and Yeater (1949) and Dressel *et al.* (1950) who used the wide spectrum of betatron produced bremsstrahlung, and by Stearns (1952), who made use of the (p, γ) reaction. The results showed that the cross section for elastic scattering was of the order of a few millibarns (in the region of the giant resonance).

Fuller and Hayward (1956) measured elastic scattering of photons in the energy range 4–40 MeV over a wide range of nuclei, using a NaI(Tl) scintillation spectrometer biased on the upper edge of the bremsstrahlung spectrum. This gave an energy resolution of a few hundred keV. They found that the energy dependence of the scattering cross section contained two maxima, one corresponding to the giant dipole resonance in the energy region of 15–20 MeV, and the second in the vicinity of, or just below, the (γ, n) threshold.

The giant resonance peak energy and maximum cross sections were found to follow a smooth A dependence consistent with the statistical theory. The corresponding parameters for the lower energy peaks were not consistent with this theory. Furthermore, the derived average level widths and level spacings were considerably larger than those found in studies of radiative decay of neutron capture states.

Reibel and Mann (1960) carried out photon scattering experiments at about 7 MeV using a (p, γ) source, with an energy resolution of about 100 keV. Their results showed values of the elastic cross section consistently below the earlier results of Fuller and Hayward by a factor of 2 or more. This may be due to the considerable difference in resolution between the two experiments.

Badalyan and Baz (1961) explained this anomalous behavior of the photonuclear reactions below 10 MeV by assuming that a few single particle (threshold) states contribute significantly to the photonuclear cross section in this energy region. These states were predicted by Baz (1959) assuming surface phenomena of nuclei in energy regions where statistical behavior is not yet fully developed.

However, Axel (1962) showed that the assumption of a Porter Thomas distribution in the ground state radiation widths at 7 MeV gave better agreement between the results of Fuller and Hayward, and Reibel and Mann, and those obtained from neutron-capture data. Furthermore, using this assumption Axel showed that the photonuclear experiments in the region of 7 MeV were in agreement with a generalized extrapolation of the giant dipole resonance. He concluded that the remaining discrepancies with the statistical theory did not justify the assumption of threshold states.

The above-mentioned experiments do not permit studies of individual levels, but only of the average properties over many levels, owing to the poor resolu-

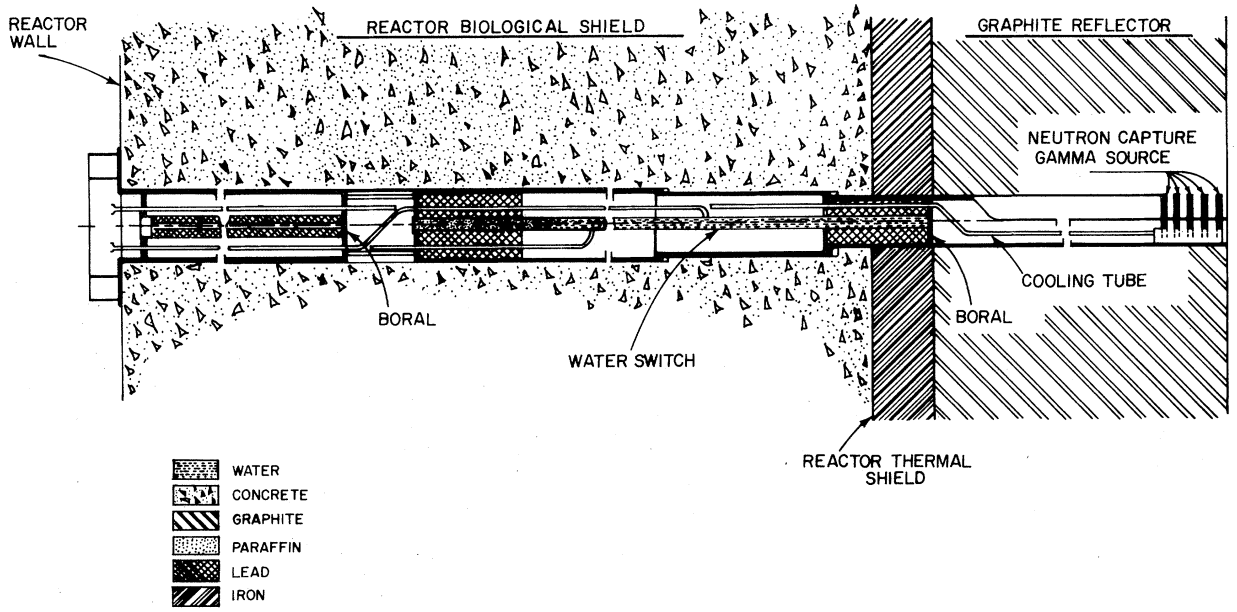

FIG. 2. Horizontal section of a tangential beam tube used in a resonance fluorescence experiment at the IRR 2 reactor. [Schlesinger *et al.* (1969)].

tion of the photon sources. In the unbound energy region, the methods of neutron resonance, and more recent threshold photoneutron studies, have revealed information on individual levels in a range up to several hundred keV above the neutron threshold (Bowman *et al.*, 1967, Baglan *et al.*, 1971). Recent studies of the fluctuations of the partial radiation widths, and of the correlation between neutron widths and the partial radiation widths, have shown discrepancies with the statistical behavior expected from the simple compound nucleus picture (see for example Lone *et al.*, 1968, Mughabghab *et al.*, 1970). Lane (1970) has explained these discrepancies in terms of single-particle-type doorway states. These states were also discussed by Bartholemew (1969) and Rimawi *et al.* (1969) to explain the anomalous shapes found in the spectra of neutron-capture γ rays.

The discovery that thermal neutron-capture γ rays can excite individual energy levels was made independently by Ben-David and Huebschmann (1962), Fleischmann (1963), and Young and Donahue (1963). Resonance fluorescence of this kind requires a chance overlap between the energy of the capture γ line and that of the resonant level. This permits studying only a random sample of levels, but over a fairly wide energy range between 6 and 9 MeV. Although this technique is useful mainly for bound levels, where there is no competition from particle emission, in favorable cases unbound levels can be excited. In addition, there may be transitions from the resonant level to low-lying levels which are not always reached through other reactions. The methods used to study the transitions from the resonant state are very similar to those used in capture γ spectroscopy. However, the two methods are in fact complimentary since the stable nuclei to which the γ resonant technique is applicable are not always accessible through the (n, γ) reaction.

Recently, many level scheme derivations have been reported using this (γ, γ') technique, including determination of the various level parameters. The accumulated data also permit statistical studies of the fluctuations in the partial level widths of transitions to the low-lying levels, and comparison with transitions from levels in the well known neutron resonance region.

The basic method described in this section relies on a random overlap between the resonance level and the discrete energy neutron-capture γ line. However, several techniques exist for varying the energy of the γ line, thus increasing the range of levels accessible to study. Two of these methods—mechanical variation of the energy, and the use of a capture γ-ray monochromator—will be described below.

Mechanical variation of the energy may be achieved by rotating the scattering target. With peripheral velocities of the order of 450 m/sec, the photon energy can be Doppler shifted by 12–15 eV with respect to the target nucleus. This small energy variation is sufficient to permit determination of the energy separation δ between the γ-ray line and the resonant level. Arad *et al.* (1964b) have studied the well-known 7.28-MeV resonance level in ^{208}Pb using velocities up to 150 m/sec and deduced the parameter δ. This energy varia-

tion may also permit analysis of complex spectra in which several elastic and inelastic components are present.

The resonance scattering process itself can be used to provide a high resolution variable energy source of γ rays [McIntyre and Randall (1965)]. By varying the angle of the elastically scattered γ ray beam between 0° and 180°, an energy variation of up to 1000 eV can be achieved with a resolution of a few eV. This technique has been used by McIntyre and Randall and by Kapadia *et al.* (1968) to study the level parameters of the 7.277-MeV resonance level in ^{208}Pb, and by Moreh and Ben Yaakov (1967) in a search for new resonance levels.

III.2 Experimental Facilities and Techniques

III.2.1 General Scattering Facilities

Facilities installed at various reactors have utilized either a thermal column access hole, or radial or tangential beam tubes. A thermal column facility provides a capture γ beam almost free of fast neutrons and core γ rays, but rather low thermal neutron fluxes have been reported ($\sim 10^{10} n$ cm^{-2} sec^{-1}). Both the radial and tangential beam tubes offer the advantage of high intensity capture γ sources, the thermal neutron fluxes available being of the order of $10^{13} n$ cm^{-2} sec^{-1} or higher at the source position.

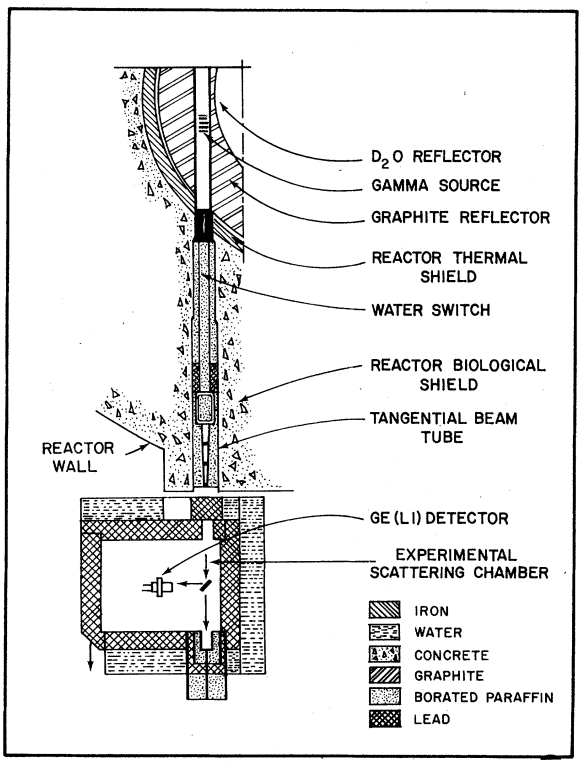

FIG. 3. Schematic representation of a scattering chamber used in resonance fluorescence experiments. [Moreh and Nof (1969)].

However, with a radial beam tube it is usually necessary to place bismuth or lead shielding in the beam to reduce the core γ rays, and there is high contamination from fast neutrons. The optimum arrangement is therefore a tangential beam facility, with the use of collimators to present "seeing" direct radiation from the core.

A typical arrangement is illustrated in Fig. 2. The γ source is attached to a special beam plug in an 11 in. tangential beam tube, permitting irradiation adjacent to the core at a flux of $2\times 10^{13} n$ cm^{-2}·sec^{-1}. The γ source is composed of several separated discs in order to reduce the neutron flux depression. The main plug includes lead collimators and borated aluminum and paraffin shielding to reduce neutron contamination at the exit of the beam. A 150-cm section of the beam aperture is used as a water switch to cut off the major part of the radiation when changes must be made in the outside scattering chamber.

A general view of an experimental scattering chamber is shown in Fig. 3. The chamber has lead, water, and paraffin shielding to reduce γ and neutron background. In order to reduce the additional neutron background caused by the (γ, n) reaction on lead, the beam catcher is lined with materials having relatively high (γ, n) threshold energies, e.g. iron.

III.2.2 Detectors and Beam Monitors

Large volume NaI(Tl) detectors have been used for absolute and relative γ-intensity measurements. However, Ge(Li) detectors (30 cm^3 or larger) are essential for accurate energy determination of the scattered γ rays, and for studying the inelastic transitions from the resonance levels.

For precise intensity measurements, such as are required in self-absorption and angular distribution experiments, it is necessary to monitor the incident capture γ-ray flux. This cannot be done accurately by monitoring the over-all reactor power, since relative neutron flux changes of several percent occur during long periods of reactor operation. Huebschmann and Alterowitz (1963) have monitored the neutron flux at the capture γ source position using a Li-coated surface barrier silicon detector. Another method described by Shikazono and Kawarasaki (1968) involves counting the low energy γ rays produced in a thin target placed in the γ-ray beam. This method has the drawback that the monitored beam includes a component arising from radioactive decay of the (n, γ) source and from scattered fission γ rays from the reactor core. During changes of reactor power the time variation of this additional low-energy component can be quite different from that of the capture γ-ray beam and cause errors in the measurement. Cesareo *et al.* (1970) and Szichman *et al.* (1970) have monitored a high energy γ ray in the direct γ-ray beam using a NaI or Ge(Li) detector to an accuracy of 1%.

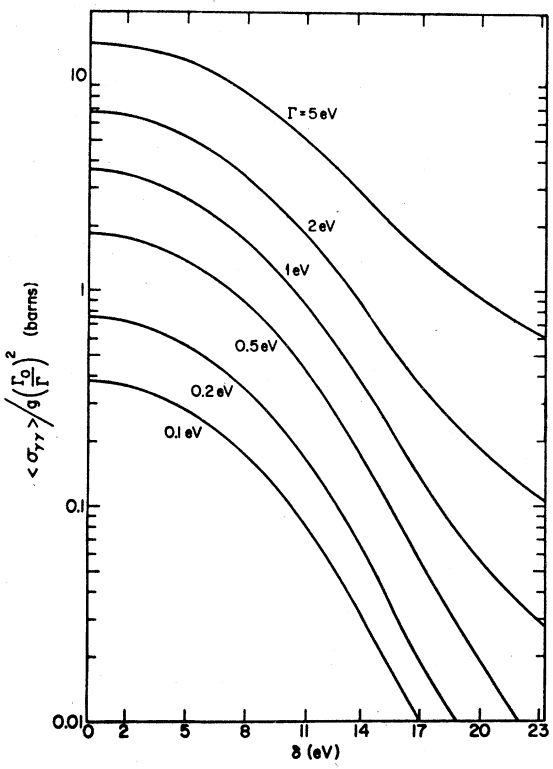

FIG. 4. Dependence of $\langle\sigma_{\gamma\gamma}\rangle/g(\Gamma_0/\Gamma)^2$ on the separation energy δ, for different values of Γ. The energy of the γ beam is taken as 8 MeV and the source Doppler width 7.8 eV.

III.2.3 Background Reduction

The nuclear resonant scattering process competes with other processes, including pair production, and Compton, Rayleigh, nuclear Thompson, and Delbrück scattering. While the latter three processes have negligible cross sections (except at very forward angles), the first two give rise to a high background. However, at angles greater than 90° to the incident beam, the energies of the scattered γ rays are predominantly below 0.5 MeV. Hence measurements are usually taken in the backward hemisphere, and the "pile-up" due to the high intensity of low-energy γ rays is reduced by using suitable shielding in front of the detector. When high Z targets are used the electrons produced by the γ-ray beam in the target generate a background of high-energy bremsstrahlung.

III.3 Derivation of Level Parameters from Various Types of Experiment

III.3.1 Absolute Beam Intensity Measurements

The intensity of a resonantly scattered γ-ray line depends on the total level width Γ of the resonance level, on the partial ground state transition width Γ_0, and on the energy separation δ, between the peaks of the resonance level and the incident γ ray.

Arad *et al.* (1964a) have expressed the measured intensity in terms of the level parameters for a plane target geometry. They show that the line shape of the incident capture γ line can be accurately expressed by the pure Doppler form

$$F(E)\,dE=C\Delta_s^{-1}\exp-[(E-E_r+\delta)^2/\Delta_s^2]\,dE, \quad (3.1)$$

where Δ_s is the source Doppler width defined by Eq. (2.6), E_r is the resonance level energy, and δ is the energy separation between the source line and the resonance level.

The incident beam is attenuated in the target by nonresonant and by nuclear absorption. However, for scattering angles greater than 15°, the recoil energy loss is sufficient to remove the scattered photons from resonance. Since measurements are usually taken at scattering angles larger than 15°, only nonresonant absorption of the scattered beam is taken into account. The special case of small-angle resonant scattering is discussed separately in Sec. III.3.5.

The number of photons in the energy interval $[E-E+dE]$, resonantly scattered by a plane target, and reaching the detector at angle θ to the incident beam, is given by

$$S(E,\theta)\,dE=DF(E)\sigma_{\gamma\gamma}(E)f(\theta)\,dE$$
$$\times\{1-\exp-[A\sigma_n(E)+B\sigma_e]\}/[A\sigma_n(E)+B\sigma_e], \quad (3.2)$$

where $\sigma_{\gamma\gamma}(E)$ is the elastic cross section defined in Eq. (2.3), $f(\theta)$ is the angular distribution function for the elastic transition, $\sigma_n(E)[=\Gamma/\Gamma_0\cdot\sigma_{\gamma\gamma}(E)]$ is the total nuclear absorption cross section, and σ_e the total nonresonant absorption cross section (essentially constant over the resonance energy interval). The constants A, B, and D include geometrical parameters, and the atomic and isotopic properties of the target.

The count rate $C(\theta)$ recorded by the detector is obtained by integrating Eq. (3.2) over the total energy region, and is given by

$$C(\theta)=\epsilon\int_0^\infty S(E,\theta)\,dE, \quad (3.3)$$

where ϵ is the relevant detector efficiency.

In order to normalize the incident beam intensity it is usual to place the detector in the incident beam (using an appropriate absorber or a reduction in reactor power). The corresponding count rate in the incident beam is then given by

$$C_0=\epsilon_0\int_0^\infty F(E)\,dE, \quad (3.4)$$

where ϵ_0 is the detector efficiency for the incident beam geometry.

The solution of the integral Eqs. (3.1)–(3.4) gives

(a)

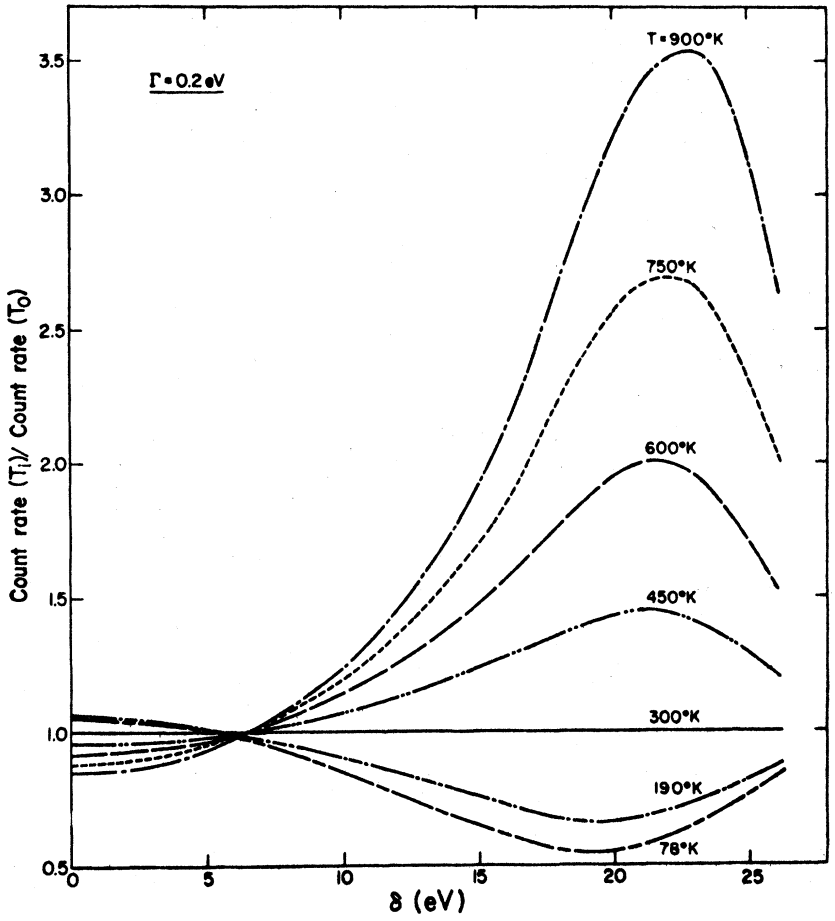

(b)

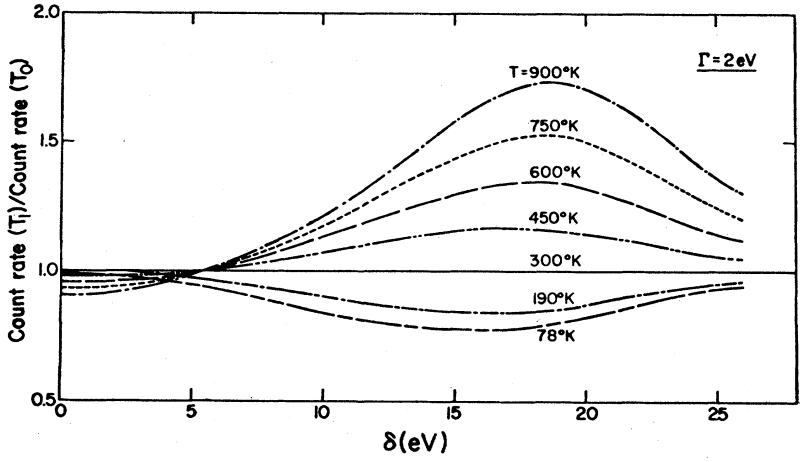

FIG. 5. Calculated intensities of resonantly scattered γ rays as a function of the energy separation δ between the incident beam and the resonant level, with the absolute temperature as a parameter. The intensities are normalized to the room temperature value. Calculations were performed for the following parameters: $E=9$ MeV, $A=200$, $g=1$, $\Gamma_0=\Gamma$, $\sigma_e=16$ b, scatterer thickness is 16 g/cm^2. (a) $\Gamma=0.2$ eV, (b) $\Gamma=2$ eV.

an implicit relationship between the level parameters Γ_0, Γ, g, and δ in terms of the experimental quantities $C(\theta)$ and C_0. In order to see the physical relationship between the level parameters, it is instructive to consider an approximation to Eq. (3.2) for the case where the nuclear absorption is much less than the total nonresonant absorption. In this case, the terms containing $\sigma_n(E)$ in the exponential term and in the denominator of Eq. (3.2) can be neglected, and the solution of Eqs. (3.2)–(3.4) can be written as

$$C(\theta)/C_0 = Kf(\theta)\langle\sigma_{\gamma\gamma}\rangle, \tag{3.5}$$

where K is a constant including the geometrical factors, and $\langle\sigma_{\gamma\gamma}\rangle$ is the effective elastic scattering cross section, averaged over the incident capture γ spectrum

$$\langle\sigma_{\gamma\gamma}\rangle = \int F(E)\sigma_{\gamma\gamma}(E)\,dE / \int F(E)\,dE. \tag{3.6}$$

The measurement of the intensities of the scattered and incident beams permits an experimental determination of the average cross section $\langle\sigma_{\gamma\gamma}\rangle$. This can then be used to derive an implicit relationship between the level parameters by using Eqs. (2.3), (3.1), and (3.6). Figure 4 shows the dependence of the ratio $\langle\sigma_{\gamma\gamma}\rangle/[g(\Gamma_0/\Gamma)^2]$ on Γ and δ, over the range of values of physical interest. The solution of the exact integral equations (3.1)–(3.4) gives a similar relationship between the level parameters. The value of g can be found from angular distribution measurements of the scattered beam, discussed below, while the branching ratio Γ_0/Γ can often be determined by analysis of the spectrum of the scattered γ rays. There then remains an implicit relationship between Γ and δ. To determine Γ and δ separately we require an additional measurement, giving a different relationship between these parameters. Some possible types of measurement are discussed below.

III.3.2 Variation of Scattered γ-Ray Intensity with Target Temperature

An independent relationship between the level parameters may be derived from the measurement of the intensity of the scattered γ rays with varying target temperature.

Inspection of Eqs. (2.3) and (3.2) shows that the temperature dependence of the scattered γ intensity comes from the Doppler broadening term $\Delta = E_R(2kT'/M_0c^2)^{1/2}$, in the expression for the cross section $\sigma_{\gamma\gamma}(E)$. The experimental ratio $C(\theta, T_i)/C(\theta, T_0)$ of the scattered intensities at target temperatures T_i and T_0—both measured at the same angle θ—thus gives an additional relationship between the parameters δ and Γ. Figure 5 shows typical values of this ratio as a function of δ for different values of T and Γ. While for a given temperature the ratio is in general a double-valued function of δ, a unique result can be found by carrying out measurements at several temperatures. Usually the larger value of δ can be ruled out from intensity considerations. This method of target temperature variation is sensitive to the parameter δ, and relatively insensitive to Γ. This can be seen if we consider the pure Doppler approximation which holds for $\Gamma \ll \Delta_s$ and $\delta < (\Delta_s + \Delta)$. Under this approximation, the ratio $C(\theta, T_i)/C(\theta, T_0)$ can be written as

$$\frac{C(\theta, T_i)}{C(\theta, T_0)} = \left(\frac{\Delta_s^2+\Delta_0^2}{\Delta_s^2+\Delta_i^2}\right)^{1/2} \times \exp\{-[(\Delta_s^2+\Delta_0^2)^{-1} - (\Delta_s^2+\Delta_i^2)^{-1}]\delta^2\}. \tag{3.7}$$

Since Eq. (3.7) has no dependence on Γ it can be used to derive a first approximation to δ.

It is usually necessary to solve the exact integral Eq. (3.3) to give the desired relationship between δ and Γ, of Fig. 5. The biggest uncertainty in these calculations comes from the evaluation of the Doppler widths, since these require a knowledge of the effective temperatures. These have been shown by Lamb (1939) to be dependent on the lattice Debye temperature. However only a few measurements have been reported of Debye temperatures for the wide variety of source and target nuclei over the relevant temperature range.

III.3.3 Self-Absorption Experiment

A self-absorption measurement is possible if the total nuclear absorption cross section is not much smaller than the nonresonant absorption cross section. This type of experiment is shown schematically in Fig. 6. A resonant absorber of the same material as the scattering target is placed in the incident γ beam between the source and the target (position A). If satisfactory geometry is used, γ rays undergoing resonant or nonresonant absorption in the resonant absorber are removed from the beam. The intensity $I(D)$ of γ rays elastically scattered from the target and reaching the detector with a resonant absorber of thickness D is then given by

$$I(D) = \int_0^\infty \exp -\{[\alpha\sigma_n(E)+\sigma_e]ND\}S(E,\theta)\,dE, \tag{3.8}$$

where α is the isotopic fraction of the isotope with the resonance level and the other parameters are as defined above.

In order to subtract the effects of nonresonant attenuation, the same absorber is now placed between the scattering target and the detector (position B). At large scattering angles, the recoil energy loss is sufficient to remove the scattered beam from resonance. The intensity $I'(D)$ for position B is given by

$$I'(D) = \int_0^\infty \exp[-\sigma_e ND]S(E,\theta)\,dE, \tag{3.9}$$

and the self-absorption ratio R, defined by

$$R(D) = [I'(D) - I(D)]/I'(D) \tag{3.10}$$

can be shown to be given by

$$R(D)=\left\{\int_0^\infty S(E,\theta)[1-\exp-\alpha\sigma_n(E)ND]\,dE\right\}\Big/ \int_0^\infty S(E,\theta)\,dE. \quad (3.11)$$

This ratio can be measured as a function of D and used to determine the various level parameters. Figure 7 shows the expected values of R for various values of Γ_0/Γ, Γ_0, and δ, for a typical experimental geometry.

The self-absorption measurement gives an additional independent relationship between the level parameters. However, owing to the experimental errors in the measurement of R, this method is only practical for relatively large values of Γ_0.

III.3.4 Mechanical Energy Variation of the Incident Neutron-Capture γ Rays

Direct variation of the energy separation δ between the capture γ-ray line and the resonant level permits an accurate measurement of the original value of δ.

Mechanical rotation of the scattering target is the most convenient technique for varying the capture γ-ray energy. With this method scatterer velocities of up to 450 m/sec may be used to produce positive or negative energy shifts in the range 12–15 eV for 6–9 MeV capture γ rays. An alternate technique is to use a capture γ ray source irradiated with monoenergetic epithermal neutrons. Theoretically this method has an unlimited range for positive energy shifts [variations of even keV have been suggested by Axel (1961)], although it permits negative energy shifts of only a few eV. However, the available intensities of the γ rays available in this latter method are several orders of magnitude lower than those attainable with the rotating target method, which seems the only one of practical interest at present.

A convenient type of rotating target is a ring target mounted on a dynamically balanced high-speed rotor. The energy of the γ rays relative to the target is shifted by an amount $E(v/c)$, where v is the component of the target linear velocity in the beam direction. The variation of the intensity of the scattered beam with target velocity can be shown to be relatively insensitive to Γ, but sensitive to values of δ, and hence the latter can be accurately determined in this type of

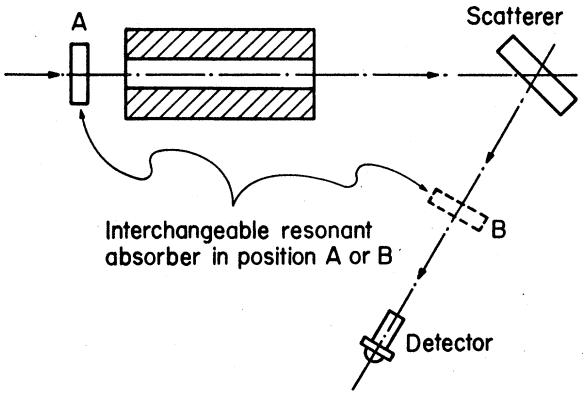

FIG. 6. Schematic arrangement of the self-absorption experiment.

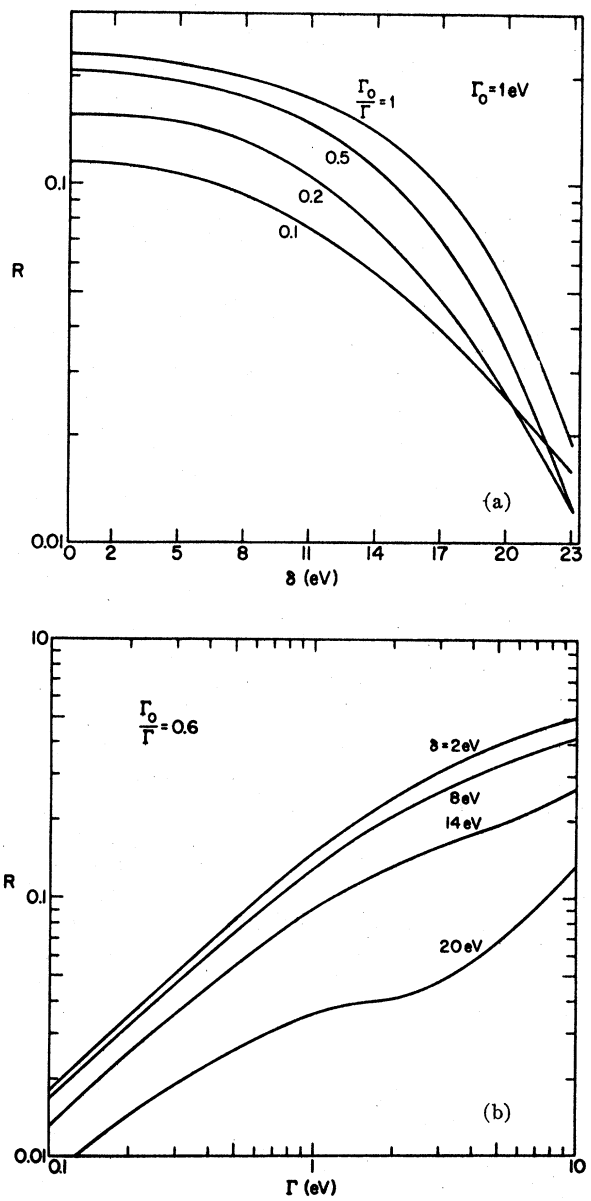

FIG. 7. (a) The self-absorption ratio R: as a function of the peak separation energy δ, for the various values of the branching ratio Γ_0/Γ; the ground state transition width $\Gamma_0=1$ eV. (b) The self-absorption ratio R as a function of the total level width, for various values of the separation energy δ; the branching ratio $=0.6$. The calculations were performed for the following parameters: $E=8$ MeV, $A=200$, $g=1$, $\sigma_e=16$ b, scatterer and absorber thickness 16 g/cm^2.

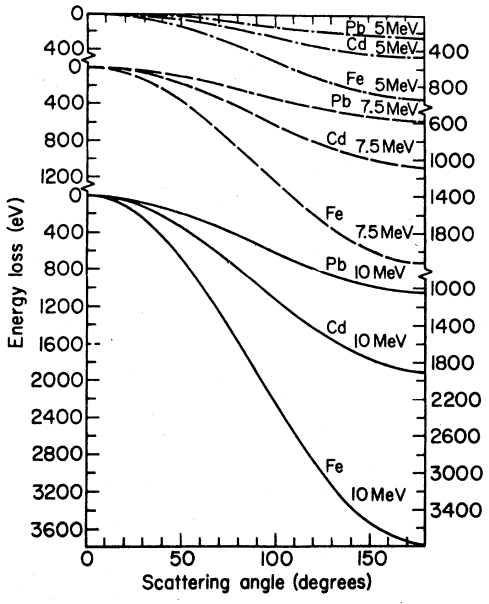

FIG. 8. Energy variation of resonantly scattered photons as a function of scattering angle for various photon energies and mass numbers.

measurement. The use of a rotor target also permits measurements at a reduced δ, resulting in increased intensities of the scattered γ rays and hence greater accuracy in measurement. In cases where more than one resonant level is excited, variation of the incident γ energy may be used to disentangle the different inelastic components and assign them to the relevant resonant levels.

III.3.5 Energy Variation of Resonantly Scattered γ Rays with Variation of the Scattering Angle

The resonance fluorescence process following γ absorption by nuclei can be regarded as a Compton-type process in which the heavy free-recoiling nucleus plays the role of the lighter electron. If the lifetime of the resonant level is shorter than the mean collision time of the recoiling nucleus, then the energy $E'(\theta)$ of the elastically scattered γ ray is given by

$$E'(\theta)=E[1+(E/\mu)(1-\cos\theta)]^{-1}, \qquad (3.12)$$

where E is the energy of the incident γ ray, μ the rest mass of the scattering nucleus in energy units, and θ the angle between the emitted γ ray and the incident beam. Thus the energy of the emergent γ ray varies with the scattering angle, and can be used as a variable energy γ ray beam, with very precise energy over a limited range of energies.

The range of the energy variation is illustrated in Fig. 8 for typical capture γ energies and scattering nuclei. Over a 180° angular variation this energy range extends from several hundred to a few thousand eV.

The energy dispersion as a function of angle is given by

$$dE=(E^2/\mu)\sin\theta\, d\theta. \qquad (3.13)$$

This energy dispersion equals 5 $\sin\theta$ eV per degree angular resolution for the 7.277-MeV γ ray elastically scattered from the resonant level in ^{208}Pb. This is of the same order as the Doppler width of the source line, which limits the resolution attainable with this resonance line to about 4 eV. The excellent energy resolution available with this technique, of the order of 1 part in 10^6, permits its application as a high-energy γ-ray monochromator.

The variable energy γ-ray beam can be used for total cross section measurements to study nuclear levels in the available energy range, using any suitable target. At small scattering angles, where the energy of the scattered beam is close to that of the original resonance level, this technique may be used to study the level parameters of the primary resonance generating the variable energy beam. In this case we use a second target having similar composition as the primary target.

The experimental arrangement used in these measurements is represented schematically in Fig. 9. The incident capture γ-ray beam strikes the primary resonance scatterer S_1, and the scattered beam is suitably collimated and allowed to strike a second target S_2 at variable scattering angle θ. The latter target may serve either as an absorber (detector position D_1) or a scatterer (detector position D_2). For cross section measurements aimed at scanning for new nuclear levels in the secondary targets, a wide energy range and hence large angular variations are required. The absorption configuration in Fig. 9 is particularly suitable for these experiments. Where the nuclear parameters of the primary resonance itself are studied, measurements are needed at forward angles to permit small energy variations within the energy interval of this resonance. Studies of this type have been carried out by McIntyre and Randall (1965) using the absorption configuration. At extreme forward angles, this configuration is impractical because of

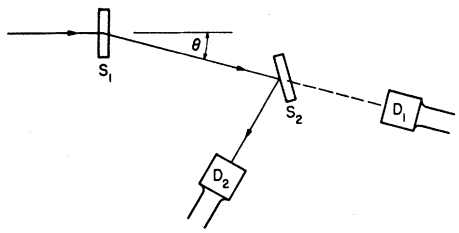

FIG. 9. Schematic representation of the γ-ray monochromator; D_1, detector in absorption geometry, D_2, detector in scattering geometry.

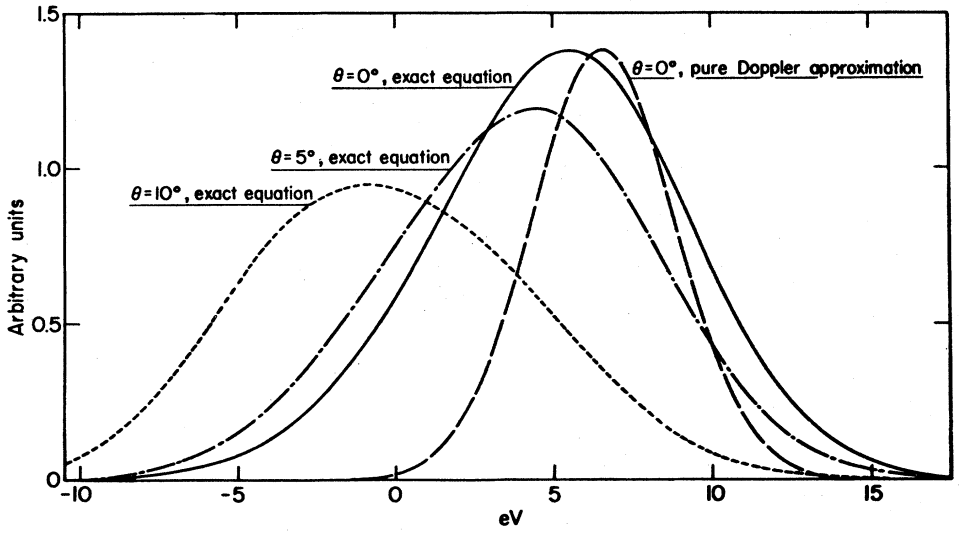

FIG. 10. Calculated line shape of 7.277-MeV γ rays resonantly scattered from a 3-cm Pb target: $z=0°$, pure Doppler approximation; $\theta=0°$, 5°, and 10°, exact equation.

interference from the forward Compton scattered photons. The scattering configuration, on the other hand, is not susceptible to such interference and has been used successfully by Kapadia *et al.* (1968) at forward angles down to 5°.

Analysis of the experimental data requires a knowledge of the energy profile of the γ beam scattered from the primary target. For the experiments carried out at small forward angles, the difference in energy between the resonantly scattered and incident beams is only a few electron volts. Hence in correcting for the absorption of the scattered beam in the primary target it is necessary to take into account resonant nuclear absorption in addition to nonresonant absorption. At scattering angles greater than 20°, as used in the total cross section work, the scattered beam may be considered to undergo only nonresonant absorption as it emerges from the target.

Kapadia *et al.* (1968) have evaluated the line shape of the scattered γ beam in this type of experiment, taking into account target absorption.

It may be noted that even at 0° scattering angle, the peak of the scattered beam is displaced from the incident capture γ peak due to the effect of level overlap. This can be seen if we consider the Doppler approximation for the scattered beam, valid for $\Gamma<\Delta$, $\delta<2\Delta$. In this approximation the spectra of the scattered beam at 0° scattering angle is given by

$$S(E,0)\,dE=K\exp-(\delta^2/\Delta_0^2)\times\exp-[(E-E_r-C)/\Delta_1]^2\,dE, \quad (3.14)$$

where the separation energy between the two maxima is δ, $\Delta_0=(\Delta^2+\Delta_s^2)^{1/2}$, $\Delta_1=\Delta_s\Delta/\Delta_0$, $C=\delta(\Delta/\Delta_0)^2$, Δ_s and Δ being the source and target Doppler widths, and E_r is the peak energy of the resonance level. The first exponential term expresses the reduction in intensity as the overlap between the incident beam and the resonance level decreases with increasing δ. Since C is always less than δ, the maximum in the spectrum given by Eq. (3.14) lies between that of the incident beam and the resonance energy E_r. In addition, the definition of Δ_1 shows that the width of the scattered line is less than either the incident line or the resonant level. Figure 10 shows the line shape of the 7.277 MeV line scattered from the resonance level in ^{208}Pb according to Eq. (3.14), compared with the result obtained from integration over the exact level shape.

III.3.6 Angular Distribution and Polarization Measurements

The angular correlation between two γ rays emitted in cascade depends on the transition multipolarities and on the level spins involved. In general the correlation is given by an expansion in even Legendre polynomials of the form:

$$W(\theta)=A_0+A_2P_2(\cos\theta)+\cdots A_{\nu\max}P_{\nu\max}(\cos\theta). \quad (3.15a)$$

The properties of this correlation have been discussed extensively following the study by Biedenharn and Rose (1953). The number of terms in this expression, and the values of the parameters A_i, depend on the properties of the transitions. The A_4 term is usually the highest found in practice.

In the present case, the first transition is the incident capture γ line exciting the resonant level, and its direction is therefore that of the incident beam. The angular correlation with respect to the exciting transition is thus

TABLE II. A summary of highly excited levels and their parameters as derived by various authors.

Scatterer (source)	Level energy (keV)	Experimental resonance level parameters				Level scheme deduced?	Reference	Remarks
		Γ_0 (eV)	Γ (eV)	Γ_0/Γ	J^π			
^{209}Bi(Se)	7416	0.14±0.09		0.6±0.2			Ramchandran and McIntyre (1969)	
^{208}Pb(Fe)	7277	0.78±0.03		1	1^+			a
^{205}Tl(Fe)	7646	~1.0		0.85±0.17	1/2		Ramchandran and McIntyre (1969)	
^{205}Tl(Fe)	7646		0.98±0.09	0.58±0.05	$1/2^{(-)}$	Yes	Moreh *et al.* (1970b)	
^{205}Tl(Fe)	7646			0.62±0.09	1/2	Yes	Cesareo *et al.* (1970)	
^{203}Tl(Ti)	6418		0.32±0.06	0.26	1/2	Yes	Moreh *et al.* (1970a)	
^{144}Sm(Ni)	8997	0.063±0.013	0.27±0.08	0.23±0.05	1		Arad *et al.* (1972)	
^{141}Pr(Cr)	8883			0.55±0.08	(5/2, 7/2)		Pavel *et al.* (1971)	
^{141}Pr(Fe)	7632		0.072±0.024	0.46±0.04	$5/2^+$	Yes	Moreh *et al.* (1970b)	
^{141}Pr(Cu)	7256				5/2	Yes	Pavel *et al.* (1971)	
^{141}Pr(Se)	7188				$5/2^-$	Yes	Pavel *et al.* (1971)	
^{141}Pr(Cl)	6115	0.133±0.020		0.43			Fleischmann and Stanek (1963b)	b
^{141}Pr(Cl)	6115		0.052±0.010	0.56±0.01	$7/2^{(-)}$	Yes	Pavel *et al.* (1971)	
^{141}Pr(Co)	6111			0.48±0.11	(5/2, 7/2)		Pavel *et al.* (1971)	
^{139}La(Cl)	8582						Szichman *et al.* (1970)	
^{139}La(Ni)	8527						Szichman *et al.* (1970)	
^{139}La(Cu)	7637						Szichman *et al.* (1970)	
^{139}La(Fe)	7632					Yes	Moreh and Nof (1970)	
^{139}La(Fe)	7279					Yes	Moreh and Nof (1970)	
^{139}La(Ti)	6760		0.060±0.030	0.15±0.02	(7/2)	Yes	Szichman *et al.* (1970)	
^{139}La(Ti)	6760					Yes	Moreh and Nof (1970)	
^{139}La(Ti)	6418		0.045±0.009	<0.86±0.01	$9/2^{(-)}$	Yes	Szichman *et al.* (1970)	
^{139}La(Ti)	6418		0.081±0.010	0.78	$9/2^-$	Yes	Moreh and Nof (1970)	
^{139}La(Cl)	6115		0.079±0.017	<0.43±0.01	$9/2^{(-)}$	Yes	Szichman *et al.* (1970)	c
^{139}La(Fe)	6018		0.05±0.01	0.50±0.04	$7/2^-$	Yes	Moreh and Nof (1970)	
^{130}Te(Ni)	7538		0.24±0.06	0.24±0.015	1	Yes	Schlesinger *et al.* (1969)	
^{120}Sn(Ni)	7696	0.07±0.02	0.12±0.03	0.58±0.01	$1^{(-)}$		Schlesinger *et al.* (1970)	
^{112}Cd(Fe)	7632	0.24±0.02		0.11±0.06	1		Giannini *et al.* (1964)	d
^{112}Cd(Fe)	7632	0.24±0.06	1.9±0.6		1		Giannini *et al.* (1965)	d
^{112}Cd(Fe)	7632	$0.6^{+0.2}_{-0.1}$		0.48±0.06	1	Yes	Min (1966)	
^{112}Cd(Fe)	7632		0.086±0.015	0.55±0.04	1^-	Yes	Moreh *et al.* (1970b)	
^{112}Cd(Fe)	7632			0.54±0.04	1^+	Yes	Cesareo *et al.* (1970)	
^{109}Ag(Fe)	7632		0.002±0.001	0.70±0.06	3/2		Moreh *et al.* (1970b)	

TABLE II (*Continued*)

Scatterer (source)	Level energy (keV)	Experimental resonance level parameters				Level scheme deduced?	Reference	Remarks
		Γ_0 (eV)	Γ (eV)	Γ_0/Γ	J^π			
^{90}Zr(Se)	8496	1.68±0.02		0.8±0.2	1		Ramchandran and McIntyre (1969)	e
^{86}Sr(Ni)	7820	0.030±0.015	0.10±0.05	0.30±0.01	$1^{(-)}$		Schlesinger *et al.* (1970)	
^{80}Se(Ni)	7820	0.030±0.007	0.09±0.02	0.33±0.11	$1^{(-)}$		Schlesinger *et al.* (1970)	
^{75}As(Fe)	7646	0.041±0.011	0.36±0.10	0.11±0.01	1/2		Moreh *et al.* (1970b)	
^{74}Ge(Fe)	6018	0.0300.007	0.09±0.02	0.19±0.02	1^-		Moreh *et al.* (1970b)	
^{66}Zn(Ni)	7696	0.10±0.02	0.21±0.04	0.48±0.01	$1^{(-)}$		Schlesinger *et al.* (1970)	
^{66}Zn(Pb)	7368	0.22±0.02		0.71	1	Yes	Shikazono and Kawarasaki (1969)	
^{65}Cu(Cr)	8488				$5/2^-$	Yes	Cesareo *et al.* (1969)	f
^{65}Cu(Cr)	7929				5/2(3/2)	Yes	Cesareo *et al.* (1969)	
^{62}Ni(Fe)	7646	$0.077^{+0.016}_{-0.012}$			1		Arad *et al.* (1964a)	g
^{62}Ni(Fe)	7646	0.15±0.02		0.71±0.07	1		Giannini *et al.* (1964)	
^{62}Ni(Fe)	7646	0.63±0.17	3.0±1.5		1		Giannini *et al.* (1965)	
^{62}Ni(Fe)	7646	0.074±0.020		0.69±0.08	1		Estes and Min (1967)	
^{62}Ni(Fe)	7646		0.48±0.05	0.64±0.05	1^-	Yes	Moreh *et al.* (1970b)	
^{50}Cr(Fe)	8888		0.75±0.20	0.90±0.07	1		Moreh *et al.* (1970b)	

[a] See complete listing in Table III.
[b] The value of Γ_0 was corrected using the g factor found by Pavel *et al.* (1971).
[c] The value of Γ in Szichman *et al.* (1970) was misprinted. The correct value is given in the Table.
[d] Originally assigned to ^{114}Cd. Data corrected for the ^{112}Cd isotope.
[e] Original isotope identification based on consistency reasoning. Confirmed by present authors who have observed weak transitions to the first excited 1762-keV 0^+ level (3.4%±0.5%) and to the 2187 keV 2^+ level (2.6%±0.5%) with a branching ratio of $\Gamma_0/\Gamma=0.94$.
[f] Spin value corrected to $5/2^-$ (P. R. Oliva, private communication).
[g] Data corrected for the isotopic abundance and branching ratio taken from Moreh *et al.* (1970b).

found by measuring the angular distribution of the secondary transition with respect to the incident beam, using a single detector. This is considerably simpler than the case for correlations in radioactive transitions, or in (n, γ) transitions, which require a coincidence measurement with two detectors, and two dimensional analysis.

In all reported measurements of resonance fluorescence with capture γ rays, the exciting transition has been found to have a dominantly dipole character. For even–even nuclei this transition is pure dipole, and the angular correlation is in general described by two terms only

$$W(\theta)=1+A_2P_2(\cos\theta). \qquad (3.15b)$$

Hence in this case measurements at two or three angles are sufficient to determine the parameter A_2. For odd–even nuclei, the primary transition may contain a dipole–quadrupole mixture, and an A_4 term in the angular distribution cannot be ruled out if the spin of the resonance level is 5/2 or more. Since many of the secondary transitions from the resonant level are also predominantly dipole, the measured angular distributions can often be used to give unambiguous values for the level spins.

However the angular distribution measurements do not give information on the parity of the transitions. In many cases measurement of the linear polarization of the γ rays can be used to determine the electric or magnetic nature of the transitions, and hence the parity of the nuclear levels.

Fagg and Hanna (1959) have reviewed the general methods of polarization measurements of nuclear γ rays. The linear polarization is closely related to the direction correlation function $W(\theta)$. If we define γ as the angle between the polarization (electric) vector

and the normal to the scattering plane of the two γ rays, then the direction polarization correlation is given generally by the form

$$W(\theta, \gamma) = W(\theta) + D(\theta) \cos 2\gamma, \qquad (3.16)$$

where the expression $D(\theta)$ depends on the parity and multipolarities of the transitions and on the level spins. The form of the $D(\theta)$ term has been described in detail in the review article of Devons and Goldfarb (1957). For the particular case of a pure dipole transition we find a maximum linear polarization at $\theta = 90°$. The degree of polarization P can be defined by the ratio of the difference and sum of the intensities for the polarization parallel and normal to the scattering plane;

$$P = (I_{||} - I_{\perp})/(I_{||} + I_{\perp}). \qquad (3.17)$$

For a pure dipole transition, P is given by $\pm 3A_2/(2 - A_2)$ where the upper $+$ sign is taken for an $M1$ transition, and the negative sign for $E1$. For the case of an elastic scattering process 0–1–0 we get complete linear polarization perpendicular to the scattering plane ($P = -1$) for $E1$ transitions, and parallel to that plane ($P = +1$) for $M1$ transitions.

A convenient method of measuring the linear polarization is by means of a Compton polarimeter, which depends on the sensitivity of the Compton scattering process to the direction of the electric vector. The relevant Klein Nishina formula, averaged over the polarization of the scattered photons is given by

$$\frac{d\sigma}{d\Omega}\Big)_{\theta} = \tfrac{1}{2} r_0^2 \frac{k^2}{k_0^2}\left(\frac{k_0}{k} + \frac{k}{k_0} - 2 \sin^2 \psi \cos^2 \phi\right), \qquad (3.18)$$

where ψ is the Compton scattering angle, ϕ the angle between the polarization vector and the Compton scattering plane, and k_0 and k are incident and Compton scattered photon energies, respectively, related by the well-known Compton equation to the scattering angle ψ. Equation (3.18) shows maximum Compton scattering intensity in a direction normal to the polarization vector and minimum intensity parallel to that vector. The polarization is measured by counting the intensities of Compton scattered photons $N_0(\phi = 0)$ in the direction parallel to the first reaction plane and $N_{90}(\phi = 90°)$ normal to that plane at a given Compton angle ψ. It can be shown that

$$P = (R+1)(N_0 - N_{90})/(R-1)(N_0 + N_{90}), \qquad (3.19)$$

where R is the asymmetry ratio of the polarimeter defined as the ratio

$$R = \frac{d\sigma}{d\Omega}\Big)_{90} \Big/ \frac{d\sigma}{d\Omega}\Big)_{0}.$$

It is clearly advantageous to have this ratio as large as possible in order to permit an accurate determination of P. The asymmetry ratio has a maximum value at an angle ψ which depends on the incident energy k_0. At zero energy, the optimum Compton angle is 90°, and the theoretical asymmetry ratio (for perfect geometry) is ∞. At 7 MeV (typical of these resonance experiments) the optimum angle is about 50°, and the value of R is 1.24.

Due to this low value of R, polarization measurements of these high-energy γ rays are difficult to perform; nevertheless, several authors [Moreh and Friedman, (1968); Moreh *et al.* 1970b; Oliva, (1970)] have reported polarization measurements in transitions from levels excited by capture γ rays. In each case the polarimeter was composed of two scintillation detectors (polarizer and analyzer) in sum coincidence, similar to that used by Bartholomew *et al.* (1967), for measuring the parity of levels populated in the (n, γ) reaction. However their polarimeter required a triple coincidence, since it is necessary to determine the direction of the first transition in the (n, γ) cascade. For the case of levels excited by capture γ rays, the direction of the first transition is again given by that of the incident beam. In this case a double coincidence experiment is sufficient, with a considerable increase in the available counting rate.

III.4 Results and Discussion

Recent results show that nearly 50% of the source-target combinations give a measurable resonance scattering effect. However, not all of these have sufficient intensities to permit accurate studies of level schemes and resonance level parameters. Table II gives a list of those resonances which have been studied in detail.

Various assumptions are usually made in deriving the level schemes. Where the resonance level de-excites via a cascade of two or more transitions it is assumed that the primary transition is that having the highest energy—the same assumption that is usually made in (n, γ) spectroscopy. However, the opposite relationship cannot be ruled out, especially where the energies of the transitions are close. A second assumption is that there are no unobserved resonance levels present, i.e., that no inelastic transition are observed where the corresponding elastic transition is too weak to be observed. This assumption seems reasonable in view of the fact that out of about 100 resonance levels studied so far only a few showed inelastic transitions stronger than the corresponding elastic ones, which were always observable. Nevertheless one cannot completely rule out the possibility of "hidden" resonance levels in the case of very weak transitions. In view of the reservations regarding the above assumptions, the assignment of new levels solely on the basis of the energies of the observed transitions must be regarded as tentative. However, the existence of new low-lying levels may be taken as confirmed if these levels are populated from different resonance levels in the same nucleus.

TABLE III. Values of Γ_0 and δ for the 7.277-MeV level in ^{208}Pb as obtained by various authors, applying different techniques.

Γ_0[a] (eV)	δ[b] (eV)	Technique	Reference
0.80±0.08	4.8±0.4	TP,[c] SA[d]	Fleischman and Stanek (1963a)
0.80±0.03	8.0±1	CS,[e] TP,[c] SA[d]	Arad *et al.* (1964a)
	6.5±1	RT[f]	Arad *et al.* (1964b)
0.86±0.06	5.0±0.5	CS,[e] TP,[c] SA[d]	Giannini *et al.* (1965)
0.70±0.20		DS[g]	McIntyre and Randall (1965)
0.56±0.08	7.50±0.60	DS,[g] TP[c]	Kapadia *et al.* (1968)
0.68±0.09	8.00±0.14	CS,[e] TP,[c] SA[d]	Ramchandran and McIntyre (1969)
0.78±0.06	7.1±0.3	CS,[e] TP,[c] SA[d]	Moreh *et al.* (1970b)

[a] $\bar{\Gamma}_0 = 0.78 \pm 0.03$.
[b] $\bar{\delta} = 7.42 \pm 0.43$.
[c] TP—Temperature dependent intensity variation measurements.
[d] SA—Self-absorption measurements.
[e] CS—Cross section measurements.
[f] RT—Rotating target method.
[g] DS—Double scattering or scattering-absorption measurements.

Where more than one resonance level is excited using a given (n, γ) source it is necessary to determine with which elastic transition each inelastic one is associated. This can be done directly using a coincidence technique, or indirectly if the different sets of transitions show a different temperature dependence. Alternatively, the intensity changes obtained when the target is rapidly rotated could be used to correlate the associated elastic and inelastic transitions.

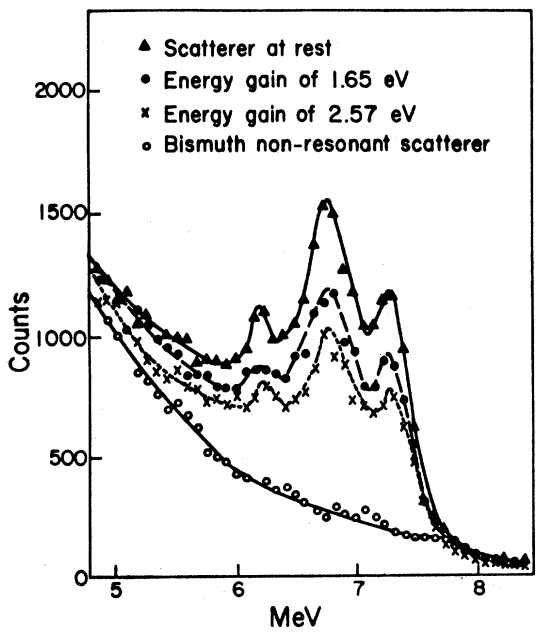

FIG. 11. Spectra of 7.277-MeV photons scattered from a rotating Pb target for an increasing energy of the incident beam as seen by the target. The curves show that the energy of the incident line lies above the resonant energy. [Arad *et al.* (1964b)].

Where multi-isotopic targets were used, the isotope containing the resonance level has been identified by comparison with previously measured low-lying levels in the individual isotopes. In some cases, the identification was confirmed using enriched isotopes.

Some of the resonances listed in Table II are discussed below as an example of the type of analysis possible with these experiments.

III.4.1 The 7277 keV Level in ^{208}Pb

The spectrum of iron capture γ rays scattered from the 7277-keV resonance level in Pb gives a very intense single line. This is one of the sources used for the γ-ray monochromator discussed in Sec. III.3.5.

This resonance has been studied by several investigators using various methods to determine the level parameters, and permits an assessment of the accuracy and self-consistency of these methods. As there are no observable inelastic components present in the scattered radiation, the branching ratio can be taken as 1. By using Pb and radio-Pb scatterers, Young and Donahue (1963) and Arad *et al.* (1964a), were able to identify the resonance isotope as ^{208}Pb. The angular distribution measurement shows clearly the dipole character of the transition, which fixes the spin of the excited state as 1, and the g factor as 3. The polarization measurement carried out by Moreh *et al.* (1970b) revealed that this line is emitted in an $M1$ transition, and hence the 7277-keV level has positive parity.

Table III summarizes the values of Γ_0 and δ obtained by various investigators, together with the experimental methods used. Since the effective cross section

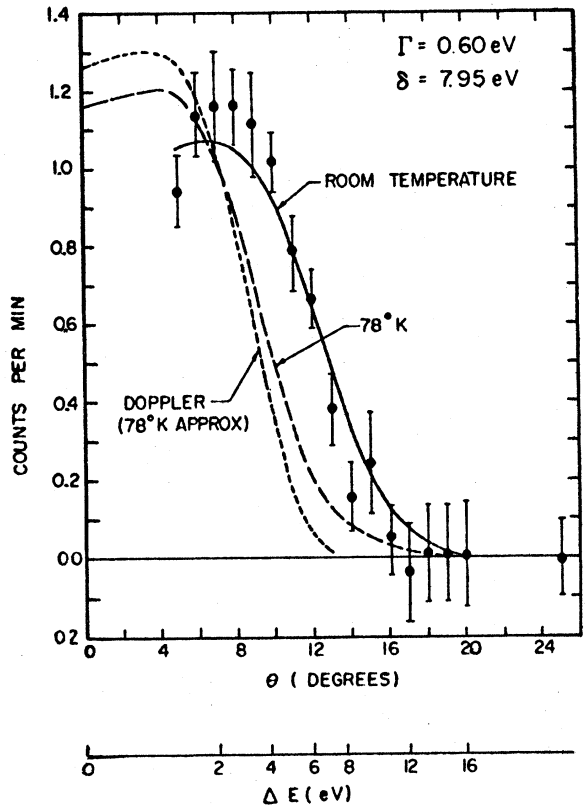

FIG. 12. Intensity of 7.277-MeV photons double scattered from Pb targets, as a function of the shift in the separation energy (or the angle of the primary scattered γ ray). From [Kapadia *et al.* (1968)].

is large, ~4 b, the self-absorption measurements gives accurate results, and most of the measurements used this method together with the temperature effect to derive these parameters. In addition, the rotating target and double scattering methods were used. Figure 11 shows the variation of the intensity as a function of the scatterer velocity, found by Arad *et al.* (1964b), which permitted an independent determination of δ. Figure 12 shows the variation of the intensity of the double scattered beam with the angle of the primary scattered γ line obtained by Kapadia *et al.* (1968). The values of Γ_0 and δ given in Table III are in generally good agreement with the weighted averages of $\Gamma = 0.78 \pm 0.03$ and $\delta = 7.4 \pm 0.4$ eV.

There are two values of δ, 4.8 and 5.0 eV, which are outside the 95% confidence intervals around the mean values, and one value of Γ, 0.56 on the edge of the 95% interval. These discrepancies are probably due either to oversimplified approximations in the calculations or to underestimated systematic errors. If these values are omitted the mean values are only slightly modified.

III.4.2 The 7646-keV Level in ^{205}Tl

The 7646-keV level excited by iron capture γ rays in natural Tl was designated by Arad *et al.* (1964a) as a level of ^{203}Tl rather than of ^{205}Tl. Since this energy is about 120 keV above the threshold for the ^{205}Tl(γ, n) reaction, they reasoned that particle emission would compete strongly with photon emission if the level belonged to ^{205}Tl. However, by using a 1-g sample enriched 92% in ^{203}Tl, Moreh and Wolf (1969a) were able to show that this level is in fact an unbound level of ^{205}Tl, having a large ground state radiative width Γ_0. Figure 13 shows the spectrum of the resonantly scattered γ rays from a natural Tl target, measured with Ge and NaI detectors. The bump in intensity around 5 MeV can be compared with the anomalous intensity bump observed in (n, γ) and $(d, p\gamma)$ reactions in the mass range $180 < A < 208$. Angular distribution measurements showed the resonant level to have a spin of 1/2. From absolute intensity measurements of the scattered radiation, temperature dependence, and self-absorption experiments, the following parameters were deduced for the resonant level: $\Gamma_0 = 0.57 \pm 0.06$ eV, $\delta = 9.3 \pm 0.3$ eV, and total level width $\Gamma = 0.93 \pm 0.09$ eV. The branching ratio Γ_0/Γ_γ was found to be 0.58, which is consistent with $\Gamma \approx \Gamma_\gamma$, and hence a small neutron width. Moreh and Wolf have suggested that the low value for Γ_n may be explained in terms of the angular momentum involved. From consideration of the measured strength, they reasoned that the resonant level had a negative parity and hence a spin and parity of $1/2^-$. Neutron emission from this level leading to the ^{204}Tl 2^- ground state, would require the angular momentum of the neutron to be $l_n = 2$, which may be strongly retarded for a neutron of about 120 keV. It is also possible that this level is a member of a group of levels combining a doorway state, as discussed below.

III.4.3 The 8535-, 7538-, and 6838-keV Levels in Tellurium

Schlesinger *et al.* (1969) measured the spectrum of Ni-capture γ rays scattered from a Te target. Three lines in this spectrum (at 8535, 7538, and 6838 keV), have energies identical to those of γ rays in the incident spectrum, and hence were attributed to three independent resonance levels in the target. The other transitions were assumed to be inelastic de-excitations of these resonance levels. Direct coincidence measurements showed that the 6698- and 5960-keV lines were due to transitions from the 7538-keV level to known levels at 840 and 1588 keV, respectively, in ^{130}Te. The intensities showed a pronounced temperature dependence in the case of the 8535- and 6838-keV elastic transitions, but none in the case of the 7538-keV transition. By examining the temperature dependence of the intensities of the inelastic transitions it was

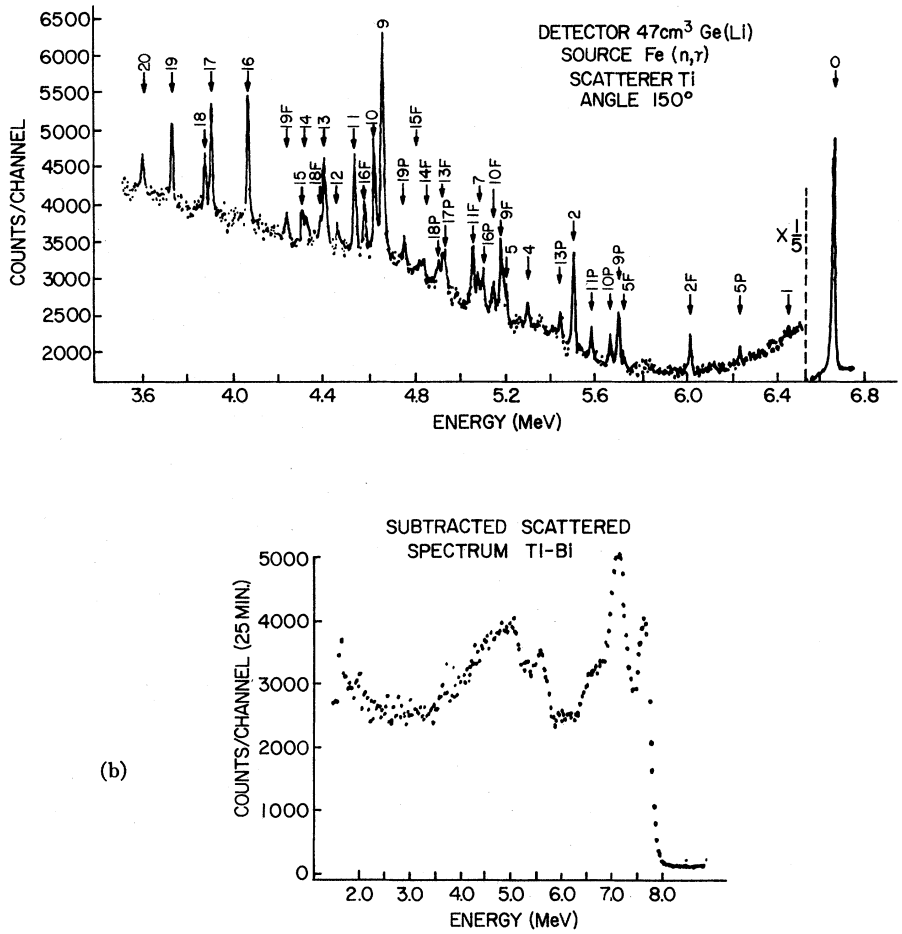

FIG. 13. Spectrum of γ rays resonantly scattered from a Tl target, as observed (a) with a Ge(Li) detector, (b) with a 5 in.×5 in. NaI/Tl) detector. The nonresonant contribution obtained with a Bi scatterer has been subtracted. [Moreh and Wolf (1969a)].

possible to assign another six of the lines to transitions from the 7538-keV resonant level.

The derived decay scheme from the 7538-keV level in ^{130}Te is shown in Fig. 14. Angular distribution measurements showed the strong transitions to be predominantly dipole, with spin 1 for the resonant level, and spin 2 for both the 840- and the 1588-keV levels. There is disagreement with the results of Cookson and Darcey (1965) for the spin of the 1588-keV level. They studied this nucleus by inelastic proton scattering, and, using an empirical intensity rule, deduced a spin of 4^+ for the 1588-keV level. The population of a 4^+ level from the spin 1 resonance level is extremely unlikely and the spin assignment can be regarded as 2^+. In this case, spin determination from the relatively simple angular correlation measurement is preferable to the use of empirical rules deduced for more complex particle reactions.

III.4.4 Levels in Lanthanum-139

These levels have been investigated by Szichman *et al.* (1970) and Moreh and Nof (1970) using various capture γ-ray sources. The level scheme of ^{139}La including the transitions from the various resonance levels is shown in Fig. 15. As can be seen, many levels are populated from different resonant levels and hence their existence is confirmed. The nuclear parameters of the various resonance levels are given in Table II.

III.4.5 Doorway States in (γ, γ′) Reactions

In recent years nonstatistical effects have been observed in photon spectra from both thermal and resonance neutron spectra, which were explained by the existence of doorway states. An example is the observation of anomalous bumps at about 5 MeV both in (n, γ) and $(d, p\gamma)$ spectra for nuclei in the mass region $180<A<208$ (Bartholomew, 1969). Lane (1970) has interpreted this phenomenum in terms of the mechanism of doorway states following the suggestions of Bartholomew and Rimawi *et al.* (1969).

The similarity between neutron-capture γ spectra and the γ spectra following excitation of a γ-resonance level suggest that similar nonstatistical effects may

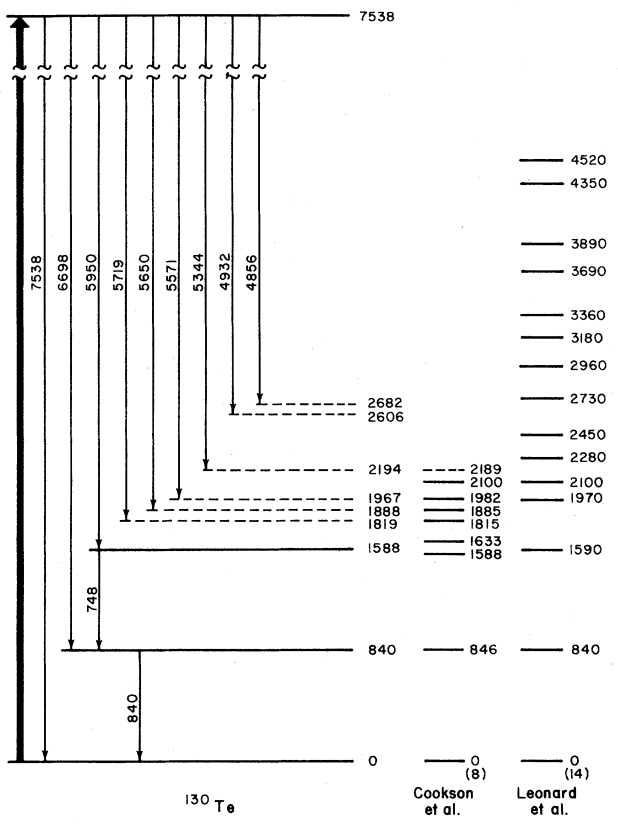

FIG. 14. Decay scheme of the 7.538-MeV level in ^{130}Te, excited by Ni-capture γ rays. [Schlesinger *et al.* (1969)].

show up in the latter case. The spectrum of 7.646-MeV γ rays scattered from a Tl target (Fig. 13) does in fact show an anomalous high concentration of γ rays at about 5 MeV. Moreh and Wolf (1969b) have reported similar anomalous intensities from other resonances in ^{203}Tl, ^{184}W, and ^{186}W. These anomalies are very similar to those observed in the (n, γ) and $(d, p\gamma)$ spectra, and show that doorway states may play an important part in the transitions from these γ-resonance states. Recently however, Loper *et al.* (1972) reported studies of thermal and resonance (n, γ) spectra in ^{197}Au. They observed the bump structure in the thermal (n, γ) spectrum but not in the resonance capture, the latter being in good agreement with the statistical model. They concluded that there is no evidence for nonstatistical behavior in gold and that the apparent bump in the thermal spectrum can be explained in terms of a Porter–Thomas distribution of individual transitions. This result throws doubts on the existence of the $2p$ $1h$ doorway states at about 5.5 MeV and also has its implication on the (γ, γ') results which must be reevaluated and checked as to whether they can be explained in terms of the statistical model and the Porter–Thomas distribution.

Some of the γ-resonance levels which show exceptionally large γ-radiation widths may also be connected with doorways.

Recently Berman *et al.* (1972) found a set of 1^+ resonances in ^{208}Pb using the threshold photoneutron reaction (see Fig. 16). These resonances, which deexcite via P wave neutrons, constitute at least half, and possibly all, the total $M1$ strength calculated for this nucleus, and may be the long sought $M1$ giant resonance. The $M1$ strength in ^{208}Pb arises from the spin flip transition in the $i_{13/2}$ neutron shell and the $h_{11/2}$ proton shell, and these particle–hole states form the doorway through which the observed compound nuclear states are reached. These authors pointed out that the 7.277-MeV 1^+ level in ^{208}Pb, excited by γ resonance fluorescence (Sec. III.4.1), may be one of the lowest members of this group of doorway states.

The 7.647-MeV level in ^{205}Tl (Sec. III.4.2) was observed to have an anomalously large value of Γ_0, and low value of Γ_n. This may also be associated with a collective doorway. The (γ, n) cross section of ^{205}Tl obtained by Antropov *et al.* (1971) shows in fact an intermediate structure at about 9 MeV which was interpreted in terms of the threshold states suggested by Baz (1959). This structure may represent an $M1$ or $E1$ collective doorway, similar to that observed for ^{208}Pb. The 7.647-MeV resonance level may belong to this doorway state although, due to the small neutron width, it could not have been seen by Antropov *et al.*

III.4.6 Radiative Widths and γ-Ray Transition Strengths of the Resonance Levels

The random nature of the resonance fluorescence method discussed in this section may give a nontypical selection of levels in this energy region. It is therefore of interest to compare the properties of these levels with the well known behavior of the radiative transitions from neutron resonance levels. Table IV lists the measured radiative parameters for some 20 levels excited by capture γ rays. The fourth and fifth Columns show the total radiative width Γ and ground state radiative widths Γ_0, respectively.

The total radiative widths can be seen to be in the range 40 meV to 2 eV, compared with the range 30–200 meV, for neutron resonance widths [see, for example, Lynn (1968)]. The spread in values of Γ in Table IV seems to be somewhat wider than that for the neutron data. However, it should be remembered that the former are measured for individual levels, while the latter are usually averaged over many levels. Since the nuclei studied by the γ-fluorescence method could not normally be reached in neutron-capture reactions a direct comparison is possible only for ^{139}La and ^{112}Cd. For ^{139}La, the value of Γ from neutron-capture studies is 99±6 meV at the neutron binding energy of 8.78 MeV compared with an average of 60±

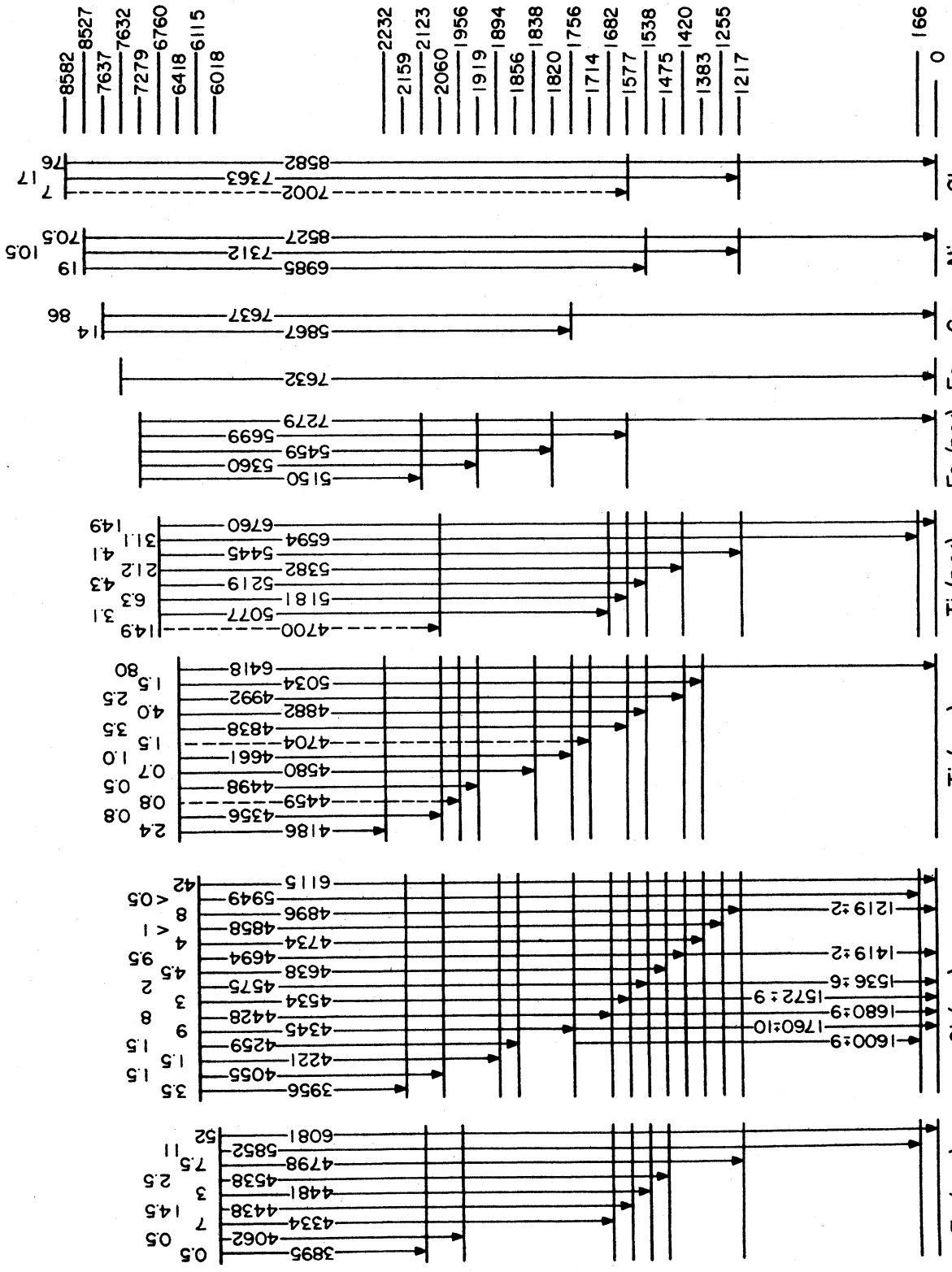

FIG. 15. Highly excited and low-lying levels of ^{139}La populated in various (γ, γ') reactions. The exciting (n, γ) source is indicated under each partial level scheme. [Szichman *et al.* (1970) and Moreh and Nof (1970)].

TABLE IV. Total and ground state radiation widths of the resonant levels, together with the reduced widths of the ground state transition. The values of Γ_0 were taken from Table II and the various references are given there.

Nucleus	J^π	Energy of resonant level (MeV)	Total width Γ (eV)	Ground state transition width Γ_0 (eV)	Level spacing D (eV)	Reduced width K_{E1} (eV·MeV^{-4})	Reduced width $K_{M1}\times10^3$	c ($\times10^5$)
^{209}Bi		7.416	0.23±0.17	0.14±0.09	250	39.0	1373	1.97
^{208}Pb	1^+	7.277	0.78±0.03	0.78±0.03	1900	29.4	1030	4.89
^{205}Tl	$1/2^{(-)}$	7.646	0.98±0.09	0.57±0.08	470	78.0	2713	3.83
^{203}Tl	1/2	6.418	0.32±0.06	0.08±0.02	425	21.0	710	1.5
^{144}Sm	1	8.997	0.27±0.08	0.063±0.013	110	28.6	786	5.67
^{141}Pr	$5/2^+$	7.632	0.072±0.024	0.033±0.011	60	47.7	1280	4.76
^{141}Pr	$7/2^{(-)}$	6.115	0.052±0.010	0.029±0.006	175	26.8	722	5.84
^{139}La	$7/2^{(-)}$	6.760	0.060±0.030	0.010±0.005	145	8.2	222	1.14
^{139}La	$9/2^{(-)}$	6.418	0.045±0.009	0.038±0.009	160	33.4	898	6.33
^{139}La	$9/2^{(-)}$	6.115	0.079±0.017	0.034±0.008	210	26.5	707	5.47
^{139}La	$7/2^{(-)}$	6.018	0.05±0.01	0.025±0.005	218	19.6	526	3.38
^{130}Te	1	7.538	0.24±0.06	0.06±0.01	300	18.1	465	6.88
^{120}Sn	1	7.696	0.12±0.03	0.07±0.02	165	38.2	930	16.20
^{112}Cd	1^-	7.632	0.086±0.015	0.047±0.008	130	35.4	822	17.34
^{109}Ag	3/2	7.632	0.002±0.001	0.001±0.0005	37	2.7	61	.93
^{90}Zr	1	8.496	2.10±0.53	1.68±0.02	1280	106.0	2141	66.00
^{86}Sr	1	7.820	0.10±0.05	0.030±0.015	980	3.2	64	2.64
^{80}Se	1	7.820	0.09±0.02	0.030±0.007	680	7.4	138	4.55
^{75}As	1/2	7.646	0.36±0.10	0.041±0.011	350	14.8	263	2.70
^{74}Ge	1^-	6.018	0.120±0.015	0.023±0.004	3293	1.8	32	3.32
^{66}Zn	1	7.696	0.21±0.04	0.10±0.02	2100	6.4	104	8.95
^{66}Zn	1	7.368	0.31±0.03	0.22±0.02	2600	12.8	210	19.83
^{62}Ni	1	7.646	0.48±0.05	0.31±0.03	4000	11.3	178	17.83
^{50}Cr	1	8.888	0.75±0.20	0.68±0.19	2500	28.5	387	52.33

15 meV at about 6.3 MeV for the four γ resonances. The corresponding values for ^{112}Cd are 120±20 meV at 9.48 MeV (neutron threshold) and 86±15 meV at the 7.632-MeV γ resonance. After correcting for the predicted energy dependence of the total radiative width (Cameron, 1959) one finds good agreement between the two types of experiment for both nuclei.

It can be concluded that the total radiative widths found for γ-resonance levels are in agreement with the radiative widths found in neutron resonance data. These present results are in disagreement with those obtained by Reibel and Mann (1960) discussed above, who reported total radiative widths several times larger than would be expected from neutron data.

The transition strengths in this energy region can be described in terms of the reduced partial widths, K_{E1} and K_{M1}. Following the notation of Bartholomew (1961), K_{E1} and K_{M1} may be defined as follows for $E1$ and $M1$ transitions

$$K_{E1}=\frac{\Gamma_{\rm obs}(E1)}{E^3A^{2/3}D}, \qquad K_{M1}=\frac{\Gamma_{\rm obs}(M1)}{E^3D}, \quad (3.20)$$

where $\Gamma_{\rm obs}$ is the measured $E1$ or $M1$ transition width in eV, E is the transition energy in MeV, A is the mass number, and D the level spacing in MeV in the neighborhood of the resonance level. Compilations of known $E1$ and $M1$ reduced partial widths for transitions following neutron capture have been given in the review article by Bartholomew (1961) and by Carpenter (1962) and Bollinger (1968). The systematics of the compiled data show a considerable spread of reduced widths, in the range $0.1\text{–}40\times10^{-3}$ eV·MeV^{-4} for K_{E1} values, and $0.1\text{–}100\times10^{-3}$ eV·MeV^{-4} for K_{M1} values.

Evaluation of the reduced widths for the resonances listed in Table IV requires knowledge of the values of D, which have not been measured experimentally for most of these nuclei. The theoretical values of D shown in Column 6 have been calculated using the formula of Cameron (1959). This formula usually gives agreement to within a factor of 3 to the measured values where these are available, although discrepancies as high as a factor of 6 in the region of closed shells were pointed out by Cameron. Since the electromagnetic nature is unknown for most of these resonances, the widths listed in Columns 7 and 8 were calculated assuming an $E1$ or $M1$ character, respectively. It can be seen from Column 7 that the K_{E1} values are in the upper range of those observed in neutron resonance reactions. This suggests that these transitions may be predominantly electric dipole, in general agreement with the direct measurements of Moreh *et al.* (1970b). It should be noted that extremely large $M1$ strengths are found for the 7.277-MeV resonance level in ^{208}Pb (1030×10^{-3} eV MeV^{-4}), and for the 7.632-MeV level of ^{141}Pr (1280×10^{-3} eV MeV^{-4}). However, the theoretical values of D used in Table IV could greatly underestimate the true values, especially for the double magic nucleus ^{208}Pb. Moreh *et al.* used larger values of D, 25 KeV for ^{208}Pb, and 700 eV as an upper estimate for ^{141}Pr. Even with these larger values they still found the $M1$ radiation strengths some five times higher than the average $M1$ strengths reported by Bollinger (1968). As discussed in Sec. III.4.5, Berman *et al.* (1972) have suggested that this 7.277-MeV level in ^{208}Pb is in fact a part of the $M1$ giant resonance in this nucleus. Since the polarization measurement on the 7.632-MeV transition in ^{141}Pr requires determination of a 1.5% asymmetry it would seem worthwhile to repeat this measurement to confirm this rather interesting enhanced $M1$ strength. A confirmation of this $M1$ strength may indicate that this level belongs to the $M1$ giant resonance reported by Pitthan and Walcher (1971). These authors found broad resonances having magnetic character at about 9 MeV in La, Ce, and Pr, using inelastic electron scattering. It should be noted that while an $M1$ assignment is probable, an $M2$ cannot be ruled out. It is therefore worthwhile to carry out more polarization measurements on the (γ, γ') resonances of ^{139}La and ^{141}Pr to clarify this problem.

It is interesting to compare these results with the ground state strength predicted by extrapolation of the giant electric dipole resonance. Axel (1962) has shown that in this case $\langle\Gamma_0\rangle/D$ is given by

$$\langle\Gamma_0\rangle/D=3.4\times10^{-6}(A/g)\times[E^4\Gamma_g/(E_R^2-E^2)^2+E^2\Gamma_g^2], \quad (3.21)$$

where E_R and Γ_g are the peak energy and level width of the electric giant dipole resonance, A is the mass number, and g the spin factor $(2I_c+I)/(2I_0+I)$.

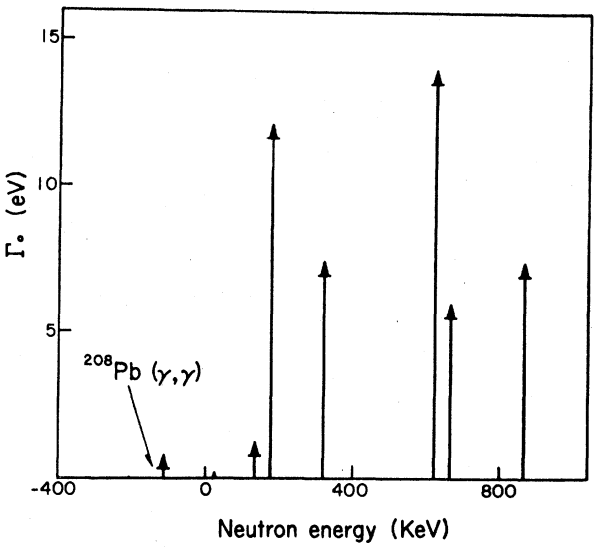

FIG. 16. Values of Γ_0 for 1^+ resonances in ^{208}Pb, which de-excite by p-wave neutrons. The level at negative neutron energies is the 7.277-MeV (γ, γ) resonance in ^{208}Pb. [Berman *et al.* (1972)].

Using the empirical expression $E_R=80A^{-1/3}$, the approximate formula in the energy region around 7 MeV can be expressed in the form:

$$\langle\Gamma_0\rangle/D=c(E/7)^5(A/100)^{8/3}(\tfrac{1}{5}\Gamma_g)(3/g), \quad (3.22)$$

where $c=2.2\times10^{-5}$, and E and Γ_g are measured in MeV.

Equation (3.22) can be used to find empirical values of the constant c from the experimental data. The results are summarized in Column 9 of Table IV. It can be seen that the values obtained are in most cases higher than the predicted value of 2.2×10^{-5}. The average value of c from Table IV is 11×10^{-5} which can be compared with the experimental mean value of 3.5×10^{-5} obtained by Baglan *et al.* (1971). This can be explained by the experimental cutoff involved in the γ resonance fluorescence method, since scattering from small resonances cannot be distinguished from background. This therefore gives a bias towards higher values of Γ_0.

It should be emphasized that one expects fluctuations in the individual results as they are based on individual levels, whereas the Axel formula (3.22) applies to the average value of the strength.

III.4.7 Fluctuations of Partial Radiation Widths From γ-Resonance Levels

Very large variations have been observed in the intensities of the partial radiation widths from the resonance levels to different low-lying levels. Estes and Min (1967) have pointed out that for both the 7.632-MeV levels in ^{112}Cd and ^{62}Ni, the first phonon

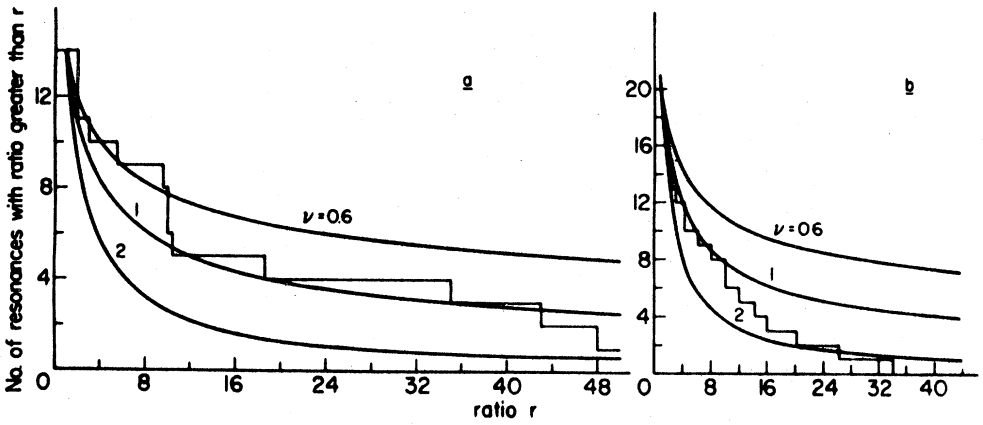

FIG. 17. Integral distribution of the ratios r of the transition intensities to the two lowest excited states: (a) For 14 resonance levels obtained in (γ, γ') experiments. [Schlesinger *et al.* (1970)]; (b) For 20 neutron resonance levels in ^{196}Pt. [Samour *et al.* (1968)].

2^+ state is strongly populated from the resonance levels. However, while the 0^+ member of the two-phonon triplet is strongly populated in both cases, the 2^+ member is very weakly populated. They attributed this effect to very different components of the wave functions of the 0^+ and 2^+ members of the two phonon triplet in each nucleus. On the other hand, Shikazono and Kawarasaki (1968) pointed out an opposite effect for the 7.368-MeV level of ^{66}Zn, where the 2^+ component of the two-phonon triplet is populated preferentially compared with the 0^+.

Schlesinger *et al.* (1970) have pointed out that these striking differences in intensity of the low-lying levels are in fact compatible with a Porter–Thomas distribution of partial radiation widths from these resonance levels. Porter and Thomas (1956) have shown that the complexity of the wave functions describing the highly excited nuclear levels leads to a normal distribution of the matrix elements describing transitions from these levels to a given final state. The distribution of partial radiation widths can then be shown to follow a χ^2 distribution with ν degrees of freedom. The Porter–Thomas distribution is defined for $\nu=1$ where one reaction exit channel is open.

The distribution in partial radiation widths from the neutron resonance levels to low-lying states has been shown to follow a Porter–Thomas distribution for a wide variety of nuclei. Samour *et al.* (1968) carried out an analysis of the fluctuation of partial radiative widths in ^{196}Pt. They measured transitions from 24 neutron resonance levels to the ground state and first two excited 2^+ states, and obtained a value of ν of 1.25 $(+0.35, -0.27)$.

For the case of the γ resonance levels, it is not possible to carry out such a direct measurement of the fluctuations in radiative widths to low-lying levels in a given nucleus, since very few resonance levels have been found in a single nucleus. Schlesinger *et al.* studied the fluctuations in the ratio r of intensities of transitions from the resonant level to the first two 2^+ states in 14 even–even nuclei. The ground state transitions were not included in this analysis owing to the experimental bias for detecting γ resonances with large values of the ground state branching ratio. Figure 17 shows the observed integral distribution in r (defined always greater than 1) for the 14 γ-resonance levels studied by these authors. For comparison, the corresponding distribution in r for 20 of the ^{196}Pt neutron resonance levels measured by Samour *et al.* (1968) is shown. If the distribution in relative partial radiative widths for each of these nuclei is taken as a χ^2 distribution with ν degrees of freedom, the distribution in r, the ratio of two partial widths, can be shown to follow a Fisher Z distribution [see, for example Cramer (1959)] given by

$$P(r,\nu)=B_{1+r}(\nu/2,\nu/2)/B_{\infty}(\nu/2,\nu/2), \quad (3.23)$$

where B_{1+r} and B_{∞} are the incomplete and complete

TABLE V. Values of ν for four resonance levels. From Moreh and Wolf (1972).

Nucleus	Resonance energy (MeV)	Number of final states	ν
^{62}Ni	7.646	16	$0.4^{+0.9}_{-0.2}$
^{66}Zn	7.368	10	$1.1^{+0.9}_{-0.3}$
^{75}As	7.646	15	$1.0^{+0.5}_{-0.5}$
^{112}Cd	7.632	18	$1.0^{+0.5}_{-0.4}$

TABLE VI. Measured differential cross sections (μb/sr) for nuclear elastic and nuclear Raman scattering from an uranium target. For comparison, the cross sections calculated using the giant dipole parameters deduced by Hass and Salzmann (1973) are also shown.

Energy (keV)	Angle	Ref.	Elastic cross section (μb/sr)		Inelastic cross section (μb/sr)	
			Experiment	Calculated	Experiment	Calculated
8 535	140°	a	8±3	13.4	8±3	8.9
8 998	140°	a	27±6	28.2	18±4	15.9
9 298	140°	a	42±9	43.8	27±7	23.7
10 830	70°	b	310±30	267	180±20	200
10 830	90°	b	230±20	209	200±20	198
10 830	120°	b	250±20	265	210±20	201
10 830	150°	b	390±40	370	200±20	209

[a] Hass *et al.* (1971).
[b] Jackson and Wetzel (1972).

beta functions, respectively. These theoretical distributions in r are shown in Figs. 17(a) and 17(b) for values of ν of 0.6, 1, and 2. The maximum likelihood fit on the γ-resonance data gives a value of $\nu_m=1.06$. A Monte Carlo calculation shows that the probability of finding a value of ν_m below 1.06 from a distribution with $\nu=1$ is 0.35, while for $\nu=2$, the probability is 0.06. The observed fluctuations in partial radiation widths are thus fully compatible with a Porter–Thomas distribution for all the observed nuclei. However, this analysis by Schlesinger *et al.* is based on the rather stringent assumption that the fluctuations in partial radiation width follow the same statistical law for all the nuclei studied.

Moreh and Wolf (1972) studied this distribution by a different approach for four different resonance levels in ^{62}Ni, ^{66}Zn, ^{75}As, and ^{112}Cd. In each case they considered dipole transitions of a given parity to between 10–18 known lower levels. The statistical distribution of reduced partial radiation widths in each case was investigated, using the maximum likelihood method; the results are shown in Table V. The values of ν are again consistent with a Porter–Thomas distribution for all these nuclei although in the case of ^{62}Ni and ^{66}Zn, values of $\nu=2$ cannot be ruled out. However, this method of analyzing radiation widths can introduce a bias in the observed distributions which has not yet been taken into account. This includes the effect of the ground state radiation widths considered in the analysis and the possibility of missing levels of appropriate spin and parity.

III.4.8 Elastic and Inelastic Scattering of Capture γ Rays in the Continuous Region—Observation of Nuclear Raman Scattering

The over-all width of capture γ rays from light nuclei is some 15 eV for energies in the range 8–10 MeV. This is considerably larger than the average level spacing for heavy nuclei in this energy region, and the effect of individual levels can be assumed to be insignificant. The scattering of high-energy capture γ rays from heavy nuclei such as U and Th can therefore be expected to be given to a good approximation by the giant dipole resonance theory.

Fuller and Hayward (1962) measured the total scattering cross section for photons on Er and Ho, using bremsstrahlung radiation. They found agreement with theory only if a tensor scattering term was included, corresponding to the so-called nuclear Raman scattering to the first excited state. However, owing to the finite resolution (some 300 keV), they were not able to resolve experimentally the Raman scattering from the nuclear elastic scattering.

Knowles (1970), Wetzel and Jackson (1971), Hass *et al.* (1971), and Jackson and Wetzel (1972) have reported measurements of nuclear elastic and nuclear Raman scattering in targets of ^{232}Th and ^{238}U, using capture γ-ray sources of Ni, Fe, and N. The use of these monoenergetic sources permits discrimination between the elastic and Raman scattering peaks, which are separated by some 45 keV.

The nuclear Raman effect is closely connected with the splitting of the giant dipole resonance in highly deformed nuclei. Fuller and Hayward (1962) have shown for a classical anisotropic oscillator that the elastic cross section for photons of energy E is given by

$$(d\sigma/d\Omega)_s = |[(\mathfrak{A}+2\mathfrak{B})/3]+D|^2[(1+\cos^2\theta)/2]. \tag{3.24}$$

The tensor scattering term, corresponding to Raman scattering to the first rotational level of even–even nuclei, is given by

$$(d\sigma/d\Omega)_t = |\tfrac{2}{3}(\mathfrak{A}-\mathfrak{B})|^2[(13+\cos^2\theta)/40], \tag{3.25}$$

where $\mathfrak{A}$ and $\mathfrak{B}$ are the intrinsic scattering amplitudes associated with the major and minor axes, respectively, of the nuclear ellipsoid. They are given by expressions of the form

$$\mathfrak{A}=\frac{e^2}{Mc^2}\frac{NZ}{A}\alpha E^2\frac{E_a^2-E+i\Gamma_a E}{(E_a^2-E^2)^2+\Gamma_a^2E^2}, \quad (3.26)$$

where E_a and Γ_a correspond to the major axis (and E_b and Γ_b being used in the similar expression for $\mathfrak{B}$), α is the dipole sum enhancement term resulting from nuclear exchange forces, and D is the Thomson scattering amplitude at $E=0$, given by $D=-Z^2e^2/AMc^2$.

It is clear that the Raman scattering cross section vanishes for nondeformed nuclei, since in this case $\mathfrak{A}=\mathfrak{B}$.

The experimental measurements of the three groups using capture γ radiation were in principle similar. Large Ge(Li) detectors were used to measure the scattered radiation at angles of 70° or more. Special care was taken to shield the detectors from the large numbers of photoneutrons produced in the targets. The experimental results of Hass *et al.* (1971) and Jackson and Wetzel (1972) for ^{238}U are summarized in Table VI.

Jackson and Wetzel (1972) have reported a ratio of Raman to elastic scattering of 0.8 for 10.8-MeV photons scattered at 90° from ^{238}U. A similar ratio of 0.7 ± 0.1 was obtained by scattering from ^{232}Th.

They showed that these results are in disagreement with the value of 1.3 predicted both by the Danos–Okamoto theory (Danos, 1958; Okamoto, 1958), and by unpublished calculations of Arenhövel based on the dynamic collective model. Jackson and Wetzel used the giant dipole resonance parameters deduced by Hass *et al.* (1971) from similar measurements at 9.3, 9, and 8.5 MeV. They obtained a ratio of 1.1 at the energy of 10.8 MeV which is still some 30% higher than their experimental results. Jackson and Wetzel concluded that these discrepancies can be explained by assuming the existence of a direct nonresonant process of some 15% in the elastic scattering.

Hass and Salzmann (1973) reanalyzed their own results as well as those obtained by Jackson and Wetzel. Using seven results (see Table VI) they performed a least-square-fit procedure to Eqs. (3.24) and (3.25) to obtain the giant dipole resonance parameters. In the calculation of the theoretical cross sections, they included the coherent contributions of Delbrück and Thompson scattering. Comparison of the experimental cross sections with the calculated ones based on the adjusted giant dipole resonance parameters shows good agreement, and hence Hass and Salzmann conclude that there is no need to include a direct reaction component in the elastic scattering.

Further measurements on other elements and at a higher energy (11.38 MeV obtained from neutron capture in the radioactive isotope ^{59}Ni) are under progress (Bar-Noy *et al.*, 1972). These measurements undoubtedly will help to decide whether a direct component is present and the accuracy to which giant dipole resonance parameters can be deduced from this kind of experiment.

III.5 Future Studies

With the experimental techniques described in this section a great deal of spectroscopic data can still be obtained through the de-excitation of single levels excited by capture γ rays. However, owing to the limited availability of separated isotopes in $\sim$100 g quantities, the technique will probably find practical applications only for nuclei having a reasonably large natural isotopic abundance (>10%). It is somewhat easier to study odd-Z than even-Z nuclei, since the former have fewer isotopes, facilitating identification of the isotope having the resonant level.

Systematic measurement of the level widths, coupled with polarization measurements of the elastically scattered component, will permit a study of the electric and magnetic dipole strengths in this interesting energy region. In addition, as more partial widths are measured in individual nuclei, it will be possible to improve the study of fluctuation properties, and the correlations between the partial widths in individual nuclei.

Doorway states have aroused great interest in recent years. These states have shown up clearly in the resonance scattering experiments via the anomalous bump at about 5 MeV in the mass region of 180–208. It therefore seems worthwhile to study resonance scattering of individual levels in this energy region, which is the lower limit of the resonances studied so far. Another way in which doorway states were ob-observed was, for example, the existence of positive correlations among similar γ-ray transitions originating in different neutron resonances. As more and more γ resonances in the same nucleus are found it will be possible to look for correlations similar to those found in resonance neutron capture studies.

While the majority of studies of individual levels have so far been concerned with bound levels, interesting results have been reported in the unbound region. Nuclear Raman scattering has been measured and parameters of the giant dipole resonance have been deduced. It seems worthwhile to extend these studies to other heavy deformed nuclei. It may be possible to carry out similar measurements in the rare earth region—despite the smaller cross sections and possible involvement of several isotopes.

IV. NUCLEAR PHOTOEXCITATION WITH A VARIABLE ENERGY COMPTON SCATTERED (n, γ) SOURCE

IV.1 Introduction

The methods described earlier for studying level widths by the resonance fluorescence technique are

somewhat limited in their applications. As pointed out in Sec. II, the recoil energy compensation needed to achieve resonance conditions in low-lying levels can be obtained only in special cases. The resonance fluorescence of highly excited levels discussed in Sec. III is also restricted since it depends on an entirely chance overlap between particular nuclear levels and capture γ lines. In order to study average level properties of a nucleus over the whole energy range it is useful to have a continuously varying γ-energy source with high-energy resolution. Seppi *et al.* (1962) have described a crystal photon monochromator using an x-ray tube as the source. This gave a well defined beam with energy resolution of 0.02–1 keV over the range 40–280 keV. McIntyre and Tandon (1963, 1968) and Mouton *et al.* (1963) extended the energy range up to 1.3 MeV by using scattered ^{60}Co radiation. The continuous variation of energy was achieved exploiting the angular dependence of the energy of the Compton scattered photons. In the higher energy range, as mentioned earlier, electron bremsstrahlung radiation has been used, with rather "poor" resolution by Fuller and Hayward (1956), Rabotnov *et al.* (1965), and many others. While recent bremsstrahlung studies have achieved a far more accurate "end-point" energy (Rabotnov *et al.*, 1970), the actual energy spectrum is extremely broad, and the cross section analysis critically depends on an unfolding procedure. O'Connel *et al.* (1962) used a bremsstrahlung coincidence monochromator, achieving moderate resolution of some 1% with however severely reduced intensity. Fultz *et al.* (1962) used monoenergetic photons from the annihilation in flight of fast positrons (obtained from a linac) with an energy resolution of some 3%. This method also gives very low intensities below 10 MeV.

Knowles and Ahmed (1966), Hall *et al.* (1970), and Fagot *et al.* (1971) have described variable photon energy "monochromators" using Compton scattered (n, γ) radiation. These combine the advantages of relatively high intensities with moderate energy resolution (about 2%) over the energy range 0.5–9 MeV. They have been used for resonance fluorescence and photofission experiments. The resonance fluorescence experiments are discussed in detail in this chapter, while the photofission experiments are discussed in detail in the next chapter. Table VII compares the intensities and resolutions obtained by the different γ sources.

TABLE VII. Comparison of photon beams in the energy range of 5–9 MeV used for photonuclear experiments.

Photon source	Effective photon intensity at target position in eV^{-1} cm^{-2} sec^{-1}	Energy resolution ($\Delta E/E$ in %)
Bremsstrahlung monochromator[a]	$\sim(0.05-1)\times10^{-3}$	1[d]
Microtron (bremsstrahlung)[b]	1	3[d,e]
Electron Linac		
Bremsstrahlung[b]	10	3[d,e]
Positron time of flight	10^{-2}	4[d]
(n, γ) reaction[c] followed by Compton scattering	1	2[d,e]
(n, γ) direct[c]	10^{6}	10^{-4}

[a] The photon intensity at the target is limited by the high random counting rate. The lower limit of 0.05×10^{-3} eV^{-1} cm^{-2} sec^{-1} corresponds to high-Z targets.

[b] The accelerators cannot be used at their full intensities for (γ, γ) experiments because of pile up.

[c] Estimates of intensity assume $3\times10^{15}n$ sec^{-1} absorbed in a Ti source 12m from the target.

[d] In (γ, γ) experiments, the resolution improves to the inherent resolution of the detectors used [~7 keV for Ge(Li)].

[e] The resolution is determined mainly by the uncertainties in the spectrum shape and the unfolding techniques involved.

IV.2 The Variable Energy Source

If a γ ray of energy E_0 undergoes Compton scattering into an angle θ, the scattered photon has an energy E given by

$$E=E_0/[1+\alpha(1-\cos\theta)], \qquad (4.1)$$

where α is the ratio of E_0 to the electron rest mass. Variation of the Compton scattering angle between 0° and 90° results in an energy variation from the full energy E_0 down to below 0.511 MeV.

We will here consider the external scattering geometry γ monochromator described by Knowles and Ahmed as typical of these Compton scattering (n, γ) facilities. This facility was set up in a 12-in. tangential beam tube of the NRU reactor, in Chalk River Ont., with the γ source located near the center of the tube. The experimental geometry is shown schematically in Fig. 18. The source S, the Compton scatterer C, and target T lie on a focusing circle F. This arrangement has the property that all the photons from the source S are Compton scattered toward the target with the same angle θ. The Compton scatterer C has a curvature matching that of the focusing circle. The source and pivot are fixed while the target is constrained to move along a straight line at a fixed angle of 67° with respect to the beam tube axis. At each Compton angle, the curved scatterer is arranged to coincide with the changing focusing circle by appropriate rotation about the pivot P. Since all the converging γ rays at the target are scattered at the same angle θ, they have the same energy E, as given by Eq. (4.1).

Figure 18 shows the scatterer geometry for a scattering angle of 6°. At small angles the γ radiation is incident on the full length of the curved scatterer. For

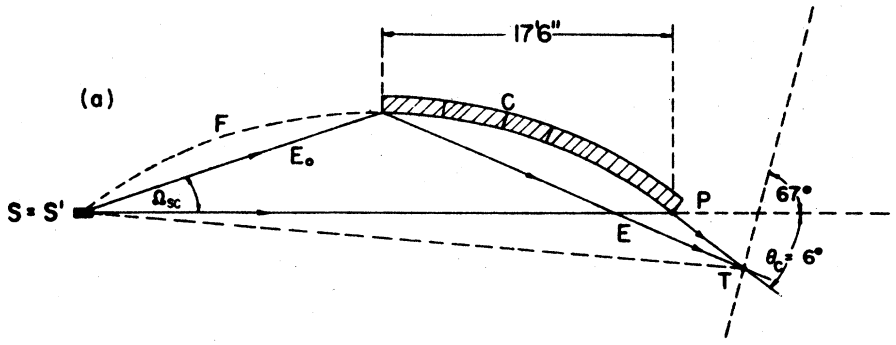

FIG. 18. Schematic representation of the scattering geometry for a Compton angle $\theta_c = 6°$: p, pivot; T, target; F, focusing circle; Ω_{SC}, constant solid angle subtended by the Compton scatterer C at the source S. [Knowles and Ahmed (1966)].

larger angles, the target is moved linearly away from the beam axis while the scatterer length is reduced, in order to keep constant the solid angle Ω_{sc} subtended by the scatterer at the source. At large scattering angles, only 20% of the scatterer is utilized. For good resolution the focusing conditions of this geometry require a thin source (ideally a line source as viewed from the scatterer position), hence a source with an appreciable (n, γ) cross section is needed. In addition it is desirable that the source emit a simple spectrum of a few intense lines. Nickel and titanium fulfill these requirements, and therefore both were used in a combined double source. This source could be rotated about a vertical axis presenting to the scatterer C either the titanium or nickel plate as an effective line source of variable width. The nickel source (having lines at 8.526 and 8.998 MeV) was used for high-energy experiments, while the more intense Ti source (having lines at 6.753 and 6.413 MeV) was the more convenient for low-energy experiments.

The γ radiation from the source emerges as a beam with an angular divergence of 1.4–3° and is Compton scattered from the variable length sectioned aluminum scatterer approximately 60-cm high and 6-m long (at maximum length).

In resonance fluorescence experiments, the resonant scatterer is held at the target position T. For photofission experiments this is replaced with either fission foils or fission chambers. A variety of detectors can be positioned inside the target chamber, including Ge(Li), NaI(Tl), and plastic film (for fission track detection).

As the capture γ spectra of both the Ni and Ti sources have two strong lines separated by only a few hundred keV, the Compton scattered beam at any angle will include two main energy components. However, other components are also present, due to weak source lines, reactor background, and bremsstrahlung, and all these components must be considered in evaluating cross sections as a function of energy. Figure 19 shows the typical energy distribution of photon beams produced by Compton scattering at the Ames facility (Hall *et al.*, 1970).

IV.3 Data Analysis and Results

When the method of Sec. III is followed, an effective cross section $\langle\sigma\rangle$ can be defined as in Eq. (3.10):

$$\langle\sigma\rangle = \int F(E)\sigma(E)\, dE / \int F(E)\, dE. \tag{4.2}$$

Since the photon spectrum is "white" it can be represented by $F(E) = C$ in the interval $[E_0, E_0 + \Delta E]$. However, as there might exist more than one level in this energy interval one has to write

$$\sigma(E) = \sum_j \sigma^j(E). \tag{4.3}$$

Inserting these expressions for $F(E)$ and $\sigma(E)$ into Eq. (4.2), one obtains

$$\langle\sigma\rangle = \sum \int \sigma^j(E)\, dE/\Delta E. \tag{4.4}$$

It has been shown by Metzger (1959) that

$$\int \sigma^j(E)\, dE = \pi^2 \lambda\!\!\!^{-2} g^j (\Gamma_0 \Gamma_i / \Gamma)^j, \tag{4.5}$$

where the parameters are defined in Eq. (2.4). Assuming n levels in the energy intervals ΔE, one then obtains from Eqs. (4.4) and (4.5)

$$\langle\sigma\rangle = \pi^2 \lambda\!\!\!^{-2} \langle g(\Gamma_0 \Gamma/\Gamma)\rangle / D, \tag{4.6}$$

where $D = \Delta E/n$ is the average level spacing, and the brackets "$\langle\ \rangle$" indicate the arithmetic average over the energy interval ΔE.

By measuring $\langle\sigma\rangle$ for both elastic and inelastic scattering and making appropriate assumptions regarding g, one can obtain the values of

$$\left\langle \frac{\Gamma_0^2}{\Gamma} \right\rangle \Big/ D \quad \text{and} \quad \left\langle \frac{\Gamma_0 \Gamma}{\Gamma} \right\rangle \Big/ D,$$

respectively. Self-absorption measurements similar to those discussed in Sec. III can be used to obtain information on the average radiation width $\langle\Gamma_0\rangle$ and the average level spacing D. A detailed analysis of these self-absorption experiments has been discussed by Axel (1962), who assumed either a pure Doppler, or a pure Lorentzian shape for the resonance levels.

The photoexcitation technique described in this chapter has been applied by Knowles and Ahmed

(1966) and Khan and Knowles (1967) to study the resonance fluorescence of various materials. Table VIII gives the energies and widths of levels in ^{208}Pb photoexcited by this technique. From this Table, is seen that the level energies are stated to an accuracy of a few keV despite the fact that the incident spectrum is about 100-keV wide.

The double closed shell nucleus ^{208}Pb is a very interesting one and has also been studied via the $(d, p\gamma)$ reaction (Earle *et al.*, 1970) and compared to theoretical predictions.

From the levels populated in the $(d, p\gamma)$ reaction, six were observed to decay to the ground state and were assigned as 1^- levels. Only two of these levels at 5288 and 5943 keV were populated strongly (10 times stronger than the other levels). The 5288-keV level is actually a part of the $S_{1/2}P_{1/2}^{-1}$ doublet. The 0^- member of this doublet was also observed and, from the (d, p) spectroscopic factor, it was concluded that this doublet has almost all of the strength of the $S_{1/2}P_{1/2}^{-1}$ configuration. Of the photoexcited levels observed by Khan and Knowles, only those at 5294 and 5512 keV can be identified with 1^- levels observed in the $(d, p\gamma)$ reactions. However, the level at 5294 keV has a width of only 5 eV, less than that of all the others. Furthermore, the 5943-keV level which according to the (d, p) spectroscopic factor contains most of the $D_{3/2}P_{1/2}^{-1}$ strength was not photoexcited (an upper limit to its width was given as 0.5 eV).

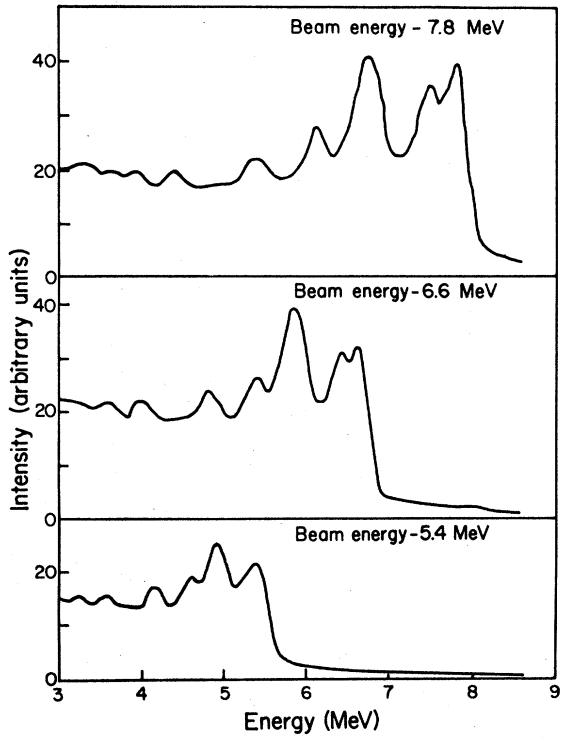

FIG. 19. Typical energy distribution of beams produced by the Compton scattering facility at various angles. [Hall *et al.* (1970)].

TABLE VIII. Photoexcited levels in ^{208}Pb (from Khan and Knowles, 1967).

Level energy E (keV)	Level width Γ_0 (eV)
5294±6	5
5512±6	15
6717±15	15
7052±3	15
7074±3	15
7325±2	35

From their results, Earle *et al.* concluded that the $S_{1/2}P_{1/2}^{-1}$ and $D_{3/2}P_{1/2}^{-1}$ strength below 7.3 MeV in ^{208}Pb is concentrated in two states and not fragmented into many states as predicted by Lane (1970) and Kuo *et al.* (1970). In addition, in this energy region, $P_{1/2}$ hole components do not account for the major part of the $E1$ photo excitation cross section in contradiction to the predictions of Pal *et al.* (quoted by Lane, 1970). The origin of the strong photoexcited resonances is so far unexplained.

In the low-energy region the widths of individual levels can be measured directly, since the sum in Eq. (4.3) and the succeeding equations can be replaced by a single term representing the energy interval covered by the resolution of the detector. However, there seems to be no advantage to this method over the resonance fluorescence of low energy bremsstrahlung (Seward, 1962).

IV.4 Conclusions

The Compton scattered (n, γ) and bremsstrahlung techniques seem to compliment each other. The latter method—using a microtron or linac as the bremsstrahlung electron source—has the advantage of higher intensities and covers a wider energy range than available with the Compton scattering method. However, severe pile up problems due to low-energy photons prevents using the electron machines at their full capacities for resonance fluorescence experiments. For this type of experiment the available intensities per energy interval are actually higher in the (n, γ) Compton scattering arrangements in the energy range 6–9 MeV.

The intrinsic energy resolution of the Compton-scattering technique is about 2%. However, for resonance fluorescence experiments in the vicinity of the (γ, n) threshold, the energy resolution is limited only by that of the Ge(Li) detector (~7 keV). The photoexcitation may in general still cover many levels. In order to simplify interpretation of the results, it is therefore desirable to use monoisotopic targets. For the Compton scattering facilities at present available

at medium power reactors, the quantity of target material required for photoexcitation is of the order of a few hundred grams, which restricts the experiments to a few targets. The target size could be greatly reduced if such facilities were installed at high flux reactors. This would make it feasible to use separate isotopic targets and thus open a wider range of stable nuclei for study.

V. PHOTOFISSION REACTIONS

V.1 Introduction

The photofission reaction can contribute to the understanding of low-energy nuclear fission, especially near the threshold energy. This is because the photons are absorbed by heavy nuclei either with E_1 or E_2 multipolarities resulting in compound nuclear states with a small selection of momenta. The general picture of the fission mechanism developed over three decades ago by Bohr and Wheeler (1939) is still believed to have general application. In this picture, the heavy nucleus goes through a quasiequilibrium saddle configuration, which represents a minimum potential energy pathway towards actual scission. There is a rapid transition from the saddle point to the scission point, where the nucleus splits into two large fragments, which then gain kinetic energy due to mutual Coloumb repulsion.

Simple liquid drop calculations predict a single potential barrier with respect to nuclear deformation, with a maximum corresponding to the saddle point. Strutinsky (1962) showed that the addition of shell correction terms to the liquid drop deformation energy can cause the appearance of a second minimum in the potential energy curve. This has permitted an interpretation of many structural phenomena observed in near threshold and subthreshold fission.

Bohr (1955) has pointed out that, despite the very high excitation energy of the fissioning nucleus, most of this energy is in deformation energy. The transition states near the saddle point therefore represent quite simple collective excitations of the nucleus which can be described in terms of the quantum number K, the component of angular momentum along the symmetry axis. Low-energy photofission is an excellent means of studying these transition states, since the electric dipole or quadrupole absorption involved can only excite low order levels. For example, for even–even nuclei, dipole absorption gives values of $K=0$ or $K=1$ for the saddle point configuration. On the other hand, fission induced by charged particles or neutrons gives a large variety of momentum states. Photofission is particularly useful for studying the shape of the potential barrier below the neutron threshold, which of course cannot be studied with neutron induced fission. Measurements of the photofission cross sections and of the fragment angular distributions permit the determination of the relative contribution of the various fission channels at different excitation energies [see, for example, Huizenga (1972)].

Early photofission studies on heavy elements were carried out by several groups using betatron bremsstrahlung. These have been summarized by Katz *et al.* (1958).

Bowman *et al.* (1964) studied the photodisintegration of ^{235}U using nearly monochromatic photons obtained from the annihilation in flight of fast positrons. This technique gives an energy resolution of 3% in the region of the resonance peak of about 13 MeV. However, owing to the reduced yield of low-energy annihilation photons, they were not able to extend their measurements below 9 MeV, and so also used bremsstrahlung measurement in the region of the fission threshold.

More recently Rabotnov *et al.* (1970) have reported measurements using microtron bremsstrahlung. The (γ, f) yields, as well as the angular distribution of the fission fragments, were measured as functions of the γ energy. The general form of the fission cross sections as a function of energy is shown in Fig. 20. The curves are typical of a photonuclear process, with a threshold energy in the region of 5–7 MeV, a broad resonance peak at about 14 MeV, and a quite rapid drop above 20 MeV. The peak cross sections are in the region of one hundred to a few hundred millibarns, and vary

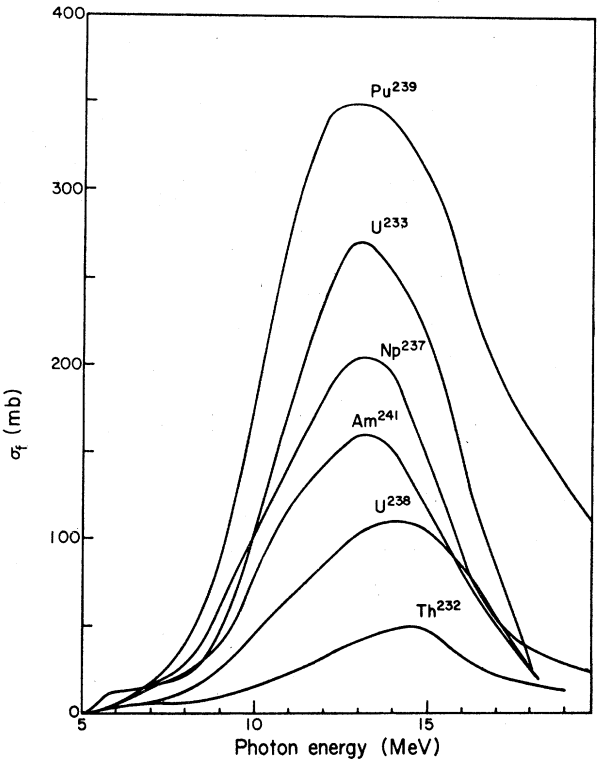

FIG. 20. Photofission cross section of various fissionable materials versus photon energy. [Katz *et al.* (1958)].

approximately as Z^2/A, the fissionability parameter. Some secondary minima were reported just above threshold for several of the nuclei, but the positions and amplitudes of these minima remain uncertain. In even–even nuclei the angular distribution of the fission axis with respect to the photon beam was found to be anisotropic, of the form $a+b\sin^2\theta+c\sin^2 2\theta$. The degree of anisotropy decreases by some three orders of magnitude between threshold energy and an energy 20 MeV above threshold.

Although the end point bremsstrahlung energies in the above studies are usually known to better than a few hundred kiloelectronvolts (and approaching 25 keV in the more recent work), the differential cross section is given with far less precision. This is because the bremsstrahlung energy spectrum $f(E, E_{\max})$ is very broad, with minimum intensity at the maximum energy $E_{\max}$. The cross sections are obtained from the integral yield curves $Y(E_{\max})$ by solving integral equations of the form

$$Y(E_{\max})=C\int_0^{E_{\max}}\sigma(E)f(E,E_{\max})\,dE. \quad (5.1)$$

However, as Rabotnov *et al.* pointed out, the determination of $\sigma(E)$ from this equation is in fact an improperly formulated problem, and is subject to "swinging" of the solutions. This makes it difficult to study detailed structure within an energy interval of less than 100 keV. Due to the exponential nature of the low-energy cross section and the shape of the bremsstrahlung spectrum, the most reliable cross sections from the bremsstrahlung data are those in the vicinity of the fission threshold.

Since the characteristics of the photofission phenomenon near threshold are of great importance in elucidating the mechanism of nuclear fission, it is clearly worthwhile to carry out additional measurements in this energy region. Khan and Knowles (1972) have studied the photofission of ^{232}Th, ^{238}U, and ^{235}U near threshold using the variable energy Compton scattered (n, γ) source mentioned in the previous chapter. Although this method also requires an unfolding procedure to unravel the cross sections, there is the advantage that the Compton scattered γ spectrum is peaked at the maximum energy. This method can therefore be used to compliment the bremsstrahlung data.

In order to resolve the inherent uncertainties involved in the unfolding procedure, there is need to carry out photofission measurements at discrete photon energies. De Carvalho *et al.* (1962, 1963, 1965) and Manfredini *et al.* (1965, 1966, 1969a, b) have carried out photofission studies using direct beams of capture γ rays. The use of capture γ rays in studying photofission permits measurements at precise energies; however, there are considerable limitations both in that the choice of energies is restricted and that usually several lines contribute to the photofission yield. Lindner (1965) used a similar technique to study the competition between neutron emission and fission in ^{238}U as a function of photon energy. He showed that this ratio is consistent with a constant value $\Gamma_n/\Gamma_f\sim 4.0$ in the energy range 6–9 MeV, but with experimental errors of the order of 50%.

V.2 Photofission Cross Section Measurements

Khan and Knowles (1972) measured the fission cross sections of ^{232}Th, ^{238}U, and ^{235}U near threshold using a variable energy beam of γ rays obtained by Compton scattering of capture γ rays. The Compton scattering monochromator is described in the previous chapter. The fission cross sections were measured using ion chambers coated with the fissionable material at the beam target position. The energy resolution of the beam was some 4%–5% for this target geometry. The derived fission cross sections for ^{232}Th and ^{238}U are shown in Fig. 21. The errors shown are the relative errors due to the unfolding procedure, and do not include a ±22% error due to uncertainty in the absolute beam intensity measurements. The results are compared with similar measurements of Yester *et al.* (1972) and the bremsstrahlung results of Katz *et al.* (1958) and of Rabotnov *et al.* (1970). The cross section of ^{238}U shows peaks at 5.2, 5.7, 6.2, 7.1, and 7.8 MeV, which are not well resolved in the bremsstrahlung studies. The ^{232}Th cross section shows peaks at 5.5 and 6.4 MeV.

De Carvalho *et al.* (1962) measured the photofission cross sections at precise capture γ energies at a reactor tangential beam hole facility. Special care was taken to remove neutrons from the beam to reduce the competing (n, f) reaction.

The fission targets were prepared from uranium or thorium acetate loaded nuclear emulsions. They were irradiated with the emulsion normal to the beam; because of the photofission asymmetry, this arrangement gave a concentration of fission tracks in the emulsion plane. The emulsions were processed to give visible tracks only for fission fragments and scanned manually with a microscope.

The initial experiments were carried out with a titanium capture γ beam having three prominent lines at 6.753 MeV (41%), 6.550 MeV (6.2%), and 6.413 MeV (29.5%). These experiments were extended by Manfredini *et al.* (1965, 1966, 1969b) using a series of 12 capture γ sources to measure the photofission cross sections of ^{232}Th and ^{238}U in the energy region 6–9 MeV. The cross sections were evaluated from the photofission yields by an iterative process assuming a smooth curve for the fission cross section as function of energy. Usually the second iteration was sufficient, giving cross sections within 1% of the final values. The experimental error in the cross sections includes a contribution of 3% due to statistical and observer errors in counting the fission tracks, an error of 6% in the

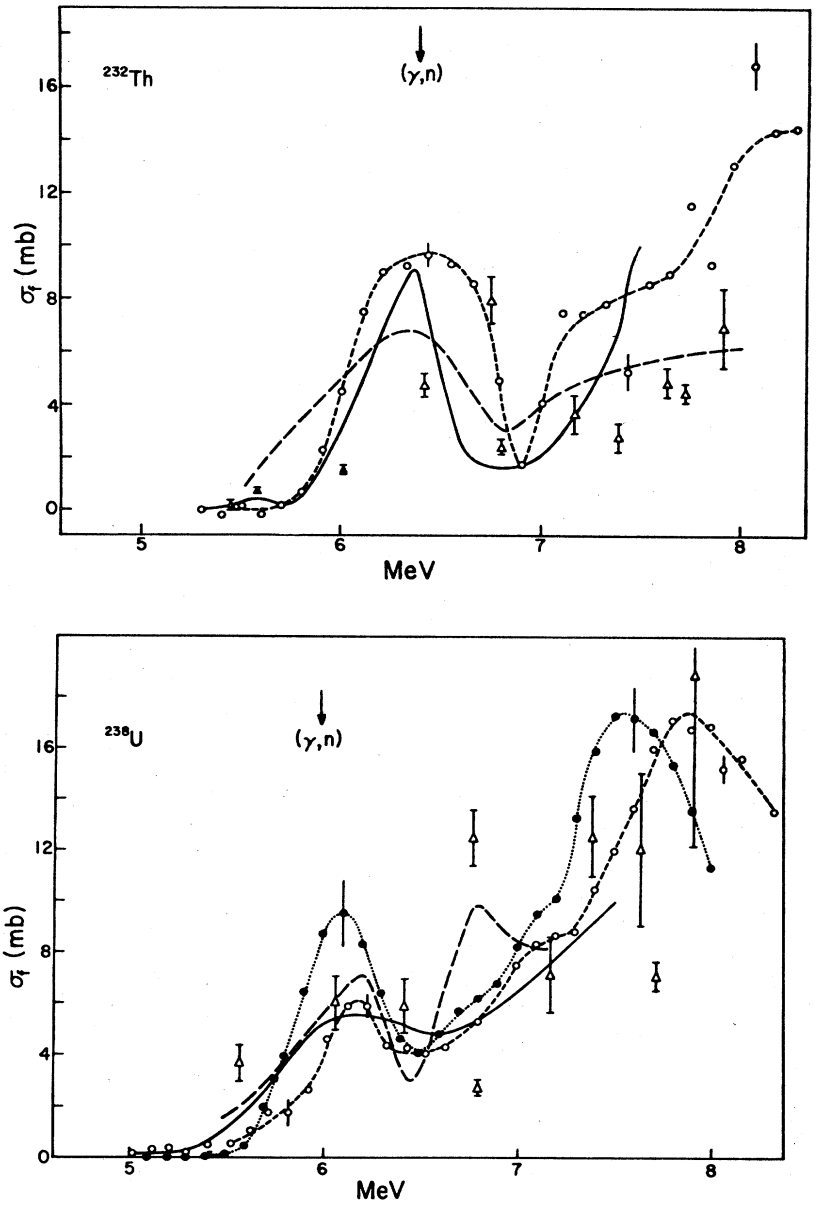

FIG. 21. Photofission cross sections: (a) ^{232}Th and (b) ^{238}U. - - -, Katz *et al.* (1958); —, Rabotnov *et al.* (1970); ⊖-⊕-⊖, Knowles *et al.* (1970); +, Yester *et al.* (1972); ⧋, points from Manfredini *et al.* (1969b).

target mass, and an error of 7% in relative γ flux measurements. There is an additional 10% error due to the uncertainty in the absolute γ flux determination.

The cross sections obtained by Manfredini *et al.* (1969b) are also shown in Fig. 21. These show considerable fluctuation about the results of Khan and Knowles. The increase at 6.8 MeV for ^{232}Th and ^{238}U has been confirmed in similar studies by Mafra *et al.* (1970) who measured relative photofission cross-sections using a fission chamber.

The discrepancies between the results of Manfredini *et al.*, and those of Khan and Knowles may be due to the fact that the former are picking out individual levels in the cross sections.

Khan and Knowles estimated the photofission transmission factors from the ^{232}Th and ^{238}U cross section results. Using a phenomenological model they give a qualitative description of the shape of these transmission factors—but not of the narrow widths observed. They suggest that such structure could be accounted for using the second minimum in the fission potential well. Huizenga (1972) has analyzed the cross section data of Khan and Knowles in terms of the penetrability through a single humped fission barrier and obtains the following parameters for the fission barrier, $B(J=1,\ K=0)$ 6.3 MeV, $B(J=1,\ K=1)$ 6.75 MeV, $\hbar\omega$ (describing curvature of barrier) 0.535 MeV.

V.3 Angular Distribution of the Fission Fragments from Photofission

De Carvalho *et al.* (1963) measured the angular distribution of the fission fragments in the fission of ^{232}Th and ^{238}U induced by 6.61-MeV Ti capture γ rays. The measurements on ^{238}U and ^{232}Th were extended using many capture γ sources by Manfredini *et al.* (1969a, 1971) with a similar experimental procedure as for the cross section measurements discussed above. The nuclear emulsions were exposed to the collimated γ-ray beam at a grazing angle, and processed to give minimum distortion and shrinkage. The emulsions were then scanned for fission events, measuring for each event the fission track orientation, with corrections made for scanning efficiency. If we assume that the photofission reaction takes place only through dipole and quadrupole absorption, the angular distribution can be shown (e.g., Huizenga, 1972) to be generally of the form

$$W(\theta, E)=a(E)+b(E)\sin^2\theta+c(E)\sin^2 2\theta, \quad (5.2)$$

where a and b are mixed coefficients (arising from both dipole and quadrupole fission), c is entirely due to quadrupole fission.

The experimental data were analyzed by least squares and by Fourier analysis, permitting independent evaluation of the parameters a, b, and c. The values of b/a and c/b for ^{238}U are shown in Fig. 22 and compared with the bremsstrahlung data of Rabotnov *et al.* (1970) and the results of Knowles *et al.* (1970). The results for the ratio b/a are in general agreement above 5.6 MeV. Below this energy no data are available from the capture γ studies.

The high values of (b/a) at low energies shows the dominance of the 1^-, $K=0$ state at the saddle point. This ratio decreases with increasing energy as 1^-, $K=1$ states contribute to the fission process. The energy variation of b and a permit an evaluation of the relevant barrier parameters for the 1^-, $K=0$ and 1^-, $K=1$ levels. The fission cross section formula near threshold has been given by Halpern (1959) and Kivikas and Forkman (1965) in the form

$$\sigma=\text{const}\int_0^E \frac{\exp(-U_f/T)}{1+\exp[(B-U_f)/E_p]}\,dU_f. \quad (5.3)$$

Manfredini *et al.* fitted the parameters of the above expression to their experimental results. They found values for T—the nuclear temperature of 0.547 MeV, B—the barrier height of 5.6 MeV, and E_p—the penetrability factor of 0.126 MeV for the 1^-, $K=0$ state. The corresponding values for the 1^-, $K=1$ state were $T=0.642$, $B=6.57$, and $E_p=0.162$ MeV. These are in good agreement with the values found by Kivikas and Forkman, and Rabotnov *et al.* (1965).

Both Rabotnov *et al.* and Knowles *et al.* found a

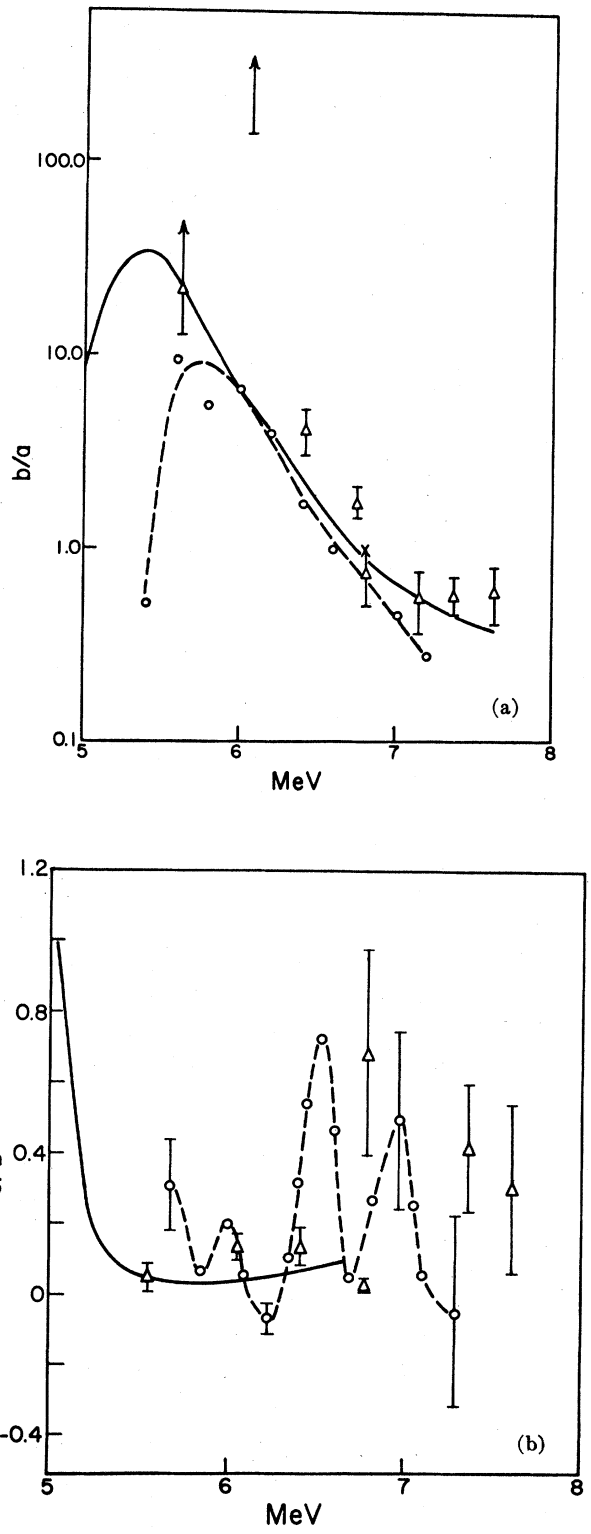

FIG. 22. Ratios b/a and c/b for ^{238}U. —, Rabotnov *et al.* (1970); ⊖–⊖–⊖, Knowles *et al.* (1970); ⏃, Manfredini *et al.* (1969b); (the values of c as defined by Manfredini *et al.* are four times the c values shown in the figure).

maximum in the (b/a) ratio in the region of 5.5 MeV. This can be explained qualitatively by the fact that the two fission barriers corresponding to the $I=1^-$, $K=0$ and $I=1^-$, $K=1$ states differ only near the top of the barrier. In this case the ratio of penetrabilities becomes equal to unity both at high energies and in the deep subbarrier region and has a maximum at some intermediate energy. Rabotnov *et al.* showed that a detailed analysis of the position of this maximum was inconsistent with a single peaked potential barrier, but could be interpreted in terms of the double-humped barrier.

The results of Rabotnov *et al.* (1970) below 5.5 MeV show an increase in c/b showing the increased relative importance of quadrupole fission in the subbarrier region. The results of Knowles *et al.* (1970) for this ratio show resonance structure with peaks about 200 keV wide at 6.9, 6.5, and possibly 6.0 MeV.

V.4 Discussion

The results of the total photofission cross sections and angular distribution results show inconsistencies between the bremsstrahlung, the variable energy Compton scattering method, and the direct (n, γ) technique. It is clearly of importance to resolve these outstanding differences in the different methods. In comparing the results, however, it should be remembered that in the first two methods the cross sections at each energy are averaged over many hundreds of levels in the target nucleus, and hence represent the gross energy dependence. In the case of capture γ beams, the narrow lines may overlap with individual nuclear levels of the target nucleus to give an accentuated cross section, or they may be in a region of fewer nuclear levels and thus give a reduced cross section. Without further experimental investigation it is difficult to say whether these effects are responsible for the discrepancies between the two methods. The method using direct capture γ rays could be improved using more accurate methods of beam intensity normalization and by using additional neutron shielding to reduce the competing (n, f) reaction. In particular, the rather sharp discontinuity in the cross section observed at 6.8 MeV for both ^{238}U and ^{232}Th may be in part due to an incorrect subtraction of the neutron background. The Ti and Be targets responsible for the above mentioned discontinuity can be expected to scatter reactor neutrons in a different manner than the heavy Bi target used for background correction. The use of calibrated mica or glass fission detectors may permit more accurate measurements of the fission yields and angular distribution. Manfredini *et al.* (1971) reported b/a values for ^{232}Th photofission an order of magnitude less than the results of Rabotnov *et al.* (1970). Since clearly a systematic error is involved, it would seem advisable to repeat these measurements.

The interpretation of the angular distribution data and comparison with the Strutinsky model is dependent on the details of the b/a ratio at low energies. Since, however, there are significant differences in the results of Rabotnov *et al.* and Knowles *et al.* in the subbarrier region it would seem important to recheck this ratio. The method using discrete capture γ rays would not be useful in this low-energy region since the low level density would make overlap effects predominant.

VI. PHOTONEUTRON CROSS SECTIONS

VI.1 Introduction

The photoneutron reaction was first studied using bremsstrahlung produced at electron accelerators, for example by Fuller and Weiss (1958). Similar work has been done using positron annihilation γ rays by Bramblett *et al.* (1963) and Bergère *et al.* (1968). These techniques have the advantage of giving intense and stable γ-ray beams, with energies variable over a wide range. However, they have the drawback of poor or moderate energy resolution, of the order of some hundreds of keV in the earlier work and some tens of keV in recent studies. Hence the experimental (γ, n) cross sections are averaged over a broad energy region, and precise determination of the threshold energy of the reaction is difficult. The monoenergetic line of the Li(p, γ) reaction has been used to study (γ, n) cross sections by Hartley *et al.* (1956). The results are restricted to energies in the vicinity of 17 MeV, which lies in the giant dipole region, far above the threshold of (γ, n) reactions. Recently the powerful threshold photoneutron technique has been developed (see, for example, Bowman *et al.*, 1967). This technique permits studying photoneutron cross sections to about 1 MeV above the (γ, n) threshold, with a resolution several orders of magnitude higher than was possible with previous techniques. Baglan *et al.* (1971) have reported measurements on over 200 resonances. The results yield interesting information on the $E1$ strength function, analog states, doorway states, and the $M1$ giant resonance.

The availability of a wide variety of lower energy monoenergetic capture γ lines offers the possibility of checking photoneutron cross sections at discrete energies in the threshold region. In addition, accurate measurements of the threshold energies can be made.

Eriksen and Zaleski (1954) made early measurements of the photoneutron cross section of Be using capture γ sources of Fe, Ti, S, Cu, and Al. Owing to the poor quality of the data then available on capture γ intensities, their results, which were estimated to have an accuracy of about 20%, showed discrepancies of as much as 50% when compared with the accelerator data.

In recent years, several studies on the photoneutron

TABLE IX. Summary of measured cross sections in millibarns [Welsh and Donahue (1961)].

Reaction	γ-ray source energy (MeV)									
	Co 7.49	Fe 7.64	Al 7.73	Cu 7.91	Cl 8.56	Ni 8.997	Fe 9.30	Cr 9.72	Fe 10.16	N 10.83
$^{181}Ta(\gamma, n)^{180}Ta^{m}$	0±0.05	0.5±1	4.8±1.6	14±5	32±16	44±15	...	83±33	...	120±48
$^{197}Au(\gamma, n)^{196}Au$	...	...	...	0±2	34±17	44±11	64±30	80±30	...	...
$^{165}Ho(\gamma, n)^{164}Ho$	...	...	...	0±0.1	29±15	30±18	64±21	86±31	...	260±93
$^{93}Nb(\gamma, n)^{92}Nb$	...	...	...	...	...	0.008±0.005	1.0±0.4	2.4±0.7	...	...
$^{107}Ag(\gamma, n)^{106}Ag$	...	...	...	...	...	0±0.1	...	4.4±1.5	22±16	23±7.5

reaction have been carried out using capture γ rays. Two methods for determining the reaction yields were used, one being measurement of the γ activity following the (γ, n) reaction, and the other being direct photoneutron counting.

VI.2 Experimental Results and Discussion

Welsh and Donahue (1961) measured (γ, n) cross sections indirectly by measuring the γ activity which followed the (γ, n) reaction. Since this method proved to be inaccurate Green and Donahue (1964) and Hurst and Donahue (1967) directly measured the neutrons emitted in the (γ, n) reaction.

Table IX summarizes the (γ, n) cross section found for different targets and γ ray sources by the method of γ activity measurement. Where a capture γ source emitted more than one γ line above the threshold energy for neutron emission, a smooth relationship between cross section and energy was assumed. For example, in order to measure the (γ, n) cross section of Ta at 9.00 MeV, a Ni source was used. However, in addition to the 9.00-MeV line, Ni also emits γ rays of 7.82 and 8.53 MeV, both above the (γ, n) threshold for Ta. Thus the (γ, n) yield from Ta was measured first using an Al (n, γ) source, having a γ energy of 7.72 MeV. In this case it is the only γ ray above

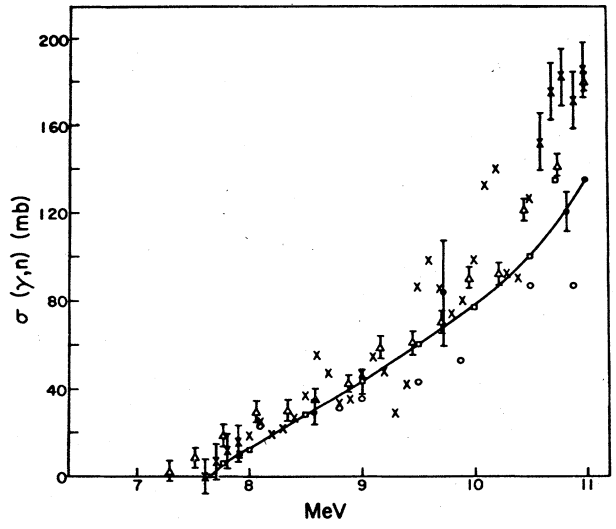

FIG. 23. (γ, n) cross section of ^{181}Ta. □, Fuller and Weiss (1958); ○, Bramblett *et al.* (1963); ●, Green and Donahue (1964); △, Bergère *et al.* (1968); ×, Ishkhanov *et al.* (1969). The solid line is a smooth curve drawn through the results of Green and Donahue.

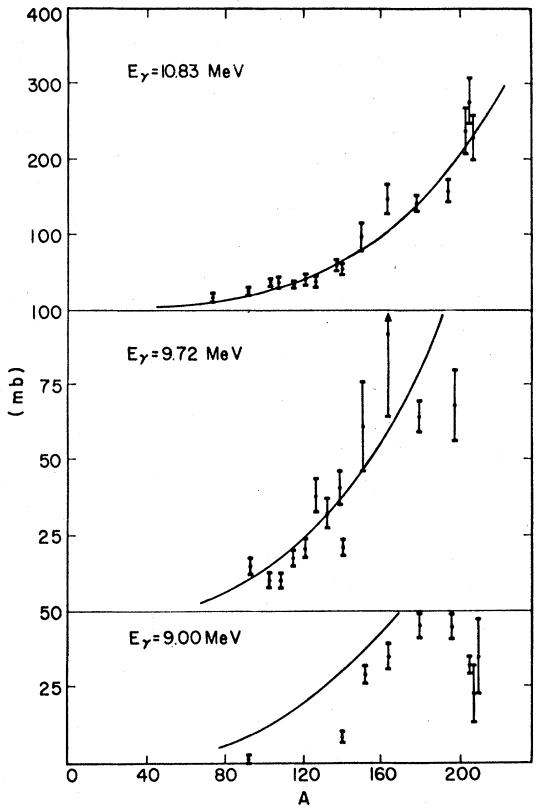

FIG. 24. Photoneutron cross section as a function of target mass for γ-ray energies at 9.0, 9.72, and 10.83 MeV. The solid lines are the giant dipole extrapolations. [Hurst and Donahue (1967)].

TABLE X. Summary of directly measured photoneutron cross sections (millibarns). [Green and Donahue (1964)].

Source	Energy (MeV)	Targets				
		^{181}Ta	^{7}Li	^{6}Li	^{13}C	^{10}B
Aluminum	7.72	4.1±0.4	0.06±0.01	1.13±0.12	1.7±0.2	...
Copper	7.91	10.8±1.0	0.07±0.01	1.1±0.2	0.97±0.13	...
Chlorine	8.56	29±6	0.17±0.12	...	...	...
Nickel	9.00	44±6	0.16±0.06	1.6±0.3	0.6±0.1	0.11±0.01
Nitrogen	10.83	121±12	1.07±0.25	...	4±2	0.9±0.2
Chromium	9.72	84±25	0.55±0.25	...	...	0.23±0.05
Iron	7.64	0.0±0.9	0.079±0.014	1.3±0.2	0.23±0.05	...
Iron	9.30	...	...	...	...	0.09±0.03
Lead	7.38	...	0.068±0.035	1.2±0.2	0.3±0.3	...
Sulphur	5.43	...	...	0.42±0.07		
Sodium	6.41	...	...	0.6±0.1		
Titanium	6.75	...	...	1.3±0.2	...	...
Titanium	6.61[a]	...	...	...	0.32±0.04	...
Manganese	7.16[b]	...	...	0.9±0.1	0.4±0.1	...
Zinc	7.88	...	...	1.0±0.2	1.2±0.2	

[a] Weighted average of 6.75-, 6.55-, and 6.41-MeV γ rays.
[b] Weighted average of 7.26-, 7.15-, and 7.05-MeV γ rays.

threshold and is close to the 7.82 MeV line of Ni. Next, a Cl source was used, having γ rays at 7.77 and 8.56 MeV. If one assumes a smooth variation of cross section with energy, these results permit evaluation of the 7.82- and 8.53-MeV contributions for the Ni source, and hence determination of the 9.00-MeV cross section. The contribution of the two lower energy lines of Ni is 25% of that of the 9-MeV line for the Ta (γ, n) reaction.

As already mentioned, the γ-activity method introduced considerable errors in evaluation of photoneutron cross sections. Although the capture γ yields and energies are now known to much better accuracy than previously, determination of absolute γ activities can involve errors of the order of several percent. Where more than one capture γ line contributes to the activity the corrections needed are also uncertain, since it is not known to what extent the photoneutron cross section is indeed a smooth function of energy in the region concerned. In addition, with the close proximity between sample and source, the photo-induced activity contains a contribution from Compton scattered γ rays which is difficult to evaluate accurately.

Direct counting of the photoneutrons, on the other hand, avoids many of the above difficulties and permits direct comparison of the results with those obtained by other methods. Table X shows the (γ, n) cross sections of ^{181}Ta, ^{7}Li, ^{6}Li, ^{13}C, and ^{10}B as determined by photoneutron counting. The chief source of errors given in the Table is an uncertainty of some 10% in the γ intensities. The cross sections obtained for Ta is also shown in Fig. 23, together with the earlier bremsstrahlung measurements of Fuller and Weiss (1958) and the more recent measurements of Ishkanov *et al.* (1969). The positron annihilation data of Bramblett *et al.* (1963) and Bergère *et al.* (1968) are also shown in this Figure. There is satisfactory agreement between the capture γ method and the bremsstrahlung measurements, though there seems to be disagreement with the positron annihilation data near threshold. The value obtained for the (γ, n) threshold in Ta is 7.64±0.04 MeV, in excellent agreement with the value of 7.64±0.1 obtained by Mattauch *et al.* (1965) and of 7.64±0.02 obtained by Geller *et al.* (1960).

In some cases, such as the one discussed above, the assumption of a smooth cross section curve is justified by the good agreement with the bremsstrahlung results. Indeed, this seems to be a good method for checking the smoothness of the energy dependence. However, if there are deviations from the smooth curve this method cannot be used to study fine details of the energy dependence of the cross section.

The cross sections for the (γ, n) reactions have been measured by Hurst and Donahue (1967) for a number of target nuclei with mass numbers between 59 and

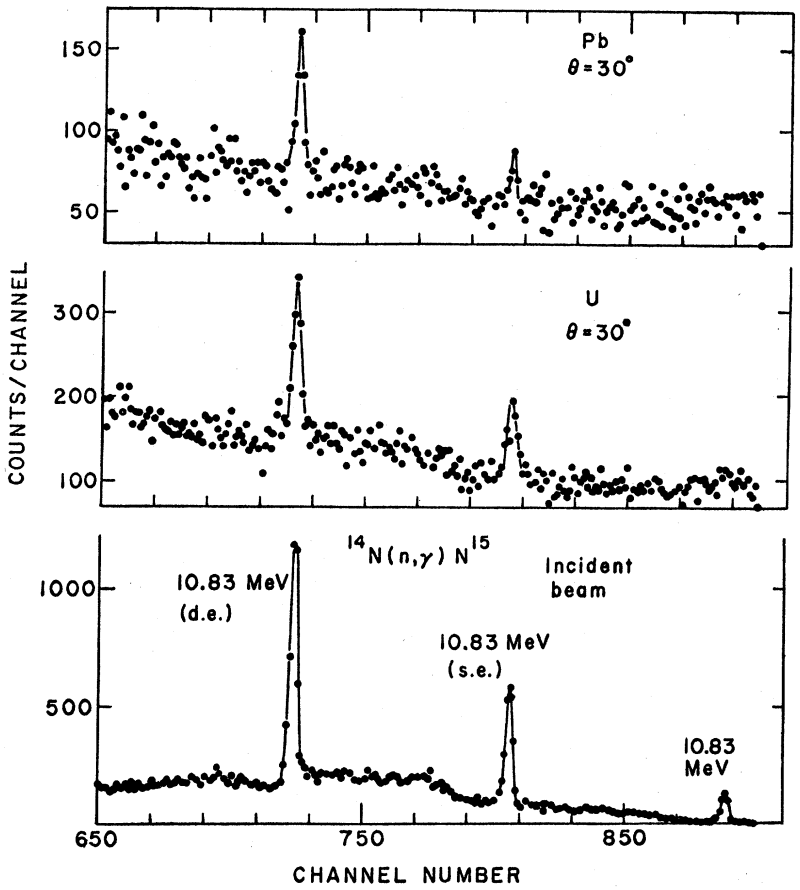

FIG. 25. High-energy region of the incident spectrum of 10.83-MeV γ rays, and spectra of photons scattered through 30° by Pb and U targets. [Jackson and Wetzel (1969)].

209 at photon energies of 9.00, 9.72, and 10.83 MeV, using capture γ sources of nickel, chromium and nitrogen. The results are shown in Fig. 24. The good agreement between the photoneutron cross sections at 10.83 MeV and those predicted by the Lorentzian energy dependence of the giant resonance (Axel, 1962) is of interest and shows the absence of structure effects at this energy. However, there seem to be some discrepancies at 9.72 and 9.00 MeV. In view of the recent improvement in the accuracy with which the energies and intensities of capture γ rays have been determined it would be worthwhile to repeat these measurements with higher precision to see whether the remaining discrepancies can be resolved.

As both the bremsstrahlung and positron time-of-flight methods have inherent uncertainties in determining beam energies and intensities, the capture γ method discussed here offers the advantage of absolute normalization at precise energies.

VII. DELBRÜCK SCATTERING USING CAPTURE γ RAYS

One of the important developments of quantum electrodynamics is in the field of nonlinear electromagnetic effects in vacuum. The lower-order predictions of the theory, including second-order shifts in hydrogenic atoms, and the anomalous magnetic moment of the electron, have been extensively checked against experiment and confirmed to an accuracy as high as one part in 10^{10}.

The scattering of photons in the nuclear Coulomb field, first predicted by Delbrück, is a fourth order nonlinear process involving virtual creation and annihilation of electron pairs. Delbrück scattering can be regarded as a radiative correction to nuclear Thomson scattering. The imaginary part of the Delbrück scattering amplitude corresponds to scattering by the real electron pairs produced in the Coulomb field, and can be used, through the well known rules of dispersion relations, to calculate the real part of the amplitude, which is related to the vacuum polarization. Thus, precision measurements of Delbrück scattering could be used to confirm the use of dispersion relations in quantum electrodynamics.

Delbrück scattering is coherent with other elastic scattering processes, namely Rayleigh, nuclear Thomson, and nuclear resonance scattering. Fortunately, however, in a certain range of forward scattering angles, and at higher energies, the Delbrück effect

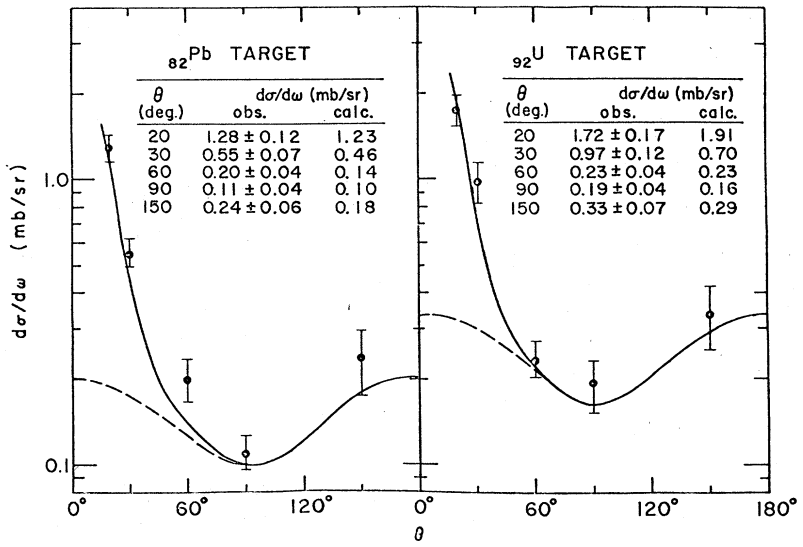

FIG. 26. Differential elastic scattering cross sections for 10.83-MeV photons. Points, experimental; solid curve, calculated; dashed curve, values calculated neglecting Delbrück scattering. For scattering angles greater than 90°, the contribution from Delbrück scattering is negligible. [Jackson and Wetzel (1969)].

has a reasonably high cross section and can be separated from these competing processes. Early experiments carried out at energies in the region of 1 MeV, using strong radioactive sources, did not succeed in identifying Delbrück scattering conclusively, owing to the predominance of Rayleigh scattering at these energies. In fact, Standing and Jovanovich (1962) showed that all the studies reported prior to 1962 were in fact consistent with the calculated Rayleigh scattering amplitude.

Since the Delbrück scattering amplitude increases with energy while the Rayleigh scattering amplitude decreases, it is clearly of advantage to study the former phenomenum at higher energies. Moffat and Stringfellow (1960) found conclusive evidence for the imaginary part of the Delbrück scattering amplitude using 87-MeV bremsstrahlung, and Stierlin *et al.* (1962) obtained similar results using 17-MeV Li(p, γ) radiation. However, due to the broad energy range of the incident γ beam and the poor resolution of the detectors, it was not possible to resolve the elastic from inelastic processes.

Capture γ rays in the energy region 7–12 MeV are particularly suited to the study of Delbrück scattering. Rayleigh scattering is small at these energies except at extreme forward angles, while nuclear resonance scattering is dominant only at large scattering angles in the backward hemisphere. Observation of the interference effects between Delbrück, Rayleigh, nuclear Thomson, and nuclear resonance scattering can thus be used to measure the contribution of the imaginary and real components of the Delbrück scattering amplitude.

Bosch *et al.* (1963) carried out measurements with 9-MeV Ni(n, γ) radiation, using NaI(Tl) detectors. Because of the poor resolution of these detectors they were unable to separate the elastic from the Compton scattering at forward angles. However, from a study of the angular distribution of the scattered radiation from Pb and U targets they were able to obtain conclusive evidence for the imaginary part of the Delbrück scattering amplitude.

Jackson and Wetzel (1969), and Moreh *et al.* (1971) used capture γ radiation of 10.8 MeV (nitrogen source) and 9 MeV (nickel source), respectively, and measured the scattered radiation with Ge(Li) detectors. Jackson and Wetzel used a melamine sample ($C_3H_3N_6$) as the (n, γ) source. The incident spectrum and the spectrum of γ rays scattered at 30° from Pb and U targets are shown in Fig. 25. The combined use of the high-resolution Ge(Li) detector and the monoenergetic (n, γ) beam permits the resolution of the elastic peak from the general background even at forward angles. The angular distribution of the scattered radiation in the range 20°–150° are shown in Fig. 26, where they are compared with theoretical distributions including the Delbrück amplitudes calculated by Ehlotzky and Sheppey (1969). The results provide an excellent confirmation of the contribution of the imaginary part of the Delbrück scattering amplitude, which is predominant below 40°. Between 40° and 100° there is strong interference between the real part of the Delbrück scattering amplitude and nuclear resonance scattering. Above 120° the results could be used to evaluate the real part of the Delbrück scattering amplitude, but more accurate measurements are required for this purpose.

The results of Moreh *et al.* are shown in Fig. 27. The angular distribution was measured between 8° and 20°, thus extending the earlier work of Bosch to smaller angles. The theoretical curves show the influence of the contributions of the different coherent effects.

The solid curves represent the values of the upper and lower limits of the Delbrück amplitudes of Ehlotzky

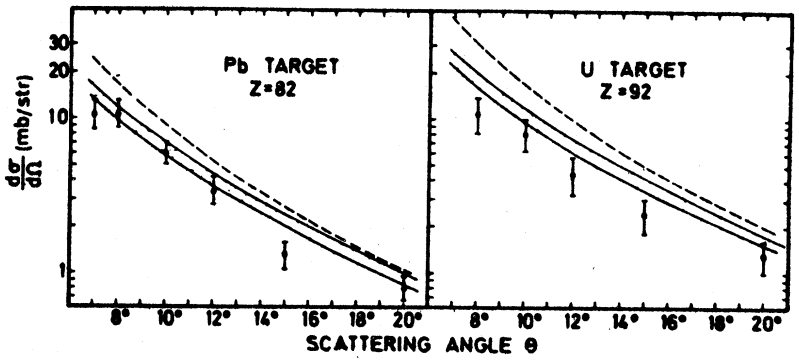

FIG. 27. Differential scattering cross sections for 9-MeV photons. The solid curves represent the calculated values of the upper and lower limits of the Delbrück amplitudes including Thompson and nuclear resonance scattering only. The dashed curves represent the calculated values if Rayleigh scattering (according to Bethe's form factor formula) is included. [Moreh *et al.* (1971)].

and Sheppey. They also include the contribution of the Thomson and nuclear resonance scattering amplitudes, without however the Rayleigh amplitudes. It is clear that the solid curves are in much better agreement with experiment than the upper dashed curve, which includes the Rayleigh amplitudes obtained from the Bethe form factor formula. The contribution of the Rayleigh amplitudes is considerably reduced if a correction factor taken from the low energy calculations of Brown and Mayers (1957) is applied.

These results again give conclusive evidence for the imaginary component of the Delbrück scattering amplitude. The existence of the real part, however, cannot be unambiguously confirmed from these results, since the theoretical scattering cross sections are sensitive to the Rayleigh scattering amplitude, which has not been calculated in this energy range.

To sum up, the use of capture γ rays has given conclusive evidence for the imaginary component of Delbrück scattering to an accuracy of about 10%. By repeating the measurements, it should be possible to improve the accuracy to about 3% and permit the verification of the existence of the real component. However, this will require more accurate calculations of the Rayleigh and Delbrück scattering amplitudes at these energies.

VIII. FUTURE RESEARCH USING NEUTRON CAPTURE γ RAYS

The capture γ-ray techniques described in this review have proved their versatility and achieved definitive results in a wide variety of applications. The great advantage and disadvantage of these capture γ-ray beams is that they are limited to discrete source energies. As such they are ideal for precision measurements at the discrete energies, which can be used for calibrating the results of the more versatile bremsstrahlung and positron annihilation techniques. As an example, precision measurements of total attenuation coefficients have been carried out at discrete energies of the capture γ rays (Bartlett and Donahue, 1965; Moreh *et al.*, 1969). Such measurements can be extended to cover a full range of nuclei.

In some of the applications, the scope for further exploration would seem limited, but there is considerable scope for additional research in the remaining fields.

The Mössbauer studies reported using on-line capture γ rays have established useful nuclear parameters for several nuclei. This on-line technique is however difficult to apply and, if available, a conventional radioactive Mössbauer source is to be preferred for studying a given element. On the other hand, there may be special cases, where, for example, it is required to work with Mössbauer source and absorber of identical chemical composition, where the capture γ technique may find application. In addition, it can be used to study the radiation damage caused by the (n, γ) reaction itself in various source materials. In one case, that of the ^{40}K source, there is no alternative radioactive source available. However, the very small changes in the mean square nuclear radius between the ground and excited states and the properties of the strong potassium binding have not permitted us to obtain much useful information from experiments with this nucleus.

The recoil compensation resonance fluorescence method of measuring level widths using the (n, γ) cascade itself can be applied only in a few isolated cases. This is because there are stringent conditions on the properties of the (n, γ) cascade permitting recoil compensation; the requirement of a reasonably high neutron cross section of the lighter isotope; and the availability of at least 100 g quantities of the two adjacent stable isotopes. Both the bremsstrahlung method and the variable energy Compton scattering (n, γ) source seem to be more suitable for the resonance fluorescence of low-lying levels. While these two latter techniques involve an incident photon spectrum with relatively poor energy resolution, the use of Ge(Li) detectors permits identification of transitions from the individual levels.

The photoneutron and photofission studies carried

out using direct capture γ beams can supplement the bremsstrahlung work. The capture γ method is ideal for normalizing the data of the bremsstrahlung technique, which require an unfolding analysis to obtain the relevant cross sections. The discrepancies in the photofission cross sections near threshold show that it is important to carry out these measurements to a higher degree of accuracy. Unfortunately, most capture γ sources have more than one line above the particular reaction threshold. Thus the minor line contributions must be evaluated to extract the contribution of the dominant γ line. This is usually performed by assuming a smoothly varying cross section without the presence of sharp resonances. Where there are deviations from a smooth cross section due to overlap with individual nuclear levels, it will generally be difficult to evaluate accurately the contributions from the different source lines. For this reason it would not be feasible to study subthreshold photofission using discrete capture γ beams, since at these energies the effect of the overlap with individual levels will predominate. In certain cases the structure of the cross sections near specific γ lines could be studied using the high resolution γ ray monochromator discussed in Sec. III.3.5, or using the rotating target method of Sec. III.3.4. These methods give a γ beam having a width of several hundred eV, or some ten eV, respectively. Both these methods would be limited from intensity considerations to reactions with cross sections of at least some tens of millibarns. There would be obvious advantages in carrying out such experiments using capture γ beams from a high flux reactor.

The variable energy Compton scattering capture γ source provides a promising means of studying the photofission reaction over a broad energy band with a resolution of about 100 keV. Such studies are of special interest in the near-threshold region, where detailed angular distribution measurements have shown effects due to the double-humped potential barrier. This method may have some advantages over the bremsstrahlung experiments since the photon spectrum includes a prominent peak at the upper end of the spectrum, and the unfolding procedure may therefore be less subject to "swinging" of the solutions. Since the resolution attainable with this technique is limited mainly by intensity considerations, it would also be advantageous to install this type of facility at a high flux reactor.

By using the two complementary methods of excitation—namely, chance overlap of the capture γ lines with individual levels, and the variable energy Compton scattering (or bremsstrahlung) source—it should be possible to make a comprehensive study of the ground state transition strengths in the interesting energy region between the pigmy resonance at about 5 MeV and (γ, n) threshold. This would yield values of $\langle\Gamma_0\rangle/D$ and $\langle\Gamma_0\rangle$, and hence D, throughout this energy region. The excitation of individual levels can be expected to give additional spectroscopic data on the level schemes of stable nuclei, both in the low-lying region and in the energy region up to 10 MeV.

The measurements of elastic and inelastic scattering of high-energy capture γ rays from heavy nuclei have permitted the direct observation of both Delbrück and nuclear Raman scattering. In the former case, more accurate measurements are required in a variety of target nuclei to permit verification of the imaginary and real components of the Delbrück scattering amplitudes. The extension of the nuclear Raman scattering to other deformed nuclei in the heavy and medium mass region will permit an independent evaluation of the giant dipole parameters.

ACKNOWLEDGMENTS

The authors would like to acknowledge the assistance of the many investigators who made available their published and unpublished results, with special thanks to L. M. Bollinger, D. I. Donahue, M. Giannini, Z. Gozani, Y. Kawarasaki, J. W. Knowles, J. A. McIntyre, R. Moreh, P. Oliva, N. Shikazono, D. Salzmann, and D. J. Zaffarano.

One of us (B.A.) would like to thank the Department of Nuclear Physics at the McMaster University, Hamilton, Ontario, for its hospitality during the period in which this review was written.

We would also like to extend special thanks to Mrs. E. Berger, Miss F. Broderson, and the Department of Technical Information at the Soreq Nuclear Research Centre for their assistance in editing and preparing the manuscript.

REFERENCES

Antropov, G. P., I. E. Mitrofanov, A. I. Prkof'ev, and V. S. Russkikh, 1971, Bull. Acad. Sci. USSR, Physical Series **34,** 108.
Arad (Huebschmann), B., G. Ben-David (Davis), I. Pelah, and Y. Schlesinger, 1964a, Phys. Rev. **133,** B684.
——, G. Ben-David, and Y. Schlesinger, 1964b, Phys. Rev. **136,** B370.
——, G. Ben-David, and Y. Schlesinger, 1964, Nucl. Inst. Meth. **53,** 277.
——, G. Ben-David, Y. Schlesinger, and M. Hass, 1972, Phys. Rev. **C6,** 670.
Axel, P., 1961, Phys. Letters **4,** 320.
——, 1962, Phys. Rev. **126,** 671.
Bäckström, G., 1959, Nucl. Inst. & Meth. **4,** 5.
Badalyan, A. M., and A. I. Baz, 1961, Soviet Physics JETP **13,** 383.
Baglan, R. J., C. D. Bowman, and B. L. Berman, 1971, Phys. Rev. **C3,** 672.
Barlett, R. H., and D. J. Donahue, 1965, Phys. Rev. **137,** A523.
Barnoy, T., R. Moreh, and J. Rajewsky, 1972, Bull. Israel. Phys. Soc. A-1, 5.
Bartholomew, G. A., 1961, Ann. Rev. Nucl. Sci. **11,** 259.
——, 1969, *Neutron Capture Gamma-Ray Spectroscopy* (I.A.E.A. Vienna, 1969) 553.
——, and L. A. Higgs, 1958, Compilation of Thermal Neutron Capture γ Rays (Atomic Energy of Canada Ltd. Report No. 669).
——, M. R. Gunye, and E. D. Earle, 1967, Can. J. Phys. **45,** 2063.
Bauminger, E. R., J. Gal, B. Khurgin, and S. Ofer, 1968a, Israel Atomics Report NRCN 222.

——, J. Gal, B. Khurgin, and S. Ofer, 1968b, private communication.
Baz, A. I., 1959, Adv. Phys. **8,** 349 (1959).
Ben-David, G., and B. Huebschamnn, 1962, Phys. Letters **3,** 87.
Bergère, R., H. Beil, and A. Veyssière, 1968, Nuclear Physics **A121,** 463.
Berman, B. L., R. I. Baglan, and C. D. Bowman, 1972, *Proceedings of the International Conference on Statistical Properties of Nuclei,* edited by J. B. Garg (Plenum, New York), p. 611.
Biedenharn, L. C., and M. E. Rose, 1953, Rev. Mod. Phys. **25,** 729.
Bohr, A., 1955, Proc. Intern. Conf. Peaceful Uses At. Energy, 1st Geneva **2,** 151.
Bohr, N. and J. A. Wheeler, 1939, Phys. Rev. **56,** 426.
Bollinger, L. M., 1968, *Proceedings International Symposium on Nuclear Structure, Dubna* (Internation Atomic Energy Agency, Vienna), p. 317.
Bösch, R., J. Lang, R. Müller, and W. Wölfli, 1963, Helv. Phys. Acta. **36,** 1625.
Boulter, J. F., W. V. Prestwich, and B. Arad, 1969, Can. J. Phys. **47,** 591.
Bowman, C. D., G. F. Auchampaugh, and S. C. Fultz, 1964, Phys. Rev. **133,** B676.
——, G. S. Sidhu, and B. L. Berman, 1967, Phys. Rev. **163,** 951.
Bramblett, R. L., J. T. Caldwell, F. G. Auchampaugh, and S. C. Fultz, 1963, Phys. Rev. **129,** 2723.
Brink, D. M., 1957, Nucl. Phys. **4,** 215.
Brown, G. E., and D. F. Mayers, 1957, Proc. Roy. Soc. **A242,** 89.
Cameron, A. G. W., 1959, Can. J. Phys. **37,** 322.
Carpenter, R. T., 1962, Argonne National Laboratory Report ANL–6589.
Cesareo, R., M. Giannini, P. R. Oliva, D. Prosperi, M. C. Ramorino, 1969, *Proceedings of the International Symposium on Neutron Capture Gamma Ray Spectroscopy* (IAEA, Vienna), p. 491.
——, M. Giannini, P. R. Oliva, D. Prosperi, and M. C. Ramorino, 1970, Nucl. Phys. **A141,** 566.
Cookson, J. A., and W. Darcey, 1965, Nucl. Phys. **62,** 326.
Cramer, H., 1951, *Mathematical Methods of Statistics* (Princeton U. P., 1951), p. 241.
Danos, M., 1958, Nucl. Phys. **5,** 23.
De Carvalho, H. G., A. Manfredini, M. Muchnik, M. Severi, R. Bösch, J. Lang, R. Müller, and W. Wölfli, 1962, Nuovo Cimento **25,** 534.
——, A. Manfredini, M. Muchnik, M. Severi, R. Bösch, and W. Wölfli, 1963, Nuovo Cimento, 29, 463.
——, A. G. Da Silva, R. N. Alvew, R. Bösch, and W. Wölfli, 1965, *Proceedings Symposium Physics and Chemistry of Fission, Salzberg* (International Atomic Energy Agency, Vienna), Vol. 2, p. 343.
Devons, S., and J. B. Goldfarb, 1957, *Handbuch der Physics* (Springer Verlag, Berlin), Vol. 42, p. 362.
Dressel, R., M. Goldhaber, and A. O. Hanson, 1950, Phys. Rev. **77,** 754.
Earle, E. D., A. J. Ferguson, G. Van Middelkoop, G. A. Bartholomew, and I. Bergqvist, 1970, Phys. Letters **32B,** 471.
Ehlotzky, F., and G. C. Sheppey, 1969, Nuovo Cimento **33,** 1185.
Eriksen, V. D., and C. D. Zaleski, 1954, J. Phys. Radium **15,** 492.
Estes, G. P., and K. Min, 1967, Phys. Rev. **154,** 1104.
Fagg, L. W., and S. S. Hanna, 1959, Rev. Mod. Phys. **31,** 711.
Fagot, J., R. Lucas, H. Nifenecker, and M. Schneeberger, 1971, Nucl. Inst. & Meth. **95,** 421.
Fink, J., and P. Kienle, 1965, Phys. Letters, **17,** 326.
Fleischmann, H. H., 1963, Ann. Physik **12,** 133.
——, and F. W. Stanek, 1963a Z. Phys. **175,** 172.
——, and F. W. Stanek, 1963b, Z. F. Natur. For. **18,** 555.
Fuller, E. G., and E. Hayward, 1956, Phys. Rev. **101,** 692.
——, and E. Hayward, 1962, Nucl. Phys. **30,** 613.
——, and M. S. Weiss, 1958, Phys. Rev. **112,** 560.
Fultz, S. C., R. L. Bramblett, J. T. Caldwell, N. E. Hansen, and C. P. Jupiter, 1962, Phys. Rev. **128,** 2345.
Gaerttner, E. R., and G. L. Yeater, 1949, Phys. Rev. **76,** 363.
Gal, J., E. R. Bauminger, and S. Ofer, 1968, Phys. Letters **27B,** 552.
Geller, K. N., J. Halpern, and E. G. Muirhead, 1960, Phys. Rev. **118,** 1302.
Giannini, M., P. Oliva, D. Prosperi, and S. Sciuti, 1964, Nuovo Cimento **34,** 1116.
——, P. Oliva, D. Prosperi, and S. Sciuti, 1965, Nucl. Phys. **65,** 344.
Goldhaber, M., and E. Teller, 1948, Phys. Rev. **74,** 1046.
Goldstein, S., and I. Talmi, 1956, Phys. Rev. **102,** 589.
Green, L., and D. J. Donahue, 1964, Phys. Rev. **135,** B701.
Groshev, L. V., A. M. Demidov, V. N. Lutsenko, and V. I. Pelikhov, 1959, *Atlas of Gamma Ray Spectra from Radiative Capture of Thermal Neutrons* (Pergamon, London).
——, A. M. Demidov, V. I. Pelekhov, L. L. Sokolovskii, I. V. Kurchatov, G. A. Bartholomew, A. Doveika, K. M. Eastwood, and S. Monaro, *1967, 1968, 1969, Nuclear Data Tables* (Academic, New York) Section A, **3,** 367–650, **5,** 1–242 (1968), **5,** 243–431 (1969).
Hafemiester, D. W., and E. Brooks Shera, 1965, Phys. Rev. Letters **14,** 593.
Hall, J. E., R. G. Strauss, and D. J. Zaffarano, 1970, Ames. Laboratory Report IS-2335.
Halpern, I., 1959, Ann. Rev. Nuc. Sci. **9,** 245.
Hannaford, P., C. J. Howard, and J. W. G. Wignal, 1965, Phys. Letters **19,** 257.
Hans, H. S., G. E. Thomas, and L. M. Bollinger, 1966, *International Conf. on the Study of Nuclear Structure with Neutrons,* edited by M. Nève de Mévergnies, P. Van Assche, and J. Vervier (North Holland Publ. Co., Amsterdam), p. 514.
Hartley, W. H., W. E. Stephens, and E. J. Winhold, 1956, Phys. Rev. **104,** 178.
Haas, H., and D. Salzmann, 1973, Phys. Rev. C (to be published).
——, R. Moreh, and D. Salzmann, 1971, Phys. Lett. **36B,** 68.
Huebschmann, B., and S. Alterowitz, 1963, Res. Reactor J. **3,** 11.
Huizenga, G. R., 1972, Nucl. Tech. **14,** 20.
Hurst, R. R. and D. J. Donahue, 1967, Nucl. Phys. **A91,** 365.
Ishkhanov, B. S., I. M. Kapitonov, E. V. Lazutin, I. M. Piskarev, O. P. Shevchenko, 1969, JETP Letters **10,** 51.
Jackson, H. E., and K. J. Wetzel, 1969, Phys. Rev. Letters **22,** 1008.
——, and K. J. Wetzel, 1972, Phys. Rev. Letters **28,** 513.
Jarczyk, L., H. Knoepfel, J. Lang, and W. Wölfli, 1959, Bull. Am. Phys. Soc. **4,** 477.
——, H. Knoepfel, J. Lang, R. Müller, and W. Wölfli, 1961, Nucl. Inst. & Meth. **13,** 287.
Kapadia, C. I., V. E. Michalk, and J. A. McIntyre, 1968, Nucl. Inst., **59,** 197.
Katz, L., A. P. Baerg, and F. Brown, 1958, *Second U.N. International Conference on The Peaceful Uses of Atomic Energy* (International Agency Atomic Energy, Geneva), Vol. **45,** 188.
Khan, A. M., and J. W. Knowles, 1967, Bull. Am. Phys. Soc. II **12,** 538 (GE6).
——, and J. W. Knowles, 1972, Nucl. Phys. **A179,** 333.
T. Kivikas and B. Forkman, Nucl. Phys. **64,** 420.
Knoepfel, H., P. Scherrer, and P. Stoll, 1959, Z. Physik **156,** 293.
Knowles, J. W., 1970, Bull. Am. Phys. Soc. **15,** 805.
——, and N. M. Ahmed, 1966, Atomic Energy of Canada Ltd. Report 2535.
——, A. M. Khan, and W. G. Gross, 1970, Izv. Akad. Nauk SSSR (Ser. Fiz) **34,** 1620 (1970).
Kuo, T. T. S., J. Blomqvist, and G. E. Brown, 1970, Phys. Letters **31B,** 93.
Lamb, W. E., 1939, Phys. Rev. **55,** 190.
Lane, A. M., 1970, Phys. Letters **31B,** 344.
Lea, D. E., 1934, Nature **133,** 24.
Lindner, M., 1965, Nucl. Phys. **61,** 17.
Lone, M. A., R. E. Chrien, O. A. Wasson, M. Beer, M. R. Bhat, and H. R. Muether, 1968, Phys. Rev. **174,** 512.
Loper, G. D., L. M. Bollinger, and G. E. Thomas, 1972, Bull. Am. Phys. Soc. **17,** 580.
Lynn, J. E., 1968, *Neutron Resonance Reactions* (Oxford U.P., London).
Mafra, O. Y., S. Kuniyoshi, and F. G. Bianchini, 1970, Brazilian Report Publicacao IEA-No. 211.
Manfredini, A., L. Fiore, C. Ramorino, H. G. De Carvalho, and W. Wölfli, 1969a, Nucl. Phys. **A123,** 664.
——, L. Fiore, C. Ramorino, H. G. De Carvalho, and W. Wölfli, 1969b, Nucl. Phys. **A127,** 687.
——, L. Fiore, C. Ramorino, W. Wölfli, 1971, Nuovo Cimento **4A,** 421.

——, M. Muchnik, L. Fiore, C. Ramorino, H. G. De Carvalho, J. Lang, and R. Müller, 1965, Nucl. Phys. **74,** 377.
——, M. Muchnik, L. Fiore, C. Ramorino, H. G. De Carvalho, R. Bösch, and W. Wölfli, 1966, Nuovo Cimento **44,** 218.
Mattauch, J. H. E., W. Thiele, and A. H. Wapstra, 1965 Nucl. Phys. **67,** 1.
McIntyre, J. A., and J. D. Randall, 1965, Phys. Letters **17,** 137.
——, and G. K. Tandon, 1963, Phys. Letters **4,** 117.
——, and G. K. Tandon, 1968, Nucl. Inst. **59,** 181.
Metzger, F. R., 1959, Prog. Nucl. Physics **7,** 53.
Min, K., 1966, Phys. Rev. **152,** 1062.
Moffat, J., and M. W. Stringfellow, 1960, Proc. Roy. Soc. (London) **A254,** 242.
Moreh, R., and G. Ben Yaakov, 1967, Israel Atomics Report IA1163.
——, and M. Friedman, 1968, Phys. Letters **26B,** 579 (1968); and Phys. Letters **31B,** 642.
——, and A. Nof, 1969, Phys. Rev. **178,** 1961.
——, and A. Nof, 1970, Phys. Rev. **C2,** 1938.
——, A. Nof, and A. Wolf, 1970a, Phys. Rev. **C2,** 249.
——, D. Saltzmann, and G. Ben-David, 1971, Phys. Letters **34B,** 494.
——, D. Salzmann, and Y. Wand, 1969, Phys. Letters **30B,** 536.
——, S. Shlomo, and A. Wolf, 1970b, Phys. Rev. **C2,** 1144.
——, and A. Wolf, 1969a Phys. Rev. **182,** 1236.
——, and A. Wolf, 1969b, in *Neutron Capture Gamma-Ray Spectroscopy* (I.A.E.A., Vienna), p. 483.
——, and A. Wolf, 1972, *Proceedings International Conference Statistical Properties Nuclei,* edited by J. B. Garg (Plenum, New York,), p. 257.
Mössbauer, R. L., 1958, Z. Physik **151,** 124.
Mouton, W. L., J. F. P. Sellschop, and G. Wiechers, 1963, Phys. Rev. **129,** 361.
Mughabghab, S. F., R. E. Chrien, and O. A. Wasson, 1970, Phys. Rev. Letters **25,** 1670.
Nathan, O., and S. G. Nilsson, 1965, in α, β, *and* γ*-Ray Spectroscopy,* edited by K. Siegbahn (North-Holland Publ. Co., Amsterdam, 1965), Chapt. X.
O'Connel, J. S., P. A. Tipler, and P. Axel, 1962, Phys. Rev. **126,** 228.
Okamoto, K., 1958, Phys. Rev. **110,** 143.
Oliva, P. R., 1970, Lett. Nuovo Cimento Series II, **1,** 77.
O'Shea, D. M., and H. C. Thacher, 1963, Am. Nucl. Soc. **6,** 36.
Pavel, D., G. Ben-David, Y. Schlesinger, and H. Szichman, 1971, Nucl. Phys. **A160,** 409.
Pitthan, R., and Th. Walcher, 1971, Phys. Letters **36B,** 563.
Porter, C. E., and R. G. Thomas, 1956, Phys. Rev. **104,** 483.
Rabotnov, N. S., G. N. Smirenkin, A. S. Soldatov, L. N. Usachev, S. P. Kapitza, and Y. M. Tsipeniuk, 1965, *Physics and Chemistry of Fission,* Proceedings Symposium Salzburg (IAEA, Vienna), p. 135.
——, G. N. Smirenkin, A. S. Soldatov, L. N. Usachev, S. P. Kapitza, and Y. M. Tsipenyuk, 1970, Sov. J. Nucl. Phys. **11,** 285 (1970) (Yad Fiz. **11,** 508).
Ramchandran, S., and J. A. McIntyre, 1969, Phys. Rev. **179,** 1153.
Reibel, K., and A. K. Mann, 1960, Phys. Rev. **118,** 701.
Rimawi, K., R. E. Chrien, J. B. Gary, M. R. Bhat, D. I. Garber, and D. A. Wasson, 1969, Phys. Rev. Letters **23,** 1041.
Samour, C., H. E. Jackson, J. Julian, A. Bloch, C. L. Lapata, and J. Morgenstern, 1968, Nucl. Phys. **A121,** 65.
Schlesinger, Y., M. Hass, B. Arad, and G. Ben-David, 1969, Phys. Rev. **178,** 2013.
——, H. Szichman, G. Ben-David, and M. Hass, 1970, Phys. Rev. **C2,** 2001.
Seppi, E. J., H. Henrikson, F. Boehm, and J. W. Du Mond, 1962, Nucl. Inst. **16,** 17.
Seward, F. D., 1962, Phys. Rev. **125,** 335.
Shikazono, N., and Y. Kawarasaki, 1968, Nucl. Phys. **A118,** 114.
——, and Y. Kawarasaki, 1969, J. Phys. Soc. Japan **27,** 273.
Standing, K. G., and J. V. Jovanovich, 1962, Can. J. Phys. **40,** 622.
Stearns, M. B., 1952, Phys. Rev. **87,** 706.
Steirlin, U., W. Scholz, and B. Povh, 1962, Z. Physik **170,** 47.
Strutinsky, V. M., N. Ya Lyashchenko, and N. A. Popov, 1962, Zh. Eksp. Teor. Fiz. **43,** 584.
Szichman, H., Y. Schlesinger, G. Ben-David, and D. Pavel, 1970, Nucl. Phys. **A148,** 369.
Tseng, P. K., S. L. Ruby, and D. H. Vincent, 1968, Phys. Rev. **172,** 249.
Welsh, R. E., and D. J. Donahue, 1971, Phys. Rev. **121,** 880.
Wetzel, K. J., and H. E. Jackson, 1971, Bull. Am. Phys. Soc. **16,** 579.
Wilkinson, D. H., 1956, Physica **23,** 1039.
Yester, M. V., R. A. Anderl, and R. C. Morrison, 1972, Bull. Am. Phys. Soc. **17,** 441.
Young, C. S., and D. I. Donahue, 1963, Phys. Rev. **132,** 1724.